Reconstruction of historic fossil CO_2 emissions using radiocarbon measurements from tree rings.

Margaret Wilson Norris

A thesis submitted to Victoria University of Wellington in partial fulfilment of requirements for the degree of Master of Physical Geography.

School of Geography, Environment and Earth Sciences, Victoria University of Wellington

February 2015

Abstract: Reconstruction of historic CO$_{2ff}$ emissions using radiocarbon measurements from tree rings

This project aims to reconstruct historic fossil fuel derived CO$_2$ (CO$_{2ff}$) emissions from two closely located point sources in Taranaki, New Zealand. The Vector gas processing plant and the Ballance agri-nutrients ammonia urea plant have combined emissions of ~0.16 TgC yr^{-1} since 1970 and 1982 respectively. Previous work found 2–5 ppm CO$_{2ff}$ in short term integrated samples collected 600m downwind of the Vector plant. This study extends the dataset back 30 years using radiocarbon measurements in tree rings.

Trees incorporate CO$_2$ from the local atmosphere into their annual growth rings. Measurements of ^{14}C in polluted and clean air trees were compared to the Baring Head Δ^{14}CO$_2$ atmospheric record. As CO$_{2ff}$ emissions are devoid of ^{14}C addition of CO$_{2ff}$ will cause a decrease in ^{14}C directly related to the amount of CO$_{2ff}$ present.

Trees growing immediately downwind of the Vector plant and from clean air locations in Taranaki and Baring Head Wellington, were cored and cut into one year growth increments. Two cellulose preparation methods were tested to confirm effectiveness at removing mobile extractive components and lignin. Radiocarbon and stable isotope results showed that the ANSTO method was more effective than the Rafter method. The clean air trees compare well with the Baring Head atmospheric record whereas trees growing downwind of the Vector plant demonstrate lower ^{14}C content consistent with CO$_{2ff}$ addition. Historic CO$_{2ff}$ emissions were reconstructed for the polluted trees, with 1–3ppm of CO$_{2ff}$ in the Luscombe chestnut tree and 4–7 ppm CO$_{2ff}$ in the Vector pine tree. CO$_{2ff}$ observations were compared with reported emissions from the Vector and Ballance plants. Observed CO$_{2ff}$ increased by 10% in the Vector pine tree for the period 1994–2012 relative to pre-1994 levels, whereas combined CO$_{2ff}$ emissions increased by 64%. No increase was observed in the Luscombe chestnut tree for the same time period. Meteorological analysis was performed to assess the relative contribution of CO$_{2ff}$ from the sources to the trees. It is proposed that the trend observed in the Vector pine is due to the dominance of emissions from the Ballance plant and a relatively minor contribution from the Vector plant.

Acknowledgements

Table of Contents

List of Tables

List of Figures

List of Equations

1.0   Introduction

Climate change is one of the great challenges facing society in the 21st Century. The Intergovernmental Panel on Climate Change (IPCC) has released their latest synthesis report that gives a clear message that human influence is causing unequivocal warming of the climate system through the release of greenhouse gases with resultant changes to the climate, oceans and atmosphere. Observations of recent changes in these climate systems are unparalleled with past changes (IPCC 2013). In terms of direct radiative effects CO_2 is the second most important greenhouse gas after water vapour and is considered the most dominant driver of climate change because it is both a long lived greenhouse gas and it has a strong influence on radiative forcing of the climate (IPCC 2013). Releases of greenhouse gases primarily CO_2, perturbs the overall global energy balance through enhancement of the natural greenhouse effect causing re-absorption of radiated energy and warming of the atmosphere and oceans. If emissions continue unchecked continued warming is predicted to result in dangerous and irreversible climate impacts with resulting economic and social consequences (Soloman et al. 2009, Smith et al. 2009). Lowering the risk of climate change "requires substantial and sustained reductions of greenhouse emissions" (IPCC 2013). This requires the implementation of green technology that minimises or removes the need for fossil fuels, climate policy to implement changes and better understanding of the carbon cycle through measurements of CO_2 as it is partitioned through the carbon cycle.

While measurement of atmospheric CO_2 concentrations is one of the best known elements of the carbon budget, better estimates of size of CO_{2ff} emissions and improved estimates of the fluxes into ocean and land sinks would improve carbon budget information (Le Quéré et al. 2014). CO_{2ff} emissions are based on reported energy statistics, and are subject to large uncertainties particularly in developing countries (Guan et al. 2012, Marland et al. 2012). The development of climate policy that seeks to limit those emissions needs to be based on independent and robust statistical and empirical data. Improvement of collection of statistical information is important but the development of methodology that can independently verify emission fluxes and thus validate reported emissions is essential. Networks of monitoring of CO_2 concentrations already exist but there is a paucity of information on a local or regional scale (Meijer et

al. 1995, Levin et al. 2010, Graven et al. 2012). Climate mitigation regulations set emission reductions based on national or regional targets which requires monitoring of CO_2 concentrations on the same scales (Weiss and Prinn 2011).

Evaluation of regional CO_{2ff} emissions is achieved using atmospheric measurements of CO_2 using a tracer to determine the CO_{2ff} component and a model to calculate emission fluxes with uncertainties. The observed fluxes can then be compared with reported emissions. Currently the best agreement obtainable between reported emissions and observations using top down approaches is in the region of ± 20%, (Vogel et al. 2010) therefore techniques to assess emissions require improvement. A strategy to increase $^{14}CO_2$ information on a regional scale is to utilise measurements of $^{14}CO_2$ content in plant material to complement current sampling strategies, e.g. (Hsueh et al. 2007) corn leaves, (Palstra et al. 2008) wine and (Turnbull et al. 2014) grass. The collection of plant material is a simple, quick and cost efficient activity.

1.1 Aims of the study and scope of the thesis

This aim of this project is to develop an experimental technique that can be used to reconstruct past annual mean CO_{2ff} emissions from a point source using measurements of radiocarbon ^{14}C in tree rings in a top down approach and assess the methods ability to evaluate these emissions. A point source with known CO_{2ff} emissions is chosen as a test site. The Vector gas processing plant and the Ballance agri-nutrients ammonia urea plant are located at Kapuni in Taranaki New Zealand, make combined emissions of CO_{2ff} ~0.16 TgC yr^{-1}. It is possible to assess the CO_{2ff} component of CO_2 by utilising measurements of the ^{14}C content of CO_2 expressed as $\Delta^{14}CO_2$.

Trees incorporate CO_2 from the local atmosphere into their cellulose which is laid down in annual growth rings during photosynthesis. To relate this to the CO_{2ff} content of the air we measure ^{14}C in annual tree rings at a local clean air site and compare this to measurements of ^{14}C in the annual ring for the same year at our test site. CO_{2ff} is devoid of ^{14}C so addition of CO_{2ff} will cause an observed decrease in ^{14}C in samples directly related to the amount of CO_{2ff} present.

To provide a check or truth for tree ring results it was necessary to establish that trees sample $^{14}CO_2$ in a representative way. A tree was sampled at a clean air site Baring Head

in Wellington and ^{14}C measured in tree rings and compared to a record of atmospheric $^{14}CO_2$ extracted from air samples collected at Baring Head (Currie et al. 2011). This technique was then applied to polluted trees at the Kapuni site to evaluate CO_{2ff} emissions from the plant. This thesis describes the development of a technique to assess CO_{2ff} using measurements of ^{14}C in tree rings and presents historic CO_{2ff} results for trees growing downwind of the point source. The results will be compared to reported emissions, analysed and interpreted using meteorological information. Tree ring results coupled with a model analysis will provide material for a later publication.

1.2   Research Process

1.2.1   Sample collection and measurement

Field work was carried out at the Kapuni site in Taranaki to assess trees for sampling that were considered to be likely to receive a signal from the Ballance and Vector Plants. Trees were sampled close to and downwind of the plant using an incremental corer and in a distant upwind location to represent clean background air. The counting, preparation and sampling of the tree cores was carried out by a summer student Marcus Trimble (Details of the trees and methodology is described in the methods chapter). Measurement of ^{14}C in a sequence of annual rings provides a historical record of $^{14}CO_2$ at the site which should capture a history of CO_{2ff} input from the Vector and Ballance plants. Cellulose was extracted from annual rings using the method established by the cellulose testing experiments, combusted, graphitised and the ^{14}C content measured using Accelerator mass spectrometry (AMS).

The first section of this thesis will compare the cellulose extraction method used at the Rafter Laboratory, GNS Science with a method used by the ANSTO laboratory for cellulose extraction for ^{14}C analysis in tree rings (Hua et al. 2000), and determine which to apply to the project samples. The initial experiment will test the Rafter and ANSTO cellulose methods on modern tree ring samples, known age wood and infinitely old "blank wood" and will establish a working method to use to prepare the rest of the tree ring samples. This will provide information on the suitability and effectiveness of cellulose method(s) for the laboratory and will form the basis of a methods publication.

1.2.2 Data analysis

The $^{14}CO_{2ff}$ record for the polluted trees was compared to reported emissions and the variability in CO_{2ff} analysed using meteorological information to assess the data for effects of variation in atmospheric transport.

1.2.3 Site information

The site chosen for the study is located in Kapuni, Taranaki NZ, 39.477° S, 174.1725° E 170 m.a.s.l. in a rural dairying area surrounded by pastureland with two closely located known sources of CO_{2ff} (Figure 2.2). There are little other sources of CO_{2ff} and the magnitude of emissions are well known, are testable by the method, there is plant material available and climate information for the site can be obtained and used to interpret the data in a qualitative manner. To compare the measured data with the reported emissions in a more absolute manner modelling work can be applied to estimate the dispersal of emissions from the plant.

1.2.4 Previous data for site

Previous data for $^{14}CO_2$ levels at the Kapuni gas processing plant have been obtained in a pilot study made in 2011–2012 (Turnbull et al. 2014). The study compared three different methods of collecting $^{14}CO_2$ samples to establish if the magnitude of the CO_{2ff} emissions from the plant could be estimated by measurements of $^{14}CO_2$ in the environment in a top down approach. Turnbull et al. (2014) found that the $\Delta^{14}C$ content in grass samples 600m downwind of the site contained 2–5 ppm of CO_{2ff} and a similar amount of added CO_{2ff} is anticipated in the tree ring samples. Levels of CO_2 downwind of the Vector plant at surface level can be enhanced by several ppm, since a 1ppm increase in CO_{2ff} results in a decrease of 2.6‰ $\Delta^{14}CO_2$ the technique should be applicable to tree ring cellulose and give similar results to the grass samples. The advantage in using tree cores rather than annual plant is that trees will contain a "time capsule" of historic of emissions from the plant, and will allow annual emissions from the last year right back through to the earliest tree ring available.

1.2.5   CO$_{2ff}$ sources

The CO$_{2ff}$ sources are discussed here. Vector operates a gas processing plant to process natural gas from onshore wells in Taranaki. The extracted gas has a high ~40% content of CO$_2$ which is removed during processing with a small proportion collected for industrial applications, but the majority is vented into the atmosphere resulting in emissions of approximately 3.3 kgC s^{-1} or 0.1Tg as C yr^{-1}, since 1970 (Table A6.6) (Turnbull et al. 2014). As the gas is fossil derived it is completely devoid of ^{14}C. The plant was expanded in 2003 and emissions increased significantly in the 2004–2007 period (Taranaki Regional Report 2013a).

The Ballance agri-nutrients ammonia urea plant is located 500m west of the Vector gas processing plant and was commissioned in 1982 to produce ammonia and urea using local methane gas as a feedstock and it is powered by natural gas from the Vector plant, emitting the resultant CO$_2$ to the atmosphere. Data available about CO$_{2ff}$ emissions from the plant includes annual emissions of CO$_{2ff}$ and tonnes of urea (Table 4.6). Reported emissions based on CO$_2$ data are ~0.05 Tg C yr^{-1} (Taranaki Regional Council 2013b). Emissions of CO$_{2ff}$ can be calculated independently using urea production statistics and a factor from urea lifecycle analysis (Ledgard et al. 2011). Calculation of emissions from urea data suggests emissions of ~0.06 Tg C yr^{-1} (Troy Baisden pers comm).

1.3   Determining CO$_{2ff}$ from Δ^{14}C measurements

A Lagrangian approach is used to assume atmospheric transport conditions, and allows the calculation of CO$_{2ff}$ without the use of an atmospheric transport model. The Lagrangian approach assumes that a parcel of air with a CO$_2$ concentration denoted by CO$_{2bg}$ and radiocarbon concentration Δ$_{bg}$ travels through a source of pollution which alters the radiocarbon and CO$_2$ concentration denoted by CO$_{2obs}$ and Δ$_{obs}$. This requires radiocarbon measurements at the background location Δ$_{bg}$ and the polluted location Δ$_{obs}$ and CO$_2$ concentration measurements at a suitable background. A mass balance equation is to calculate the mole fraction of CO$_{2ff}$ in the cellulose or air samples. The equation used by to calculate the mole fraction of CO$_{2ff}$ in the grass samples is given below (equation 1.1) (Levin et al. 2003, Turnbull et al. 2009, Turnbull et al. 2011a, Turnbull et al. 2014).

$$CO_{2\,ff} = \frac{C_{bg}\left(\Delta_{obs} - \Delta_{bg}\right)}{\Delta_{ff} - \Delta_{obs}} - \beta$$

Equation 1.1   Mass balance equation

In the above equation C_{bg} is the CO_2 concentration at a background location, Δ_{obs} is the ^{14}C content of the tree ring, and Δ_{bg} is the ^{14}C content of background. Δ_{ff} is a term used to denote the ^{14}C content of fossil fuel, and is defined as -1000‰. β is used as a term for correction.

Measurements of CO_2 concentration of background air is required for the CO_{2bg} variable in this equation. The CO_2 concentration data are obtained from the record of CO_2 concentrations measured at Baring Head (Brailsford et al. 2012, Stephens et al. 2013). We intended to use tree ring material from an Oak tree located 3km upwind of the Kapuni site (Kapuni Oak, Figure 2.2) to provide background measurements of $\Delta^{14}C$ for the background (Δ_{bg}) term of the mass balance equation. Although ^{14}C measurements from the Oak generally agreed with the Baring Head $^{14}CO_2$ record, early annual rings in the tree had rather variable agreement, and so the Baring Head $^{14}CO_2$ record was chosen instead for the background term instead. If the CO_2 concentration at a background location (C_{bg}), the ^{14}C content of the tree ring (Δ_{obs}) and Δ_{bg} are measured; then CO_{2ff} can be calculated, using the fact that the ^{14}C content of fossil fuel (Δ_{ff}) is -1000‰.

Beta (β) is a correction term to account for the fact that $\Delta^{14}C$ of CO_2 from other sources may be slightly different from the atmosphere and may include contributions from heterotrophic respiration, oceanic CO_2 sources and nuclear industry produced $^{14}CO_2$. These were considered by Turnbull et al. (2014) to be adequately accounted for in the background term so no additional correction was required. In this study we are using the same source and almost identical location, and have used the $^{14}CO_2$ record from Baring Head instead as the background term for calculating CO_{2ff}. Influences on the background at Baring Head and Taranaki are fairly similar and we make the assumption that any influence from other factors will be identical at both locations and therefore β to can be set to 0 for this study.

1.4 Background: Literature review

1.4.1 Changes in CO_2 concentration and anthropogenic influence

Measurements of CO_2 trapped in ice cores has revealed that the levels of carbon dioxide, methane and nitrous oxide measured today are higher now than any time in the past 800,000 years (IPCC 2013). Annual emissions from fossil fuel burning and cement manufacturing, estimated to be 9.9 ± 0.5 Gigatonne of Carbon (GTC) in 2013, are 61% larger than corresponding emissions in 1990 (Le Quéré et al. 2014). Other anthropogenic activities that result in CO_2 releases are land-use change; deforestation and land clearing for economic or agricultural activities. Since preindustrial times on a cumulative basis the contribution from these activities is 70% from fossil fuel burning and 30% from land use change (Le Quéré et al. 2014). Although there is a recent downward trend in emissions from land use change, CO_2 emissions from fossil fuel burning shows no abatement (Le Quéré et al. 2014). Release of carbon dioxide emissions has resulted in a current global average atmospheric concentration of 398.28 ppm, and this is currently increasing by 2.43 ± 0.09 ppm per year (Dlugokencky and Tans 2014).

CO_2 displays a large seasonal and diurnal variability which is caused by uptake by photosynthetic activity by vegetation during daylight hours in the growing season. This cycle is reversed in autumn when photosynthesis slows down and respiration by heterotrophic and autotrophic organisms that release CO_2 is more dominant. Carbon dioxide also varies on a spatial basis, the majority of fossil fuel CO_2 emissions are made in the Northern hemisphere; this creates plumes of CO_2 that are depleted in ^{14}C concentrated around large urban or industrial sources, (Randerson et al. 2002, Levin et al. 2003, Turnbull et al. 2006, Turnbull et al. 2009). The plumes are transported by air masses so that CO_2 becomes well mixed globally in a space of a year, however on a regional basis CO_2 can vary greatly (Nisbet and Weiss 2010). In the southern hemisphere CO_2 is characterised by latitudinal gradients of ^{14}C because of interaction with the ocean sink, which releases re-entrained CO_2 from deep ocean water that has less ^{14}C than the atmosphere (Braziunas et al. 1995, Levin and Hesshaimer 2000).

Emissions of CO_2 are partially offset by uptake of CO_2 by land and ocean based sinks. Continued emissions have resulted in perturbation of the carbon cycle with much more carbon being taken up by the atmosphere, terrestrial biosphere and oceans than would have naturally occurred (Ballentyne et al. 2012). Approximately equal amounts of anthropogenic CO_2 are absorbed by oceans 25% and about 30% by land sinks with the remaining 45% remaining in the atmosphere (Friedlingstein et al. 2010, Le Quéré et al. 2014).

The oceans absorb 90% of the increase in energy in the climate system (IPCC 2013). Addition of CO_2 to the ocean is causing warmer oceans, rising sea levels, and less sea ice. It also increases the acidification of the oceans through uptake of CO_2 which perturbs the bicarbonate chemistry leading to a decrease in pH (Bates et al. 2012). Warmer oceans will cause rising sea levels through thermal expansion, and a decrease in the extent of sea ice. An increase to sea level of 0.19m ±0.02 from 1900–2010 has been reported mostly as a result of thermal expansion and melting of glaciers and is predicted to increase further (Church et al. 2013). Predicted future rises in sea level will not be uniform across the globe and will affect some regions disproportionately (Lyu et al. 2014). The ocean sink has absorbed more CO_2 in response to increasing emissions but the extent of long term change to the ocean sink is not clear with difficulties in disentangling trends from model analysis (Keller et al. 2014, Le Quéré et al. 2014, Sitch et al. 2015).

Estimates of net flux from land use change and land cover (LULCC) emissions account for the largest uncertainty in the global carbon budget. It is calculated from models that incorporate satellite data that shows land cover, fires and statistics (Houghton et al. 2012). Land use change data is subject to large uncertainties as it is inferred from modelled information and is affected by the inter-annual variability of uptake by other sinks. There is evidence that emissions from deforestation and land use change have been declining since 2000's through a slowing of deforestation (Le Quéré et al. 2014).

Reported increases in greenhouse gases will result in climate change (even if no further CO_2 emissions are made) through to the next century and beyond (IPCC 2013). The resulting climate change will have a forcing effect resulting in further increases to CO_2 concentrations and other changes; warmer oceans and air temperature, less snow and

ice and more CO_2 in the atmosphere. At the current rate of emissions under the business as usual scenario estimates of possible warming generated by the IPCCC indicate warming by an average of 4 °C by 2100 (IPCC 2013). This level of warming will likely invoke critical irreversible climate impacts such as; loss of ocean life due to acidification, loss of sea ice and sea level rise leading to inundation of coastal areas, and changes of ocean and atmosphere circulation patterns, failure of agriculture due to extreme weather patterns, with resulting severe economic impacts (Solomon et al. 2009, Smith et al. 2009).

1.5   Mitigation of greenhouse gases

Global concerns about the rate of increase and concentration of greenhouse gases coupled with indications of climate radiative forcing has prompted actions by world governments. Various policies have been implemented to reduce and monitor emissions. Agencies that monitor the emissions and effectiveness of climate change mitigation include Intergovernmental Panel on Climate Change (IPCC). The IPCC established by the WMO and UNEP in 1988 is the leading authority for assessment of climate change. The IPCC does not conduct its own research but assesses the latest findings from scientific, technical, and socioeconomic research and produces synthesis reports that summarises current knowledge on climate change. The reports include the latest climate research, and predicted impacts on climate. The latest report, AR5, includes projections based on Representative Concentration Pathways (RCPs); these cover a range of scenarios for predicted climate change based on different levels of greenhouse gas emissions.

1.5.1   International treaties

The United Nations Framework Convention on Climate Change (UNFCCC) has the ultimate objective of "stabilisation of greenhouse gas concentrations in the atmosphere at a level that would prevent dangerous anthropogenic interference with the climate system."(UNFCC 1992) To strengthen the original UNFCC agreement the Kyoto protocol was formed after the third conference of parties (COP3) to the UNFCCC in 1997. Whereas the UNFCCC convention encouraged countries to reduce their greenhouse gas emissions the Kyoto protocol legally commits members to adhere to internationally

binding emission reduction targets. There are two commitment periods in the Kyoto protocol 2008–2012 and 2013–2020 usually relative to the base year 1990. Since the inception of the Kyoto protocol other international agreements have been added. The Copenhagen accord in 2009 created an agreement for signatory countries to stabilise the levels of greenhouse gases to limit warming to no more than 2 °C average above preindustrial levels (UNFCCC 2009, 2010).

Despite the Kyoto protocol growth in CO_2 emissions remains strong (Peters et al. 2013). To achieve the 2 °C target requires large and sustained emission reductions. It is complicated to calculate the size of emissions reductions required because the levels of warming created by greenhouse gas emissions are poorly understood because of uncertainties in the understanding of the carbon cycle (Meinhausen et al. 2009). A useful metric used to calculate future warming scenarios is cumulative emissions, and works on the principle that global temperature change is intimately and more robustly linked to estimates of cumulative emissions (Allen et al. 2009, Matthews et al. 2012). The calculated cumulative emissions of CO_2 linked to the 2°C degree limit is one trillion tonnes of carbon (3.67 trillion tones of CO_2) (Allen et al. 2009). It is recognised that two-thirds of the quota of carbon emissions have already been released (Friedlingstein et al. 2014, Le Quéré et al. 2014) and that not all remaining carbon reserves can be combusted (Meinhausen et al. 2009). Achieving the 2°C target requires reductions of emissions by about 5% per year with future stabilisation of emissions by introducing negative carbon emissions through introduction of carbon capture and storage and bioenergy technology (Fuss et al. 2004, Raupach et al. 2014).

1.5.2 Reporting of emissions

A mandatory requirement of the Kyoto protocol requires parties to keep a national registry to track and record their fossil emissions. These are reported to the UNFCCC where an independent record is kept. Presently the method in which emissions are estimated is by a bottom up approach using guidelines for calculating greenhouse gas inventories produced by the IPCC Guidelines for National Greenhouse Gas Inventories (IPCC 2006). Fossil emission estimates are calculated from energy data using statistics on fuel production and consumption utilising coal, gas and fuel sales data and transport patterns rather than measured values. Data is calculated by emitters and reported to

central Governments and then to the UNFCCC. Emissions are known reasonably accurately in developed countries but with large uncertainties in developing countries e.g. ± 10% in China (Gregg et al. 2008, Le Quéré et al. 2014). When there is a combination of very large emissions with a corresponding large uncertainty the actual size range of the calculated emissions can vary by a huge amount. Guan et al. (2012) report that China's emissions vary by 18% when using two approaches that should give the same result, the inconsistencies mainly arise from differences in coal consumption statistics. The 18% uncertainty is equivalent to 1.4 billion tonnes of CO_2 (Marland et al. 2012). It is also important to consider who is responsible for the emissions. The strong growth in recent CO_2 emissions is linked to economic growth in developing countries (Davis and Caldeira 2010, Peters et al. 2011). From 1990–2008 there has been a large shift in emissions from the traditional carbon emitters in Annexe B countries to developing Annexe A countries (Peters et al. 2011, Le Quéré et al. 2014). A large proportion of emissions in developing countries is attributable to the production of goods destined for western countries (Davis and Caldeira 2010, Peters et al. 2011).

1.5.3 Verification of emissions

Another requirement of the Kyoto protocol is the independent verification of emissions reporting (Tans et al. 1999, Weiss and Prinn 2011, Levin et al. 2011). In principle the approach used to quantify anthropogenic emissions is a combination of "top down" atmospheric concentration measurements and modelling which attempt to map and quantify the airborne fraction of CO_2. This is difficult because anthropogenic emissions of CO_2 are partitioned between the atmosphere, oceans and biosphere and there are large uncertainties in calculation of the exact fluxes into each reservoir, and the anthropogenic signal needs to be separated from natural sources of CO_2. Improvement in the coverage of measurement stations and improved models would reduce some of the uncertainty and help to meet the target of verifying emissions (Weiss and Prinn 2011).

Currently it is difficult to assess whether member countries are meeting their obligations to the Kyoto protocol because the sizes of reductions are smaller than the uncertainties of regional top down/bottom up estimates (Levin et al. 2011, Weiss and Prinn 2011). It may be easier to calculate the anthropogenic contribution to CO_2 concentrations

through a combination of monitoring fluxes of $\Delta^{14}CO_2$ concentration on a regional basis over an extended period of time and assessing change as trends (Levin and Rödenbeck 2007).

1.5.4   Methods to determine the airborne fraction of CO_2

Observations of the climate system including monitoring of atmospheric greenhouse gases is carried out by performing concentration measurements using a variety of methods/platforms (Meijer et al. 1995, Levin et al. 2010, Graven et al. 2012). These include ground based monitoring stations, aircraft and satellite measurements. Fluxes of greenhouse gases are then evaluated using models.

Emissions of greenhouse gases that have only anthropogenic origins e.g. chlorofluorocarbon gases (CFC's) can be quantified in a straightforward manner by making atmospheric measurements at well mixed background sites by comparing fluxes with reported emissions. However CFCs cannot be determined on local or regional scales because the mixing ratio is not well known (Miller et al. 2008, Prinn et al. 2000). Gases that have anthropogenic and natural origins and sinks such as CH_4, CO and CO_2 are more problematic but can be determined from concentration measurements alone providing the signal is large relative to variability in the background (Loh et al. 2009, Turnbull et al. 2011b, Turnbull et al. 2014).

Fluxes of CO_{2ff} can be quantified by comparing with known emissions of another anthropogenic emitted gas such as the radon isotope ^{222}Rn (Nisbet and Weiss 2010) or sulfur hexafluoride SF_6 (Turnbull et al. 2006). Global total emissions of SF_6 are known but local emissions are poorly known and are not co-located with CO_{2ff} emissions at the local scale. This approach is effective only if the emissions of the other gases are well-known, for instance ^{222}Rn is well known in a few places but not others.

There has been some use of tracers to estimate CO_{2ff} such as CO, (Turnbull et al. 2006, Vogel et al. 2010, Van der Laan et al. 2010). In these methods the aim is to measure the concentration of a more easily measured trace gas e.g. CO and if the emission ratio of CO/CO_{2ff} is known then the CO_{2ff} can be calculated (Vogel et al. 2010, Turnbull et al. 2011a Turnbull et al. 2011b). However this approach is only suitable where fossil fuel ratio to tracer gas is well known, potential variations in the ratio can be assessed and it

needs to be directly associated with the combustion of the fossil fuel (Vogel et al. 2010, Turnbull et al. 2014). This method is not applicable in this study where the only significant emitted gas is CO_2. Here emissions of CO_{2ff} will be measured by using a tracer ^{14}C which allows us to differentiate between emissions of anthropogenic CO_{2ff} and biogenic CO_2.

1.5.5 Determination of recently added CO_{2ff} in CO_2

It is possible to assess the anthropogenic contribution to the concentration of CO_2 by utilising measurements of the ^{14}C content of CO_2 which is the most direct way to quantify added CO_{2ff} (e.g. Meijer et al. 1996, Hsueh et al. 2007, Levin and Karstens 2007, Levin and Rödenbeck 2007, Levin et al. 2008, Palstra et al. 2008, Turnbull et al. 2009, Turnbull et al. 2011a). Air samples are collected either in flasks or by absorption over NaOH, the CO_2 is subsequently evolved in the laboratory and collected cryogenically before being converted into graphite for measurement of ^{14}C. In practice measurements of ^{14}C are combined with measurements of CO_2 concentration in air samples to determine the proportion or "fraction" of fossil fuel component of carbon dioxide. As fossil emissions contain no radiocarbon (Δ_{ff} = -1000‰) they can be distinguished easily from other sources of CO_2 such as heterotrophic respiration, biomass burning and plant respiration, which have radiocarbon content similar to atmospheric CO_2 currently at $\Delta^{14}C$ ~28 ‰ (Figure 1.1).

1.6 Radiocarbon

There are 3 isotopes of carbon, two of which are stable ^{13}C and ^{12}C and one unstable rare naturally occurring radioactive isotope ^{14}C. ^{12}C makes up about 98.89% of the total, there are much smaller amounts of ^{13}C (1.11%). ^{14}C forms only a very small portion of the total pool of carbon in the carbon reservoir, approximately 1×10^{-12} atoms in the atmosphere (Stuiver and Polach 1977). ^{14}C is unstable and decays to release a β particle and forms ^{14}N. ^{14}C is produced in the stratosphere by the bombardment of nitrogen atoms by cosmic ray produced neutrons (equation 1.2).

$$n + {}^{14}N + {}^{14}C + p$$
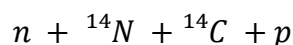
Equation 1.2   Production of ^{14}C in the atmosphere

Once the ^{14}C is produced it is quickly oxidised to form CO_2. The CO_2 produced is distributed throughout the atmosphere and it becomes partitioned between the atmosphere, the terrestrial biosphere and the ocean. ^{14}C is incorporated into plants by photosynthesis and animals by the ingestion of plants or other animals. While the plants or animals are alive they exchange carbon with their surroundings so that they remain in equilibrium with the biosphere. After death incorporation of ^{14}C ceases and because ^{14}C is unstable it decays to form nitrogen with the emission of a beta particle. Radiocarbon atoms have a half-life which has been calculated as 5730 years (Godwin 1962).

1.6.1 Reporting ^{14}C.

$F^{14}C$ and $\Delta^{14}C$ are notations that are used for reporting the ^{14}C content of a sample in common usage in radiocarbon literature (Stuiver and Polach 1977, Reimer et al. 2004). They reflect the ratio of the abundance of ^{14}C atoms compared to ^{12}C atoms in a sample versus the ratio of abundance of ^{14}C compared to ^{12}C in an oxalic acid standard, the deviation is expressed in parts per thousand ‰ after correction for isotopic fractionation. The oxalic acid standard NIST Oxalic I has a known activity.

$$\Delta^{14}C = \left(\frac{Asn\ e^{\lambda c(1950-x)}}{Aon} - 1\right).1000‰.$$

Equation 1.3   Calculation of $\Delta^{14}C$

Asn is the activity of sample, and Aabs is the activity of the standard, and y is the year of measurement, x is the year of formation or growth, and λc is the (1/8267) years^{-1} the mean half-life of ^{14}C. Δ and $\Delta^{14}C$ are comparable if measurement takes place in the same year as the sample was formed.

Fraction modern $F^{14}C$

$$F^{14}C = \frac{Asn}{Aon}$$

Equation 1.4   Calculation of Fraction Modern $F^{14}C$

A correction for decay not necessary as long as sample and standard are measured at the same time. Asn is the activity of sample, and Aon is activity of oxalic standard. Fraction modern $F^{14}C$ is not corrected for decay as it is based on a ratio of activity of

sample and standard. The ratio is of absolute activities of the sample and standard, therefore decay correction is unnecessary (Reimer et al. 2004).

1.6.2   Correction for Isotopic fractionation

Isotopic fraction needs to be taken into account in radiocarbon measurements to account for any changes in ^{14}C in a sample from the atmosphere during formation, combustion or conversion into graphite in the laboratory, it also allows the ^{14}C content of different sorts of material to be compared directly e.g. ^{14}C in atmosphere can be compared to ^{14}C in wood cellulose or cellulose ^{14}C can be compared to the oxalic acid standard. The isotopic correction applied is called normalisation it is applied to both the sample and standard. It is expressed as $\delta^{13}C$ and it is a deviation of the abundance of ^{13}C to ^{12}C atoms in the sample relative to the same ratio in a limestone standard usually VDPB Vienna Pee Dee Belenmite. The CO_2 for the standard is prepared using the limestone standard and the scale is called the PDB scale.

$$\delta^{13}\,C = \frac{{^{C^{13}}/_{C^{12}}\ sample - {^{C^{13}}/_{C^{12}}\ standard}}}{{^{C^{13}}/_{C^{12}}\ standard}} \times 1000\ ‰$$

Equation 1.5   Correction for isotopic fractionation

For cellulose analysis in tree rings it is necessary to correct for fractionation caused during uptake of ^{14}C during photosynthesis, because the ^{12}C is absorbed relatively more easily by the plant than ^{13}C and ^{14}C, from atmospheric CO_2 so plants become depleted with respect to atmospheric $\delta^{13}C$.

1.6.3   Addition of ^{14}C to the atmosphere by atmospheric nuclear testing

Atmospheric nuclear weapon testing in the 1950s and 1960s generated large amounts of ^{14}C (Currie et al. 2011, Figure 1.1). The ^{14}C produced oxidised to $^{14}CO_2$ in the atmosphere and entered the carbon cycle in exactly the same way as naturally produced ^{14}C. Bomb $^{14}CO_2$ that entered the carbon cycle became a useful tool that has enabled researchers to understand more about atmospheric circulation and exchange of CO_2 between the oceans and terrestrial biosphere e.g. (Broecker et al. 1985, Nydal and Gislefoss 1996, Trumbore 2000, Gaudinski et al. 2009, Hua et al. 2013). The $^{14}CO_2$ concentration reached a peak in the southern hemisphere in 1965 (Hua et al. 2012,

Currie et al. 2011). In 1963 the nuclear test ban treaty was signed and atmospheric nuclear testing was halted except for France and China who continued testing until 1968 and 1980 respectively (Nydal and Gislefoss 1996). Since this time the concentration of atmospheric $^{14}CO_2$ has rapidly declined due to exchange between atmosphere, oceans and biosphere (Nydal and Lövseth 1983, Levin and Hesshaimer 2000, Hua et al. 2013). In the recent atmosphere the Suess effect from fossil fuel combustion has been dominant (Turnbull et al. 2011b).

1.6.4   Baring Head atmospheric record

Baring Head atmospheric record $^{14}CO_2$ data
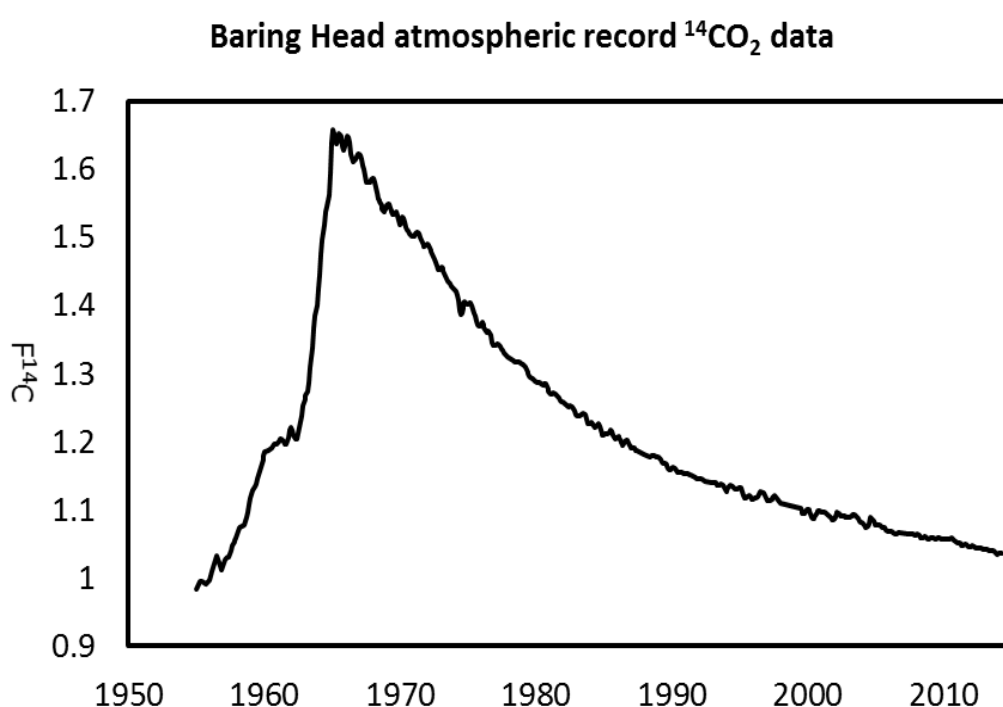
Figure 1.1   Smoothed $^{14}CO_2$ record from Baring Head Wellington New Zealand

Measurements of $^{14}CO_2$ from air samples collected at Wellington New Zealand from December 1954 until the present day are presented in Figure 1.1. The record consists of measurements of 100's of samples collected at regular intervals by GNS Science and NIWA scientists and is the longest record of tropospheric $\Delta^{14}CO_2$ in the world (Currie et al. 2011). The plot shows that levels of $^{14}CO_2$ increased by two thirds to a peak in 1966 as a result of input of ^{14}C from nuclear testing.

The current dataset has been revised and updated using high precision AMS measurements (Turnbull et al. 2015) from the original data set produced by (Rafter 1955, Rafter and Fergusson 1957, Manning et al. 1990, Currie et al. 2011). CO_2 extracted

from air was collected by static absorption over a NaOH solution for several weeks. CO_2 is evolved from the NaOH solution and trapped cryogenically and the ^{14}C content measured, details of methodology are found in Currie et al. (2011). In the early part of the Baring Head $^{14}CO_2$ record ^{14}C was quantified by gas proportional counting which measures disintegration of β particles, and after May 1995 measurements were made by counting of the number of $^{14}C/^{12}C$ atoms using AMS. Early measurements were made in the infancy of radiocarbon and the measurements were subject to large variations due to measurement uncertainties, high variability of ^{14}C around the peak of the bomb curve and sparse measurements in some years.

1.6.5   Use of radiocarbon in plant material

The use of radiocarbon measurements in plant materials to monitor the anthropogenic emissions of CO_{2ff} has been utilised by several researchers. Plants assimilate carbon from their environment during photosynthesis and reflect changes in radiocarbon in the atmosphere. Palstra et al. (2008) used radiocarbon measurements in wine ethanol, Hsueh et al. (2007) used corn leaves, Rakowski et al. (2013) tree rings, and Turnbull et al. (2014) have used grass to study effects of fossil fuel emissions in surface air either at a local, regional or continental scale. Plants growing close to sources of CO_{2ff} or in areas where recently added CO_{2ff} emissions were present had lower levels of $\Delta^{14}C$. The advantage of using plants over conventional collection methods (air flasks, tower or sodium hydroxide samplers) is that plant materials can be easily collected over wide geographic areas and thus provide a snapshot of emissions at those locations in a less labour intensive and cost effective manner than conventional methods and they allow retrospective sampling. Collection of plant materials avoids the capital outlay and setup of field equipment but still requires similar amounts of sample processing in the laboratory.

The disadvantage of using annual plants is that the sampling period cannot be controlled as plants effectively only sample air during daytime conditions averaged over the growing season and sites need to re visited at least on annual basis to accumulate a record of emissions through time. During the hours of darkness photosynthesis ceases and is replaced by respiration, which recirculates some CO_2. Plants sample the air in daylight hours when the planetary boundary layer is well mixed (Hsueh et al. 2007),

therefore plant sampling represents daytime $^{14}CO_2$ levels integrated over the growing season. The actual uptake of $^{14}CO_2$ is affected by variables in meteorology, atmospheric transport, interaction with the local biosphere and the actual rate of photosynthetic uptake (Palstra et al. 2008, Bozhinova et al. 2013). Bozhinova et al. (2013) suggests that measuring the growth period of plants would improve usefulness of this technique.

1.6.6   Applications of tree rings in environmental studies

Tree rings have been used extensively in paleoclimate studies because they reliably sample the environment they are growing in thus provide a past history of atmospheric conditions, climate, temperature, and rainfall. By sampling wood from living trees and creating chronologies that can be linked by matching patterns in rings of living trees with overlapping rings present in dead trees a fixed chronology is established that can extend thousands of years (Briffa 2000). It is possible to deduce a certain amount of environmental information from trees (temperature and rainfall and storm events) by examination of rings widths and statistical analysis alone (Fritts 1976). Analysis of wood, usually utilising the cellulose fraction from tree rings can provide detailed information on past meteorological conditions e.g. (Wilson and Grinsted (1977), Leavitt and Danzer (1993), Hoper et al. (1998), Loader et al. (2003), Harlow et al. (2006). Chronologies using long lived bristlecone pines have been used to calibrate the radiocarbon timescale (Suess 1970, Becker 1993, Stuiver and Pearson 1993, Hogg et al. 2013). Tree ring material has been used by to monitor levels of anthropogenic emissions in an urban area (Rakowski et al. 2011, 2013). Hua et al. (2000, 2004, 2013) have used tree rings to measure the global distribution of radiocarbon after the bomb spike.

1.6.7 Tree types used in this study

The two types of trees used in this study are angiosperms and gymnosperms, angiosperms are commonly called hardwood or deciduous trees, and gymnosperms are commonly called softwood or conifers. Angiosperm means "hidden seed" and bear their seeds inside a fruit or flower. Other characteristics of angiosperms are that they are broadleaved and deciduous, and they have a much greater capacity to transport water than gymnosperms examples include Oak, and chestnut. Gymnosperm means "naked seed" and they do not have flowers and instead spread their seeds into the wind, often in a cone. Gymnosperms have compact leaves or needles that are usually retained during winter, examples include pine and kauri.

1.6.8 Annual ring formation

All trees produce fresh growth every year starting in spring. Woody plants possess a layer called cambium that allows tree to grow upwards and expand in girth. Beneath the bark cells in the cambium divide and produce new cells called xylem. The xylem produced in spring are large with thin walls which enable large amounts of water to be transported up the tree to the leaves to support growth. In autumn the cambium makes xylem that has narrower thicker walls as the tree needs less water but it is also enables the tree to make strong dense wood to support the new spring growth of the following year. In this way annual growth consists of large celled early-wood and smaller denser late-wood visible as annual ring.

In angiosperm trees one annual ring consists of early-wood that has large diameter vessels and late-wood that consists of thick walled small diameter vessels, with the rings characterised by the changes in diameter rather than changes in colour. The large vessels are particularly visible in ring porous species like Oak which produce these cells at the beginning of the growing season before leaves appear. The tree likely uses stored photosynthetic products to do this (Hill et al. 1995, Switsur et al. 1995, McCarroll and Loader 2004), and this trait is suggested as the reason that ring porous trees do not produce locally absent rings (Speer 2010).
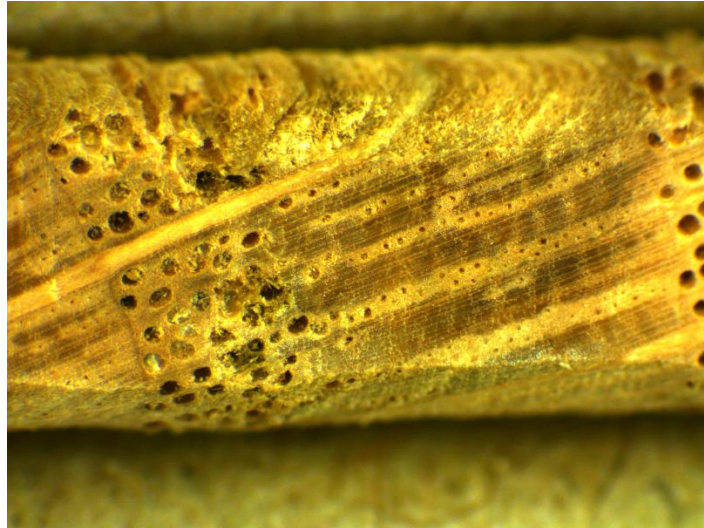
Figure 1.2   Oak tree core image annual ring boundary
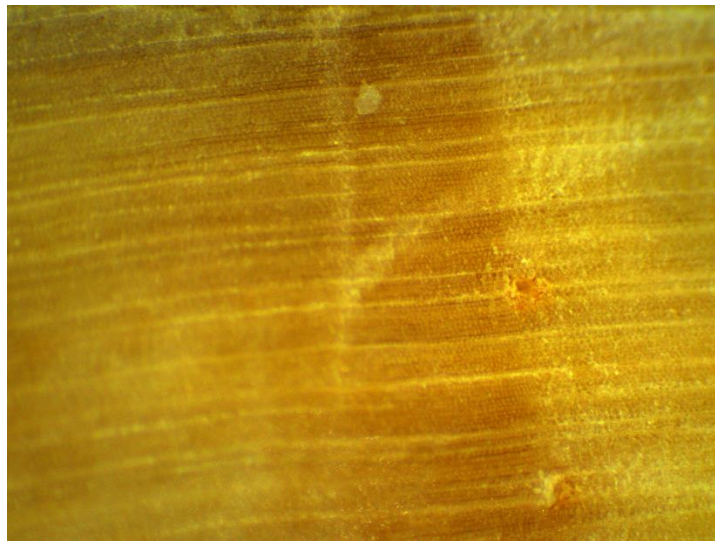
Figure 1.3   Monterey pine image annual ring boundary.

In gymnosperm trees cells do not have such a marked difference in size of cells between early and late-wood. Annual rings of gymnosperms like pine trees have a banded colour appearance, characterised by pale coloured early-wood with thin walled large diameter cells and dark coloured late-wood with thick walled small diameter cells.

Occasionally under stressful conditions trees can produce a false ring or, intrannual growth bands or conversely fail to produce a growth ring for a particular year. This is called locally absent, partial or missing rings (Fritts 1976, Hoffer and Tardif 2009, Speer 2010). Locally absent or missing rings are particularly rare in Oak (Baillie 1973, English Heritage 1998, Haneca et al. 2009). The presence or absence of rings makes the interpretation of ring counting problematic but the collection and analysis of more than

one core from the same tree or from trees nearby can help resolve the patterns as the same climatic effects will likely be reflected as the same patterns by other trees.

1.6.9 Radiocarbon measurements of tree rings

In order to obtain a radiocarbon measurement on an annual tree ring, the tree ring material must be separated into individual growth rings. This can be achieved by either taking material from a slice of wood or "biscuit" from a felled tree or in this study by taking a small core from the trunk of a living tree with an incremental coring device. The Haglöf coring device allows the removal of a pencil sized core of wood approximately 400mm long in one continuous piece without causing serious damage to the tree. Several cores are removed from each tree for comparison and are prepared to observe the rings. The process of correlation involves observing patterns of varying ring widths and cross-matching these with the other cores. Analysis of the rings in this way establishes a correlation and avoids the false interpretation of the number of rings present. If the outermost ring is present and collection date or year of felling is known then the last ring can be assigned to a fixed calendar year. The rings are counted backwards from the bark starting with the most recent ring and are marked with pins every decade, 50 then 100-years using a standard convention and separated into annual increments for analysis. Some trees sampled proved to be unusable for dendrochronology because the correlation was inconsistent.

In this study a whole annual ring is used for analysis of cellulose, but an assumption is made that growth occurs principally during the spring and summer months September through April then slows down or halts completely in autumn and winter. This is a reasonable assumption to make for angiosperms that lose their leaves but may be a poorer assumption for gymnosperms which continue to photosynthesise all year round if the temperature and sunlight permit (Barnett 1973, Striebly 2013). CO_2 concentration data is averaged using the same time period September to April the assumed sampling period by the tree. An entire annual ring is used to try to gain an "annual average" of the emissions, and in this way we hope to average out any biases created by recycling of nutrients by the tree such as starch in the early part of the season in order to create new wood growth, although this recycling of nutrients should only apply to Oak trees in this study (Hill et al. 1995, Mc Carroll and Loader 2004, Rocha et al. 2006). Cellulose is

the target material in the wood for analysis because it is considered the most reliable fraction in wood, and is directly related to formation of glucose by the tree during photosynthesis (Park and Epstein 1961). Once cellulose is formed there is no further exchange of carbon with the atmosphere, moreover the cellulose component reflects the ^{14}C assimilated by the plant during photosynthesis, unlike the formation of lignin and starch which take place after cellulose has been formed (Fritts 1976). In the laboratory the process of cellulose extraction aims to remove all other wood components particularly mobile components such as resins and lignin laid down after cellulose is formed which can have a different ^{14}C value to cellulose, to leave a relatively pure cellulose component usually defined as alfa cellulose α and refers to the components of cellulosic material that are insoluble in 17.5%w/v sodium hydroxide solution at 20°C (Anchukatitis et al. 2008). However the use of the term α cellulose tends to be applied to the final product of cellulose extraction regardless of the strength of alkali used after bleaching.

1.7   Outline of this thesis

Chapter 2 Methods: details tree sampling and tree core sample preparation, cellulose extraction methodology, combustion and radiocarbon measurement. The methods include the data collected and used and a description of the process of calculating CO_{2ff} calculations using the ^{14}C data and uncertainties. Statistical methods used to assess the measurements are described.

Chapter 3 Cellulose testing: Chapter three is divided into background information on the structure and composition of wood including a description of the development of cellulose extraction methods for stable isotope and radiocarbon analysis and describes and considers alternative cellulose extraction methods. The second part of the chapter describes cellulose experiment aims and methodology used to analyse and assess the efficacy of the methods. Results for the comparisons are presented with analysis, discussion and conclusions about the method to be used for the Kapuni tree ring samples.

Chapter 4 Tree ring results: presents ^{14}C results for all the trees sampled for the project with analysis of the results. The chapter describes the process of establishing a 'tree ring

method' by comparing agreement of the background Baring Head tree with the $^{14}CO_2$ record, and background Kapuni Oak tree at Taranaki. The tree ring method is then applied to the polluted trees and ^{14}C and CO_{2ff} results for the polluted trees are presented, compared with reported emissions and analysed using meteorological data. Results of the analysis are discussed and conclusions presented.

Appendices: Part 1: Tree sample correlation documents for the trees used for the project. Part 2: CO_{2ff} data from Luscombe chestnut and Vector pine trees. Also tables of $^{14}CO_2$ and CO_2 concentration data used to make the CO_{2ff} calculations, and Vector emissions data.

2.0   Methods

2.1   Collection of tree cores

2.1.1   Polluted locations: Kapuni Vector plant

Trees were selected for sampling based on three criteria; their age, species, and their relative location from the Vector and Ballance site. Six trees were sampled a short distance from the CO_{2ff} sources, but approximately half were not able to be used because the tree cores proved unsuitable for dendrochronology. Two trees growing close to the site provided tree cores that were able to be counted and correlated with a reasonable degree of confidence are described here. A Monterey pine (*Pinus radiata),* (referred to in the text as Vector pine) was sampled ~250m from the Vector plant stacks in a primary downwind direction and a chestnut tree (either a Chinese or sweet chestnut referred to in the text as Luscombe Chestnut) located ~850m away in a secondary down-wind direction (Figures 2.1 and 2.2).

2.1.2   Background location; Kapuni

A control sample was taken from an Oak tree (species unidentified) referred to in the test as Kapuni background Oak >3 kilometres distance upwind of the plant. The background Oak was selected to provide a local background tree for Taranaki that would see similar conditions to the polluted trees but with no influence from CO_{2ff} from the Vector or Ballance plant (Figure 2.3).
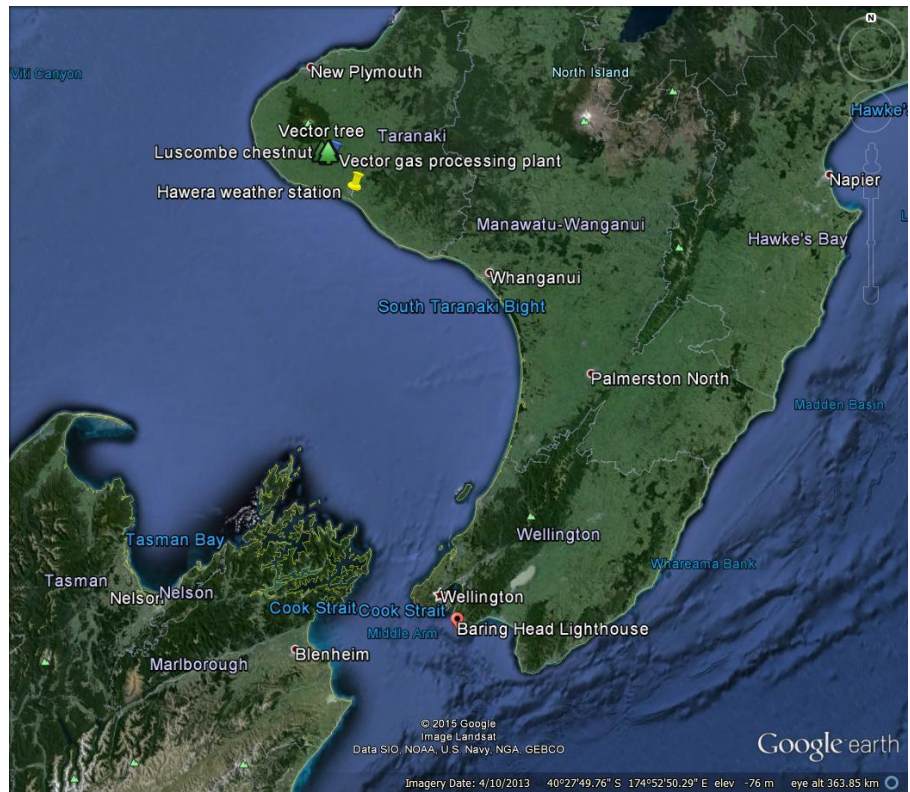
Figure 2.1   Map of North Island, New Zealand with location of Kapuni site trees and Baring Head clean air monitoring site.
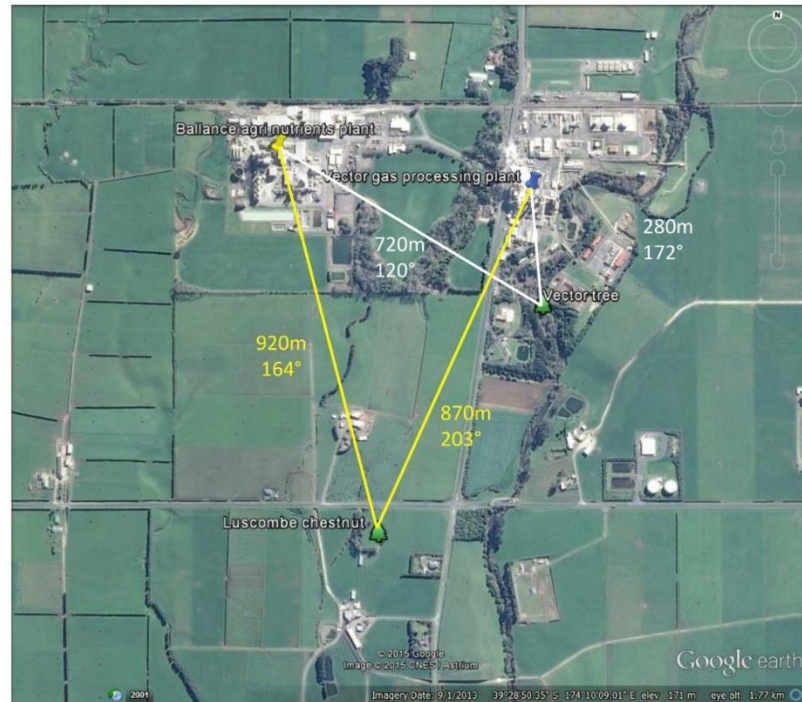
Figure 2.2   Map of Kapuni site with location of Ballance and Vector gas processing plant indicated and location of trees.
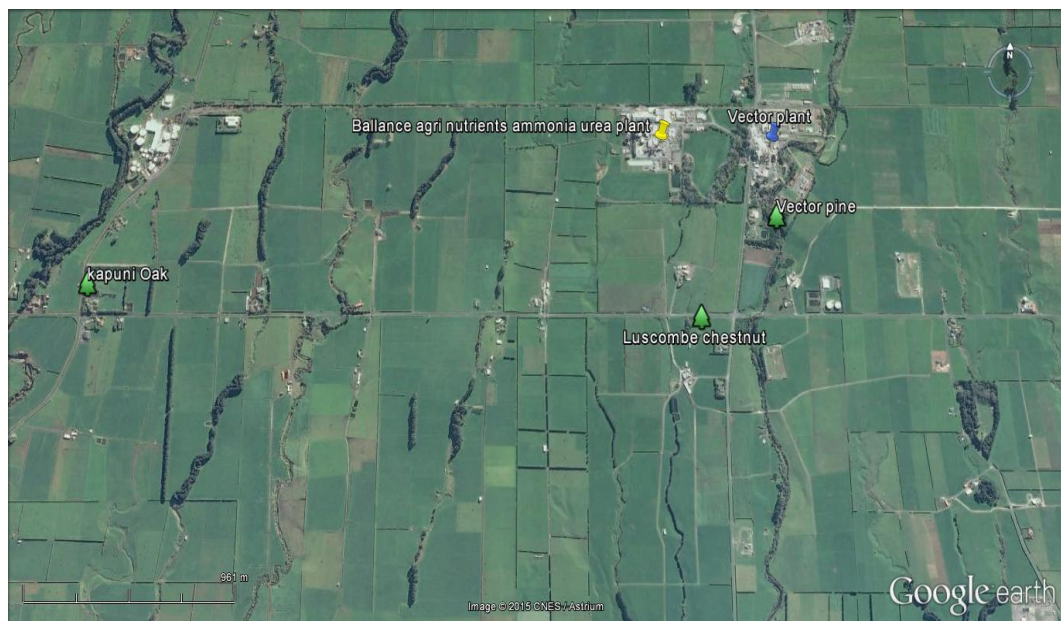
Figure 2.3   Location Kapuni Oak, Taranaki.

2.1.3   Background Location; Baring Head tree

In order to establish that tree ring ^{14}C directly reflects local atmosphere, a pine Pinus radiata (referred to as Baring Head tree) was sampled at Baring Head, Wellington, NZ

41.4167° S, 174.8667°E at the same site used for the collection of air samples for the long term Baring Head atmospheric $^{14}CO_2$ record (Figure 2.4).
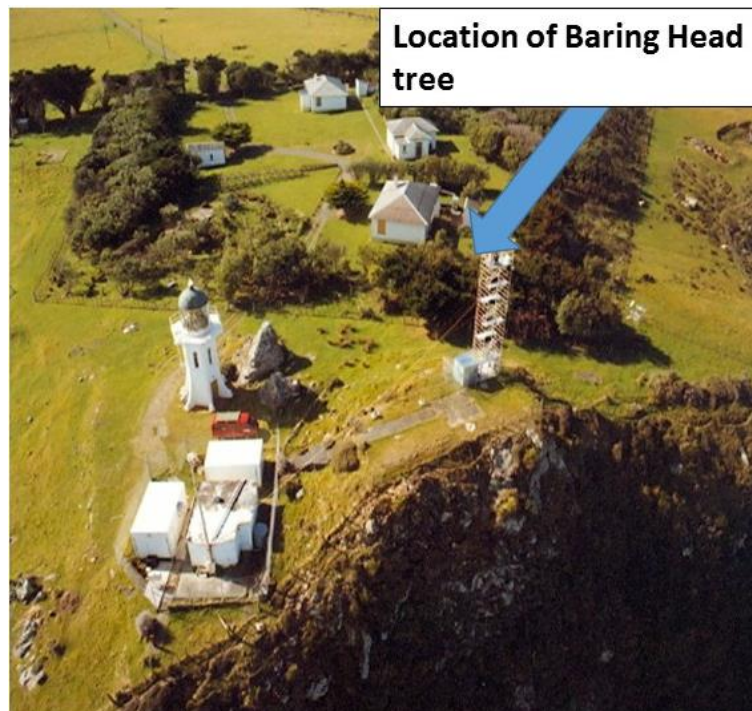
Figure 2.4 Location of Baring Head tree, Baring Head Wellington.

2.2   Sampling strategy and core preparation

Sampled trees were photographed and their coordinates recorded using GPS. The tree species was identified and particulars about location, surroundings were recorded. The tree diameter at breast height was measured using dendrochronology measuring tape and several cores taken at approximately equidistant points around the trunk from the same tree to ensure that the centre of the tree was sampled. Sampling at multiple points has several advantages, if the tree has any rot in one place it or if the core breaks and parts are lost or it proves unusable the laboratory has spare material to obtain a sample from. Having multiple cores also helps to pinpoint any inconsistencies in the rings such as false or missing rings that could cause errors in the counting process.

The cores were sampled with a Haglöf increment borer. The increment borer is a specialised piece of equipment that allows the sampling of a core of wood tissue approximately 5mm in diameter from a living tree with minimal damage. Depending on the size of the tree being sampled either a 400 or 600mm length corer was chosen to reach the pith of the tree. The corer tip is pressed into the bark then the borer screwed

fully into the trunk by the operator until the desired depth has been reached. The tree core is removed by rotating the corer one half turn and withdrawing the core by means of a long metal spatula inserted inside the coring instrument. The fresh cores were inserted into plastic drinking straws taped together to make a storage container and labelled with the sample identifier. Not all trees sampled were old enough to pre date the start of emissions from the Vector plant in 1970. For instance the estimated age of the earliest ring from the Vector Pine was 1985, after the Vector and Ballance plant started operation.

2.2.1 Core sampling strategy

An initial planning step was used to decide which rings to sample from the cores. The aim was to date tree rings that predated the Vector and Ballance plants emissions and then to create a record of emissions from the initiation of the sources through to the present day. Where a long sequence of tree rings was available rings that represented the bomb spike were included to "anchor" the tree ring record to the atmospheric curve and provide a check on results.

Particular calendar years were sampled across multiple trees in order to compare ^{14}C results for the same calendar year. The total number of unknown samples >100 were divided into groups as there were too many for a single measurement run. A measurement run consists of 40 graphite targets placed in a wheel that contains 26–28 unknown samples along with primary oxalic acid standards, secondary standards and blanks. The samples were grouped so that tree rings from the same calendar year were measured together to minimise uncertainties caused by any run to run variations.

2.2.2   Preparation of cores

Each core was allowed to air dry, then prepared for counting by creating a flat smooth surface using a scalpel blade to reveal the ring structures. Once the core surfaces were smoothed they were inspected to identify the ring boundaries using a binocular microscope and hand lens, then the rings in each core were counted using a dendrochronology approach. The cores were photographed and analysed for inconsistencies, then rings were counted from the outside bark of the tree (current year) backwards to the centre of the tree and assigned to calendar years. Rings are marked with pins every decade, using a standard convention. Individual rings were then sampled with a scalpel blade, weighed and loaded into sample vials. Some sampled cores were not used due to difficulty in cross matching rings. All the tree core preparation steps including identification of the ring boundaries, correlations between the cores, assigning rings to calendar years and cutting of the cores into rings was carried out by a summer student Marcus Trimble who also documented the ring counting and correlation of the tree core samples. These tree core correlation documents form part of the appendices (A6.11-A6.14).

2.3   Cellulose extraction and sample preparation

The following paragraphs will describe the steps of cellulose extraction and sample preparation.

2.3.1   Physical preparation

The individual tree rings were examined under a microscope and any fibres or other contaminants removed with a scalpel blade. For samples where multiple treatments were applied to one annual ring the rings were divided into equal parts longitudinally and each longitudinal section was then cut into slivers a few mm long and about 1.5 mm wide using a scalpel blade. The subsamples were weighed and a small portion of the whole wood retained for later testing. A subsample was taken from the laboratory Kauri "blank" wood standard and the known age SIRI Oak inter-comparison sample (Scott et al. 2003) and treated the same way as the tree ring samples.

2.3.2   Rafter Organic solvent washes (OSW)

Sample slivers are wrapped in a piece of GFC filter paper and placed in a glass thimble for soxhlet extraction. Samples are treated with consecutive treatments of n-hexane, 2-propanol, and acetone. Each treatment is for 90–120 minutes and observations are made about any visible extractives being removed by the solvents. If any coloured extractives are still visible after 90 minutes the extraction is continued. At the end of the extractions the samples are dried in 50°C oven.

2.3.3   ANSTO Organic solvent washes (OSW)

Sample slivers are wrapped in a piece of GFC filter paper and placed in a glass thimble for soxhlet extraction. The standard method at ANSTO is to extract the wood samples in hot consecutive treatments of a 2:1 cyclohexane ethanol mixture followed by ethanol and then deionised water for 6 hours each. It was decided for reasons of efficiency that the extractions would be reduced to 3 hours of the two organic solvents followed by a 1 hour deionised water wash at 85°C followed by rinses of deionised water and drying at 50°C.

2.3.4   Rafter cellulose method

The solvent treated wood slivers are transferred to centrifuge tubes and treated with hot washes at 85°C: 0.5M HCl, for 30 minutes, 0.1M NaOH for 1 hour (which is repeated if the solution is darker than an amber colour), followed by bleaching in 4%v/v Hydrogen peroxide at pH 11 made alkaline with 1.5g NaOH/100ml peroxide solution at 60°C. The bleaching step is repeated as necessary, most samples only require 1 treatment. The bleached product is pale yellow colour. The final step is acidification with 1.0M HCl for 30 minutes followed by rinses of deionised water to neutral pH before drying at 50°C. In between the intermediate steps the sample is rinsed to neutral pH with deionised water.

2.3.5 ANSTO cellulose method

The solvent treated wood slivers are bleached with $NaClO_2$ (15g/L) with 3ml 0.5M HCL added to adjust the solution to pH 2-3. Holocellulose extraction: sample is heated to 90°C for 60–90 minutes, and the process is repeated as necessary. The bleached product is a whiteish colour; sample is rinsed thoroughly with deionised water. Holocellulose is treated with sodium hydroxide washes designed to extract α cellulose: sample is washed with 12%w/v NaOH in a nitrogen atmosphere at 60°C for 1 hour then in 7%w/v NaOH solution in a nitrogen atmosphere at 60°C for 1 hour, sample rinsed thoroughly in deionised water. The final step is acidification with 2.0 M HCl at room temp for 2 hours followed by deionised water rinses to neutral pH and drying at 50°C.

2.3.6 Combustion Sealed tube method

Samples are loaded into quartz tubes and reagents added to supply O_2 (CuO) and remove halogens (Ag wire). The tubes are evacuated and flame sealed and placed in a muffle furnace for 2 hours at 900°C. After cooling the tubes are cracked under vacuum and the CO_2 is purified to remove water vapour and non-condensable gases such as nitrogen oxides, then the CO_2 is collected by freezing in Liquid nitrogen. The CO_2 pressure is measured to calculate the volume of gas produced and the yield of combustion calculated. The gas is transferred into a mass spectrometry bottle ready for graphitisation. A portion of the CO_2 gas is used for a measurement of $\delta^{13}C$ by isotope mass spectrometry.

2.3.7 Elemental Analyser and collection device

Pre-treated cellulose samples were loaded into tin cups then combusted using a Europa ANCA elemental analyser (EA) connected to a Europa 20–20 mass spectrometer. The CO_2 gas is split with a small amount used for $\delta^{13}C$ measurement with the remaining gas trapped cryogenically then transferred to a sample bottle (Baisden et al. 2013).

2.3.8　Graphitisation

CO_2 gas from the samples is transferred into a graphite reactor, containing 2.8mg reduced iron catalyst. The pressure of the CO_2 is measured and the number of moles of gas calculated. 2 moles of Hydrogen gas for every 1 mole of CO_2 are added to the graphite reactor. CO_2 gas is converted into carbon in the form of graphite over a Fe catalyst at 550°C. Water vapour produced during the reaction is frozen out as an ice pellet using a thermoelectric cooler. The reaction proceeds for approximately 2–3 hours until completion (equation 2.1), (Turnbull et al. 2015).

$$CO_2 + 2H_2 \xrightarrow[Fe]{} 2H_2O + C\ graphite$$
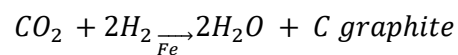
Equation 2.1　Graphitisation reaction

2.3.9　AMS Measurement

The graphite samples are packed into aluminium target holders and all three carbon isotopes are measured using accelerator mass spectrometry at GNS Science (Zondervan et al. 2015). The graphite targets were counted to over 700,000 ^{14}C counts to produce high precision counting statistics of 1.1–2.0‰ in Δ^{14}C. Standardisation is via Oxalic Acid I and results are normalised for isotopic fractionation (Zondervan et al. 2015, Stuiver and Polach 1977) standard and blank corrected using a sample processing blank Kauri wood >140,000 years old that contains no ^{14}C activity (Marra et al. 2006, Hogg et al. 2006). The Kauri blank is pretreated in the same manner as the unknown samples and is representative of sample processing conditions. The results are reported as fraction modern (F^{14}C), useful for reporting results from post bomb samples. F^{14}C is the ratio of activity of sample compared to the activity of the standard that has been background corrected and normalised to a δ^{13}C of -25‰ (Reimer et al. 2004). This is described in equation 1.4 section 1.61. Uncertainty is reported at one-sigma, based on the number of ^{14}C counts for both sample and standard, and an additional error factor is added in quadrature to account for the long-term performance of standard materials of the same type (Zondervan et al. 2015; Turnbull et al. 2015).

2.4 Data handling

2.4.1 Comparison of results with the atmospheric $^{14}CO_2$ data

The ^{14}C results from the tree rings were plotted against an established accurate record of atmospheric $^{14}CO_2$ data to allow the comparison of tree ring data with Baring Head data (Currie et al. 2011, Turnbull et al. 2015). In this way the background trees can be compared with background $^{14}CO_2$ data. Trees from the polluted locations are expected to show good agreement with Baring Head $^{14}CO_2$ data until the inception of the plant in 1970 when CO_{2ff} emissions began (Figure 1.1). After 1970 the local atmosphere around the plant will be affected by added CO_{2ff} that is devoid in ^{14}C. ^{14}C concentrations in tree rings in the polluted locations will be lowered in direct proportion by the amount of CO_{2ff} added.

2.4.2 Record of historic CO_2 concentrations for the project

CO_2 concentration data is required to make CO_{2ff} calculations. There is an established accurate record of CO_2 concentration data measured at Baring Head Wellington by NIWA scientists (Brailsford et al. 2012, Stephen et al. 2013) (Table A6.5). As the Baring Head record $^{14}CO_2$ is used to provide a basis for background conditions at Kapuni it is reasonable to apply the Baring Head CO_2 concentration record as a proxy for CO_2 concentrations at Kapuni as well.

2.4.3 Compilation of Baring Head $^{14}CO_2$ data

Baring Head $^{14}CO_2$ data was averaged for the months September to April to calculate an annual value for the purposes of the mass balance equation (Table A6.4). The uncertainty for the annual Baring Head $\Delta^{14}C$ was calculated by taking a standard deviation of the individual measurements. Results for the years 1955–1965 were subject to large variability in ^{14}C concentration and lower precision and are often based on relatively few data points.

2.4.4 Emissions data

Monthly (2004–2013) and annual emissions (1991–2004) from the Vector plant were provided by P Stephenson (Vector). Monthly emissions were summed to represent the

8 months of the year (April–September) when trees are assumed to be photosynthesising. Detailed emission information prior to 2004 could not be obtained and is based on annual figures recorded from the months from July–June The annual data for this period is the best compromise between no data or annual data and should be a reasonable proxy for the same sampling period (Table A6.6). The pre 2004 data is assumed to be subject to higher errors due to changes in the way emissions were calculated at the plant (P. Stephenson pers comm) and because of the disparity between the values produced for 2004. For the years prior to 1990 no data could be obtained about Vector's emissions.

Ballance emissions for the years 1990–2013 were obtained from the biennial monitoring report produced by Taranaki Regional Council. (2013b) (Table 4.6). Ballance reports both CO_2 emissions and tonnes of urea produced per annum. These figures were used to calculate CO_2 emissions by two methods that resulted in very good agreement. Reported emissions based on CO_2 data are ~0.05 Tg C yr^{-1} (Taranaki regional Council 2013b). Emissions of CO_{2ff} can be calculated independently using urea production statistics and a factor from urea lifecycle analysis (Ledgard et al. 2011). Calculation of emissions from urea data suggests emissions of ~0.06 Tg C yr^{-1} (Troy Baisden pers comm). Emissions data from both sources was summed and plotted against CO_{2ff} values for the Luscombe chestnut and Vector pine tree.

2.5   Atmospheric Mixing and inter-annual variability in atmospheric transport

2.5.1   Assessment of results using Meteorological data

Atmospheric mixing and transport of CO_2 are affected by inter-annual variability. Meteorological data for the Kapuni area was compiled from the Hawera Automatic Weather Station (AWS) (39.6117°S, 174.2917°E, 98 m.a.s.l.), downloaded from the New Zealand National Climate Database (CliFlo, 2014) for the years 2004–2013. Hawera is a reasonable proxy for conditions at the Kapuni Vector site; data was averaged for the months of September to April for daylight hours 08:00 to 16:00 to mimic the growing season of the plants assumed to be April to September for the years 2004–2013 to

create wind roses. The meteorological data and wind roses were supplied by Liz Keller for this project (Figs 4.19, 4.20, 4.21, 4.22).

Wind roses provide a graphical summary about wind speed, direction and frequency at a particular location over a given time period. A wind rose shows direction the winds blows from, the speed is denoted by the colour (warmer colours are faster wind speeds) and the length of the spoke the frequency of the wind speed. The wind rose data was analysed to produce data sets that represent the three main wind directions observed at the Hawera met station for each calendar year (Table A6.7). The wind types were grouped based on their trajectories, Westerly >230 and <330 degrees, South Easterly >100 and <220 and North Easterly >330 and <80. Only 2 small sectors were not included (80–100 and 220–230) and at worst this excluded about 6% of the data. Low wind speeds were considered to be a possible bias but only a tiny proportion of the data has wind speeds of <2 meters per second. Removal of low wind speeds did not affect the overall frequency of wind types so all wind speeds were retained.

The wind data was plotted as histograms and the mean wind speed calculated for each category. The wind data was used to make a qualitative assessment of correlations between CO_{2ff} concentrations and changes in frequency of wind conditions.

2.6   Mass balance equation

CO_{2ff} emissions from the Vector and Ballance plants were calculated using a mass balance equation from ^{14}C data from tree rings using a Lagrangian approach that assumes a parcel of air travels from a clean air location and collects fossil emissions that alter its CO_2 concentration and ^{14}C level. The air mass is then reflective of background conditions and the fossil emissions that it has collected. The mass balance equation requires measurement of ^{14}C in the tree of interest Δ_{obs}, CO_2 concentration CO_{2bg} and ^{14}C content of a background tree Δ_{bg}. Using the derived value for CO_{2ff} ^{14}C content (-1000‰) the CO_{2ff} can be calculated in the tree rings in ppm, following the mass balance equation (equation 1.1 section 1.3). CO_{2ff} was calculated for the polluted Vector tree(s) using ^{14}C data and CO_2 concentrations and $^{14}CO_2$ data from Baring Head as a background.

2.6.1 Calculation of Uncertainties in CO_{2ff}

We can estimate CO_{2ff} mixing ratios with uncertainties from our ^{14}C data in tree rings. Total uncertainty in the calculation of CO_{2ff} from Δ^{14}C measurements of (1.5–2.0% precision) is less than 2ppm for a single observation based on the uncertainty in CO_2 concentration measurement, and uncertainty in the ^{14}C result (described below).

The largest contribution of uncertainty in calculated CO_{2ff} comes from the uncertainty of ^{14}C measurement of the tree ring and the uncertainty of the background [14]CO_2 data. Each tree ring result is based on a single F[14]C result counted using high precision AMS ^{14}C measurement with an uncertainty of 1.1–2.0‰. The Baring Head [14]CO_2 data set consists of multiple data points per calendar year, which was averaged over an 8 month period for each calendar year from September to April to provide a value for Δ_{bg} that could be compared with the tree ring result for the same calendar year. In order to provide an uncertainty assessment of the 'averaged' [14]CO_2 data a standard deviation was taken of the individual results (Table A6.4). Years with large changes in ^{14}C results e.g. 1950–1970's resulted in large uncertainties.

CO_2 concentrations are reported to 2 decimal places with a very small uncertainty, and contributes a very minor portion of the uncertainty to the CO_{2ff} concentration data (Brailsford et al. 2012, Stephens et al. 2013). The method for calculating the uncertainty of CO_{2ff} is described here.

An uncertainty can be calculated for the fossil CO_{2ff} values using uncertainties in the terms in the mass balance equation. Uncertainties in Δobs Δbg and CO_2 concentration are propagated in quadrature. The uncertainty in Δobs is the F[14]C measurement uncertainty. For the background term (Δobs) and the CO_2 concentration term (Cbg) the uncertainties reflect the scatter of values that were averaged to calculate Δbg and Cbg. Δff is a derived value so does not contribute any uncertainty to the equation.

2.7 Calculation of student's t-test

A Student's t-test was used to compare the ^{14}C results from tree ring data with the Baring Head atmospheric $^{14}CO_2$ record. The t test is designed to determine if two data sets are significantly different from each other (equation 2.2).

The calculation used incorporates the differences between the sample pairs and the uncertainty of the results of the individual samples.

$$t = \frac{S_1 - S_2}{\sigma_t}$$

Equation 2.2   Student's t-test

Difference in sample pair is calculated S_1-S_2, where S_1 and S_2 are the measured values of the sample pair.

σ_t is calculated by adding the uncertainties in S_1 and S_2 in quadrature.

3.0   Cellulose Extraction

3.1   Introduction

The Rafter Laboratory method for producing cellulose from wood samples for radiocarbon dating is quite different to that used by other radiocarbon labs. It was developed by the Rafter lab as a faster, less toxic alternative method to traditional sodium chlorite wood bleaching and has been in use by the laboratory since the 1990's.

This project is based on the measurement of radiocarbon in modern wood samples consisting of annual tree rings. Annual rings formed around the time of bomb curve (1950–1970) when atmospheric radiocarbon was changing rapidly are predicted to contain extractible fractions with a significantly different Δ ^{14}C age from the growth year of the ring, thus removal of this contamination and extraction of a reliable cellulose fraction that represents $^{14}CO_2$ in the atmosphere during the growth year the ring was laid down is important (Wilson et al. (1963), Jansen (1970), Cain and Suess (1976) and Stuiver and Quay (1981). Cellulose is considered the most reliable fraction for analysis of radiocarbon and stable isotope studies (Park and Epstein 1961, Leavitt and Danzer 1993, Boettger et al. 2003). This initial study will compare the Rafter cellulose extraction method with a cellulose extraction method used by the ANSTO laboratory Australia (Hua et al. 2000) and determine which of the two cellulose methods is more effective and should be used to prepare the tree ring samples for this research project.

3.2   Background

3.2.1   Wood structure

Wood is a complex material that consists of four main components: cellulose, lignin, hemicellulose and extractible materials (Goldstein 2004). In scientific analysis cellulose is the target material in wood but to extract it requires mechanical and chemical processing to remove lignin, extractives and non-cellulosic polysaccharides to obtain a cellulose fraction for analysis (Boettger et al. 2007).

Cellulose forms an important part of cell walls of plants, many algae and oomycetes. Approximately 45% of wood consists of cellulose a linear polymer of glucose units linked

by β 1–4 glycosidic bonds with a degree of polymerisation of up to 30,000 glucose units (Pettersen 1984, Zink-Sharp 2004). Molecular chains are bonded with an adjacent cellulose chains via multiple hydroxyl bonds to form rather stiff rod like structures, which cause cellulose to have highly crystalline areas (Pettersen 1984). This bonding between various cellulose chains gives cellulose its structural strength and makes it impervious to hydrolysis.

Hemicelluloses are polysaccharide polymers made of many different types of sugar monomer and comprise about 25–30% of wood. They have a branched structure and consist of both pentose and hexose sugar units (Goldstein 2004). Hemicellulose has a much lower degree of polymerisation than cellulose with a random amorphous structure that can easily be hydrolysed by both acids and bases (Pettersen 1984). In softwoods hemicellulose is dominated by mannose, xylose, glucose, galactose and arabinose. In hardwoods hemicellulose consists of xylose, mannose, glucose and galactose (Goldstein 2004). The most important function of hemicellulose is strengthening the cell wall in conjunction with cellulose and lignin (Scheller and Ulvskof 2010).

Lignin is the third major cell wall component of wood and comprises between 15–35% of dry weight of wood (Zink-Sharp 2004). It has three main functions: it plays a role in the transport of nutrients and water, provides mechanical support to the plant by providing strength to cells and protects the cell wall from enzymatic attack (Goldstein 2004). Lignin is a high molecular weight complex of three dimensional cross linked amorphous polymer consisting of phenyl propane units made of three monomers p-coumaryl alcohol, coniferyl alcohol and sinapyl alcohol (Sjöström 1993). There are three main classes of lignins: guaiacyl lignin primarily composed of coniferyl alcohol found in conifers, guaiacyl-syringyl lignin composed of both coniferyl and sinapyl alcohol associated with hardwoods. The third class graminaceous lignin is made primarily of p-coumaryl alcohol units found in grasses (Pearl 1967, Sjöström 1993).

Extractives are genus or species specific wood components that can be dissolved in water or organic solvents (Goldstein 2004). Extractives include sugars, fatty acids, starches, pectin, resins, tannins, alcohols, terpenes, volatile oils and quinones. Extractives serve as intermediates for metabolism, provide energy reserves, and defend the tree against microbial attack (Pettersen 1984).

3.2.2 Dendrochronology

Dendrochronology or tree ring dating is a scientific method of dating based on the analysis of patterns in tree rings. A.E. Douglass is considered the father of dendrochronology and his original interest in looking for evidence of links between climate and sunspot activity led to creating tree ring chronologies that allowed the dating of Native American settlements before the advent of radiocarbon (Fritts 1976). Dendrochronology is based on the principle that trees produce a new growth ring each year, that reflect the climatic conditions they grew in. Trees in the same climatic area will tend to display the same pattern in their growth rings which can be compared to other trees by cross matching tree rings to create floating chronologies that go back in time. Observing patterns in rings is achieved using a skeleton plot an established technique that is used to represent the relative narrowness of tree rings and is recorded much like a bar code on graph paper or using a computer program (Stokes and Smiley 1968). Manual plotting is now largely replaced by computer plotting techniques (Cropper 1979). Once the plots have been created they are used to match ring width patterns from other cores that are linked to dated chronologies. Undated floating chronologies can then be linked to absolute chronologies by comparing to the patterns in rings preserved in dead trees or building timbers. Once linked to an absolute chronology it is possible to assign a growth ring to an exact calendar year. Chronologies have been created that cover thousands of years. Calibration of radiocarbon dates have been achieved using an 11,000 year old Oak and Pine chronology (Stuiver et al. 1986, Friedrich et al. 2004) and an 8500 year old chronology using long lived bristlecone pines (Suess 1970, Becker 1993, Stuiver and Reimer 1993, Hogg et al. 2013).

3.2.3   Photosynthesis

Trees capture a record of their environment during photosynthesis through the incorporation of carbon, hydrogen and oxygen atoms from the atmosphere into their cells. In angiosperms springtime growth is activated by warming temperatures and production of growth hormones. Water travels from roots to stems where cell division causes buds to swell, leaves emerge and photosynthesis begins. In evergreen gymnosperm trees photosynthesis can continue all year if temperatures permit (Barnett 1973, Striebly 2013). In spring time warmth accelerates photosynthesis again. Photosynthesis is a complex process where sugar is manufactured using water and carbon dioxide from the atmosphere. They are enzymatically combined to form glucose in the chloroplasts of the leaves using energy from light with oxygen formed as a by-product.

A simple way in which photosynthesis can be represented is shown below equation 3.1

$$6\,CO_2 + 6\,H_2O \xrightarrow{673\ kcal\ light\ energy} C_6H_{12}O_6 + 6\,O_2$$
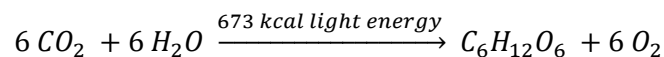
Equation 3.1   Photosynthesis

Glucose is an intermediate product which is the basis for building food or cell building materials, such as cellulose lignin and starch. If glucose is not needed for immediate food uses it can be transformed into other important cell components such as fats or proteins. During the hours of darkness trees use stored starch to provide energy which is broken down into glucose and carbon dioxide and water as the by-products. Respiration occurs continuously but is overwhelmed by photosynthesis during daylight hours (Fritz 1976). Respired CO_2 is released into the atmosphere which results in the strong diurnal cycle observed in CO_2 concentrations. Low CO_2 concentrations are observed during the daytime linked to photosynthesis and higher CO_2 concentrations observed at night time, this cycle has a higher amplitude during spring and summer months as photosynthesis and respiration are at a maximum.

A simple way to represent respiration is shown below equation 3.2.

$$C_6H_{12}O_6 + 6\,O_2 \rightarrow 6CO_2 + 6\,H_2O + 673\ kcal\ energy$$
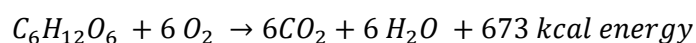
Equation 3.2   Respiration

3.2.4   Carbon Isotopes in plants

The isotopic ratio of ^{14}C to ^{12}C in atmospheric CO_2 is quite different to that in plants, this is called fractionation and occurs during photosynthesis because the lighter isotope ^{12}C is able to diffuse more readily into the leaf than the heavy isotopes ^{13}C and ^{14}C (McCarrol and Loader 2004). More fractionation occurs when glucose is formed by the photosynthetic enzymes with ^{12}C used in preference to ^{13}C *but once the cellulose has been formed it does not exchange carbon atoms with its environment*. (McCarrol and Loader 2004). It is possible to correct the ^{14}C result for this fractionation caused by the uneven uptake of carbon isotopes during photosynthesis by a process called normalisation. The δ^{13}C correction can then be applied to the ^{14}C result of the cellulose so that fractionation is removed enabling measurements of different material to be compared on the same basis. It is expressed as δ^{13}C and it is a measure of the deviation of the abundance of ^{13}C to ^{12}C atoms in the sample relative to the same ratio in a limestone standard usually VPDB Vienna Pee Dee Belenmite. Fractionation in C3 plants is about -18‰. Atmospheric δ^{13}C is changing due to addition of fossil fuels, which are depleted in ^{13}C so the ^{13}C of plant materials is also gradually decreasing since industrialisation (Freyer and Belacy 1983).

As biochemical pathway processes involved in creating different wood components differ so the wood components have different isotopic signatures (Barbour et al. 2002). Chemical changes to wood during pre-treatment cause small observable changes in δ^{13}C value from whole wood to cellulose which can be used as a qualitative indicator of the removal of non-cellulosic materials such as: lignin ~3‰ lighter and resins ~6‰ lighter (relatively more depleted) in δ^{13}C than cellulose (Wilson and Grinstead 1977, Benner et al.1987, MacFarlane et al. 1999, Loader et al. 2003 Rinne et al. 2005).

3.3   Historic wood sample preparation

Historically whole wood in tree rings was used for stable isotope paleoclimate analysis reconstruction (e.g. Craig 1954, Farmer and Baxter 1974, Libby and Pandolfi 1974). The advantage of using whole wood for analysis was that more analyses could be made as little sample processing was required. In the early days of radiocarbon and stable isotope analysis measurement uncertainties were much higher and large amounts of sample

material were required so small amounts of contaminants left by basic pre-treatment methods didn't matter. Early pre-treatments applied to wood for radiocarbon analysis were acid base acid treatments (De Vries and Barendsen 1954). This approach to wood pretreatment was demonstrated to be inadequate when Wilson et al. (1963), Jansen (1970), Cain and Suess (1976) and Stuiver and Quay (1981) found that there was evidence of ^{14}C incorporated into tree rings from nuclear testing into growth rings from pre-bomb years.

Wilson and Grinsted (1977) demonstrated that wood contains compounds of different isotopic composition and reported that dendro-climatic information could not be satisfactorily obtained from analysis of whole wood because $\delta^{13}C$ of extractives and lignin differ to that of cellulose, and vary in the amounts laid down within one growth ring, thus most recent researchers have chosen to extract cellulose. Analysis of various components extracted from wood have been used too such as; solvent extracted wood, lignin, and holocellulose (e.g. Leavitt and Danzer 1993, Hoper et al. 1998, Loader et al. 2003, Harlow et al. 2006). The use of other fractions of wood must be carefully tested to see if there is a bias introduced because of the effectiveness of the pretreatment on the type of wood species. Inadequate pretreatment of wood can lead to interpretation of false climate signals and incorrect radiocarbon measurements.

3.3.1 Cellulose extraction

Cellulose has become the most used fraction from wood for radiocarbon and paleoclimate analyses because it offers the following advantages: it is produced by a single biosynthetic pathway, and is directly related to growth of the tree because it is formed in one growing season and is deposited into an annual ring that is definitively related to that seasons growth (Park and Epstein 1961). Cellulose $\delta^{13}C$ is similar to the whole plant and it does not exchange carbon with the environment which means it records paleoclimate information at the time of formation (Leavitt and Danzer 1993). Extracting cellulose from wood avoids the influence of other wood components such as extractives and lignin which tends to be laid down in the annual ring after cellulose, causing the ratio between cellulose and lignin to vary through time or to be variable within individual trees (McCarroll and Loader 2004). Processing of wood to produce cellulose also creates a pure homogeneous product that is useful for stable isotope

analysis (McCarrol and Loader 2004). The goals of pretreatment of wood samples for radiocarbon and stable isotope analysis are similar but because radiocarbon is concerned with measuring the amount of ^{14}C left in the sample after death it is important that any exogenous carbon ^{14}C is removed from the cellulose and no additional carbon is introduced by the reagents used for the extraction. So the methods designed for analysis of stable isotopes are not necessarily suitable for radiocarbon analysis.

3.3.2 Jayme-Wise method cellulose extraction method

Since the early years of paleoclimate reconstruction that require measurement of large suites of samples researchers have been focussing on producing reliable and efficient methods to prepare wood samples. Most researchers have adopted the Jayme-Wise method to produce cellulose described by Green (1963). The method employs sodium chlorite bleaching that preferentially attacks lignin to produce holocellulose. Lignin consists of a strongly bonded polymer that is resistant to hydrolysis, but is susceptible to oxidising agents (Hedges 1990). Holocellulose is the total carbohydrate portion of plants which consists of a mixture of cellulose and hemicellulose, and polysaccharides (starch and pectins) (Pettersen 1984). The holocelluose is then treated with sodium hydroxide washes to leach out the hemicellulose and polysaccharide components, the insoluble material that remains is termed alpha (α) cellulose and is the material that most resembles the original cellulose in the wood. Although the Jayme-Wise method is used by most researchers to produce cellulose, there are various criticisms of it. It is acknowledged that the cellulose produced contains small amounts of extractives, hemicellulose and lignin (Li and Liu 2013). It is also a destructive technique that results in quite a large loss of sample mass, requires special apparatus, and is considered a time consuming process (Cullen and MacFarlane 2005). Determination of the end point of the bleaching process requires experience and is based on the appearance of the beached material (Harlow et al. 2006).

3.3.3 Alternatives to Jayme-Wise method: Brendel and Diglyme method

Two alternative methods to the Jayme Wise method have been developed for the preparation of cellulose for stable isotope analysis. The Brendel method an adaptation

of a method developed by Crampton and Maynard (1938) employs an acetic/nitric acid mixture to remove lignin and non cellulose polysaccharides (Brendel et al. 2000). Gaudinski et al. (2005) and Anchukaitis et al. (2008) have both expressed the opinion that the Brendel method introduces dead ^{14}C contamination to cellulose, and they do not recommend its use for the preparation of radiocarbon samples. Moreover, Gaudinski et al. (2005) claim that the Brendel method leaves lignin in the sample. The second alternative method developed by Wallis et al. (1997) and adapted by MacFarlane et al. (1999) called the diglyme method uses diethylene glycol dimethyl ether. Although regarded as quick and reliable the diglyme method produces crude cellulose that contains 5% lignin (Borella et al. 1998). Cullen and MacFarlane (2005) extracted cellulose from woods with differing degrees of resistance to delignification using the digylme method with an additional $NaClO_2$ oxidation. They found diglyme-HCl extraction alone was sufficient for hardwood species but conifer woods required additional oxidation using $NaClO_2$. Cullen and MacFarlane (2005) propose the difference is because softwoods are more resistant to extraction of resin and lignin.

3.3.4   Acid base acid method

An alternative treatment that is sometimes used to treat wood samples which uses a sequence of acid base acid washes and is the standard pretreatment method for non-woody plant materials and charcoal for radiocarbon analysis. It is designed to remove material absorbed by samples after death and burial including, carbonates and humic acids but this method does not produce cellulose and is generally regarded as being inadequate for wood sample preparation because treated samples still contain lipids and lignin (Gaudinski et al. 2005). The acid base acid method has also been demonstrated to produce inconsistent radiocarbon dates (Long et al. 1979, Olsson 1980, Hoper et al. 1998, Olsson and Possnert 1992).

3.3.5   Organic Solvent washes

Radiocarbon analysis of modern tree rings has demonstrated that trees that contains growth rings from the bomb period 1950–1970's contains extractive material from the bomb era that does not represent the year of growth that is deposited e.g. (Wilson Gumbley and Speddin 1963, Jansen 1970, Baxter and Farmer 1973, Olsson 1980). To

address this issue extractible materials are commonly removed by a solvent extraction process before cellulose extraction procedures are applied. Solvent extraction is recommended for softwood species such as conifers that contain large amounts of extractives (McCarroll and Loader 2004, Rinne et al. 2005), but the removal of extractible materials, may only be strictly necessary for samples where large differences are expected between the ^{14}C content in these translocatable substances and the cellulose (Southon et al. 2010). The choice of organic solvent used in washes is not universal among labs undertaking radiocarbon analysis, benzene was an early choice (Tans et al. 1978, Olsson 1980), now replaced by toluene because of the carcinogenic properties of benzene. Solvents used include; toluene/ethanol (MacCarroll and Loader 2004, Rinne et al. 2005), ethanol/chloroform water (Hoper et al. 1998), cyclohexane and ethanol (Hua et al. 2000) and hexane/isopropanol/ acetone by the Rafter lab. The application of solvent washes prior to cellulose extraction is not necessarily a standard practice either but should be regarded as a sensible precaution in pre and post bomb wood samples.

3.3.6 General principles of cellulose preparation for radiocarbon analysis

Current practice in wood sample preparation for radiocarbon analysis is often a two stage process which involves initial treatment with a sequence of organic solvents to remove extractible materials. Removal of extractives from wood is a sensible precaution as contamination could be introduced from coring equipment and handling and it removes transloacatable substances that may not reflect the age of the cellulose (Harlow et al. 2006). Solvent extraction is also particularly important for museum pieces that may have been repaired with glue and conservation products. Solvent washes if used are followed by extraction of cellulose from the wood typically using variations of the Jayme-Wise method (Green 1963). Modifications of the Jayme-Wise sodium chlorite method have been adopted as the standard treatment to prepare wood samples for radiocarbon analysis e.g. Tans et al. (1978), Hua et al. (2000), Hogg et al. (2006), Hogg et al. (2013).

3.3.7   Cellulose preparation in the Rafter Laboratory

The Rafter method was created in house and is based on pulp and paper treatment methods and was designed to produce a cellulose extract from wood using less toxic chemicals and in a shorter treatment time than the Jayme-Wise method. It involves an acid/base/oxidation cycle (ABOx), a similar procedure used by other radiocarbon labs as a rigorous pre-treatment applied to background materials, generally charcoal or wood (Southon et al. 2010 and refs within).

Results for inter-comparison wood FIRI-D wood treated using the Rafter cellulose method are all consistent with each other and $F^{14}C$ results for Rafter cellulose 0.5689 ± 0.0022 are within the 1 sigma statistical limits of the consensus age reported by other laboratories 0.5705 ± 0.0002 (J. Turnbull pers comm, Scott et al. 2003).

Two other studies (Cooper 2000, Turney et al. 2007) have demonstrated good agreement in radiocarbon ages for wood samples prepared using the Rafter method and the Jayme-Wise method, but there is no data about the purity of the Rafter cellulose or the efficacy of the cellulose treatment. Even though past studies have not shown observable differences between the Rafter method and the Jayme Wise method, it use has been limited to wood samples that are several hundred years to thousands of years old, that represent time periods with little change in ^{14}C levels, so small changes in ^{14}C caused by methodological differences would be hard to detect. While it is possible that both methods can be used interchangeably a more rigorous test using modern wood samples used by this project may highlight some differences not observed before.

3.3.8   Description of cellulose preparation methods

The ANSTO laboratory method consists of removal of resins, fats and waxes with a 2:1 mixture cyclohexane/ethanol followed by ethanol and hot deionised water washes to remove some starches and pectin (Table 3.1). The lignin component is removed by oxidation with acidified sodium chlorite solution followed by hot washes of sodium hydroxide under a nitrogen atmosphere to remove non cellulosic material (hemicellulose) with a final acid wash to remove any CO_2 absorbed by the sample during the sodium hydroxide treatment. The final product is termed α cellulose, is quite white

in colour. The method takes three working days to complete and results in sample mass loss of about 50% during the cellulose extraction.

The Rafter method uses washes of n-hexane, propan-2-ol and acetone to remove resins, fats and waxes; then employs hot washes of hydrochloric acid and sodium hydroxide (Table 3.1). The NaOH washes serve two functions they remove any humic acids absorbed during burial of wood and removes some lignin to produce a pulp that can then be bleached. Oxidation of the alkali extracted pulp to remove lignin is performed with a 4%v/v solution of hydrogen peroxide (H_2O_2) made alkaline with 1.5g/100ml NaOH, followed by an acid wash to remove any CO_2 absorbed by the sample during the NaOH and H_2O_2. After the alkali washes and H_2O_2 oxidation the final cellulose produced is a pale yellow colour. The method takes two days to compete and result in sample mass loss of about 50% during cellulose extraction.

3.3.9 Experimental design

The Rafter method uses a milder bleaching reagent and lower molarity sodium hydroxide than used in the ANSTO cellulose pre-treatment method, therefore it is hypothesised that the Rafter method may not be as effective as the ANSTO method at extracting cellulose from wood.

Six wood samples were tested: 4 modern tree rings (consisting of a single year of growth) and two known age materials; an infinitely old laboratory "blank" wood and a known age medieval wood (Table 3.2). Results are likely to be comparable for the 300 year old wood and the blank wood but may not be within statistical limits for the modern tree ring samples formed around the peak of the bomb curve because of influence of extractible components that have a large difference in ^{14}C relative to the cellulose. The wood samples were divided into four parts and tested using the Rafter method and the ANSTO method, and two variants of the methods. In addition some whole wood and Organic solvent washed only wood fractions were tested.

A)   Rafter-Organic solvent washes (OSW) and Rafter-cellulose

B)   ANSTO-Organic solvent washes (OSW) and ANSTO-cellulose

C)   Rafter Organic solvent washes (OSW) and ANSTO-cellulose

D)   ANSTO-solvent washes (OSW) and Rafter-cellulose

Pre-treated cellulose samples were combusted using a sealed tube method or using elemental analyser. The CO_2 gas was collected in bottles, converted into graphite and radiocarbon ages measured by Accelerator Mass Spectrometry (AMS) at GNS Science (Baisden et al. 2013).

3.4   Details of the samples

[14]C free wood:

Kauri wood R40142/1 is used as a blank material by the laboratory. The wood has independently dated to >140,000 years BP (Marra et al. 2006, Hogg et al. 2006).

Pre-bomb-wood:

Oak wood R40387/6 from the Sixth international Radiocarbon Inter-comparison (SIRI). This sample is part of a series of known age materials submitted to the laboratory for the purposes of participation in an international inter lab radiocarbon comparison. The Oak has an expected age of approximately 350 years BP.

Polluted samples from Kapuni site:

Luscombe chestnut R40459/25 from Luscombe farm Kapuni, located ~850m in a secondary downwind position from the Vector plant, estimated tree ring age 1990.

Vector Pine R40447/16 tree Monterey pine (*Pinus radiata)* located ~250m distance from the source and is directly downwind of Vector plant, estimated tree ring age 1999.

Clean air Oak tree:

R40444/65 Oak tree from Kapuni school field near corner Skeet and Mania Rd, Kapuni, Taranaki. Tree ring estimated age 1950. This sampling location is 3km distance upwind of the Vector and Ballance site tree ring F[14]C results should be representative of clean air $^{14}CO_2$ of samples collected from Baring Head.

R40442/56 and R40442/58 from an additional core taken from the Kapuni Oak tree as sample R40444. Tree ring estimated age 1958 and 1956 respectively.

Background clean air sample:

Baring Head pine R40454/29 Monterey pine (*Pinus radiata*) from Baring Head Wellington tree located at clean air location estimated age of ring 1986.

3.4.1   Aims of this initial experiment

To compare and assess the cellulose extraction methods for suitability for the project using radiocarbon and stable isotope analysis as the key indicator of removal of contaminants. Statistical testing will be used to assess whether there are significant differences between ^{14}C results produced by these methods and ^{14}C results will be compared to the ^{14}CO$_2$ atmospheric record as truth.

To make an assessment of the purity of the final cellulose and the efficacy of the cellulose treatments at removing unwanted fractions. The intention was to test this using Pyrolysis-gas chromatography/mass spectrometry (Py GC/MS). This analysis is able to detect traces of resin and lignin functional groups in the wood samples, however while the analysis has been done interpretation of the results were not available to include in this thesis but will be used for a future publication. Instead removal of contaminants was observed through an enrichment in δ^{13}C stable isotope measurements from whole wood to cellulose.

δ^{13}C values of untreated, OSW treated wood and cellulose will be compared between methods as an indication of the removal of extractives and lignin. It is hypothesised that Rafter cellulose will contain more residual lignin and resin than the ANSTO method. More resistant tree species such as Kauri and Pine may produce larger δ^{13}C offsets than Oak or Chestnut wood.

Table 3.1   Flow chart cellulose extraction.

Physical pre-treatment
Sample divided into 4 parts cut into slivers
Portion whole wood saved

A	B	C	D
A	**B**	**C**	**D**
Rafter OSW solvents	ANSTO OSW solvents	Rafter OSW solvents	ANSTO OSW solvents
Soxhlet extraction (120 minutes each solvent)	Soxhlet extraction (180 minutes each solvent)	Soxhlet extraction (120 minutes each solvent)	Soxhlet extraction (180 minutes each solvent)
n-hexane	2:1 Cyclohexane/ethanol	n-hexane	2:1 Cyclohexane/ethanol
2 propanol	Ethanol	2 propanol	Ethanol
Acetone	D.I. wash 85°C 60 minutes	Acetone	D.I. wash 85°C 60 minutes
Dry @50C	Dry @50C	Dry @50C	Dry @50C

A	B	C	D
A	**B**	**C**	**D**
Rafter cellulose	ANSTO cellulose	ANSTO cellulose	Rafter cellulose
0.5M HCl (85°C-30mins) (1)	15g/L NaClO$_2$ (acidified 90°C 60-90 minutes, repeat if necessary) (A1)	15g/L NaClO$_2$ (acidified 90°C 60-90 minutes, repeat if necessary) (A1)	0.5M HCl (85°C-30mins) (1)
0.1 M NaOH (85°C 60 minutes, repeat if necessary) (B1)	12% w/v NaOH (60°C 60 mins)	12% w/v NaOH (60°C 60 mins) (2)	0.1 M NaOH (85°C 60 minutes, repeat if necessary) (B1)
4% v/v H$_2$O$_2$ (1.5gNaOH/100ml) 65°C 60 minutes, (repeat if necessary) (C1)	7%w/v NaOH (60°C for 60 mins (1)	7%w/v NaOH (60°C for 60 mins (1)	4% v/v H$_2$O$_2$ (1.5gNaOH/100ml) 65°C 60 minutes, (repeat if necessary) (C1)
1.0M HCl (85°C 60 mins) (1)	2.0M HCl (120 minutes 20°C) (1)	2.0M HCl (120 minutes 20°C) (1)	1.0M HCl (85°C 60mins) (1)
Dry @50C	Dry @50C	Dry @50C	Dry @50C

Table 3.1 Notes (A1) Sample Oxidised until uniformly off white, rinsed with deionised water until no longer smells of bleach. (B1) NaOH wash is repeated if darker than amber. (C1) Sample oxidised until uniform pale yellow colour and rinsed until pH neutral. (1) Centrifuged and rinsed until pH neutral (2) Centrifuged and decanted.

Table 3.2   Wood sample details and δ^{13}C, F^{14}C results, chi square comparisons.

R number	Method	Tree species/location	δ^{13}C	F^{14}C	error	Chi
R40142/1	A	Kauri 'blank' Laboratory wood standard >140,000 yrs	-23.42	0.00322	0.00012	
	B		-21.72	0.0027	0.00011	
	C		-21.95	0.00277	0.00011	
	D		-23.32	0.00166	0.00008	
R40387/6	A	SIRI inter-comparison Oak est age 350 BP	-24.57	0.95305	0.00176	2.3 [1]
	B		-24.32	0.95488	0.00177	
	C		-24.21	0.95185	0.00176	
	D		-24.25	0.95805	0.00177	
R40454/29	A	Background clean air Monterey Pine Baring Head Wgtn c.1986	-25.17	1.19579	0.00214	1.7 [1]
	B		-24.02	1.20028	0.00211	
	C		-24.50	1.20234	0.00211	
	D		-25.62	1.19825	0.00214	
R40447/16	A	Polluted tree Vector site. Monterey Pine c.1999	-25.59	1.09327	0.00194	1.5 [1]
	B		-25.64	1.09293	0.00212	
	C		-24.84	1.08827	0.00195	
	D		-26.13	1.08982	0.00194	
R40459/25	A	Polluted tree Vector site Luscombe Chestnut c.1990	-25.82	1.16236	0.00205	0.5 [1]
	B		-25.22	1.15977	0.00206	
	C		-25.09	1.16089	0.00208	
	D		-25.52	1.16309	0.00270	
Table 3.2 continues on following page.						

R number	Method	Tree species/location	δ^{13}C	F^{14}C	error	Chi
R40444/65	WW	**'Background' tree 3km upwind Kapuni site Oak c.1950**	-25.74	0.99062	0.00138	
	OSWR		-25.50	0.9797	0.00131	
	A		-24.89	0.98566	0.00181	1.3 [2]
	A		-25.80	0.98216	0.00134	
	B		-24.51	0.97048	0.00177	0.2 [3]
	B		-24.68	0.97177	0.00161	
	C		-25.02	0.9699	0.00176	19.8 [1]
	D		-25.11	0.98164	0.00179	
R40442/58	WW	**'Background' tree 3km upwind Kapuni site Oak c.1956**	-25.01	1.0007	0.00164	
	OSW R		-24.92	0.98162	0.00161	
	OSW R		-24.83	0.99768	0.00162	
	A		-24.34	0.99202	0.00164	1.5 [4]
	B		-24.05	0.98801	0.00163	
R40442/56	WW	**'Background' tree 3km upwind Kapuni site Oak c.1958**	-24.6	1.0598	0.00175	
	OSW R		-25.25	1.05019	0.00173	
	ANSTO OSW		-24.28	1.05924	0.00174	
	A Rafter		-24.6	1.06644	0.00172	7.7 [4]
	B ANSTO					

Table 3.2 notes. Chi square comparison [1] is chi square value of F^{14}C "A,B,C,D" cellulose results. Chi square comparison [2] chi square value F^{14}C "A" cellulose fractions. Chi square [3] chi square value F^{14}C "B" cellulose fractions. Chi square [4] chi square value F^{14}C results "A and B" fractions.

3.5   Sample Information and Results

3.5.1   Observation based evidence

Judgement of endpoint of the both the Rafter and the ANSTO method bleaching process is based on visual appearance of the treated cellulose. Observations were made about the length of bleaching time and colour of the samples during cellulose extraction. During ANSTO NaClO$_2$ bleaching the colour of the wood changes from a pale yellowish brown colour to lemon yellow, and cellulose is completely decolourised to white in the subsequent extraction with NaOH. This was more noticeable in pine and chestnut samples where a yellow colour often leached out into the NaOH solution during holocellulose extraction that was not observed in the Oak samples. Overall pine and chestnut and particularly Kauri samples were more resistant to bleaching and required a 90 minute NaClO$_2$ bleaching sequence, in some instances a repeat wash was required relative to Oak samples which took less time 60–90 minutes.

Bleaching all types of all wood samples using the Rafter cellulose method required a single 60 minute wash except for the Kauri which required 2 bleaching steps. The Rafter bleaching step decolourises wood to a pale yellow colour, but generally increasing the time does not achieve a much paler product, the colour is not altered much further in the final acid wash. Quantitative testing of the cellulose for non-cellulosic materials was not carried out here, but it is suspected that the yellow colour could be indicative of unremoved contaminants. In a study of Brendel cellulose processing Brookman and Whittaker (2012) made the cautionary observation that the appearance of treated cellulose is not necessarily an indication of its purity and attest that the yellow colour removed is an artefact of resin not lignin. Although using the appearance of the ANSTO and Rafter cellulose to judge purity of cellulose could be misleading, and should be confirmed by testing for resin and lignin, other evidence such as bias in δ^{13}C and ^{14}C between the two methods is more compelling evidence of efficacy.

3.5.2   Purity of cellulose evidence from δ¹³C data

A $\delta^{13}C$ value was obtained for all cellulose fractions to normalise the $\Delta^{14}C$ result of cellulose, $\delta^{13}C$ analysis also yields qualitative information about chemical changes in the samples through the stages of pre-treatment and allows a comparison of Rafter and ANSTO cellulose. Generally the $\delta^{13}C$ of lignin is ~3‰ lower relative to cellulose (Wilson and Grinsted 1977, Benner et al. 1987, Loader et al. 2003). Resins and oils are also depleted with respect to cellulose (MacFarlane et al. 1999) so higher cellulose $\delta^{13}C$ is expected relative to that of whole wood.

$\delta^{13}C$ results were obtained from additional fractions of the Kapuni Oak samples R40444/65, R40442/56 and R40442/58 (Figure 3.1) to allow a qualitative assessment of removal of contaminants in the wood. $\delta^{13}C$ values of whole wood and OSW fractions are generally more depleted than treated wood, and as the sample gets cleaner the $\delta^{13}C$ becomes enriched reflecting removal of extractible components and lignin (Borella et al. 1998, Van De Water 2002).

Considering the comparison of $\delta^{13}C$ results of ANSTO and Rafter fractions in the cellulose tests (Figure 3.1) a fairly consistent pattern emerges, Rafter cellulose tends to produce cellulose that is more depleted (contains relatively less ^{13}C) than ANSTO cellulose. This likely indicates larger amounts of lignin and/or resin remaining in the Rafter cellulose fractions than in the ANSTO cellulose. This bias is more pronounced in tree types with more resistant lignin including the Kauri and pine samples although it is less clear in the Vector pine than the Baring Head pine. Samples that are easier to bleach such as the Oak have minor differences in ^{13}C ~0.3‰.
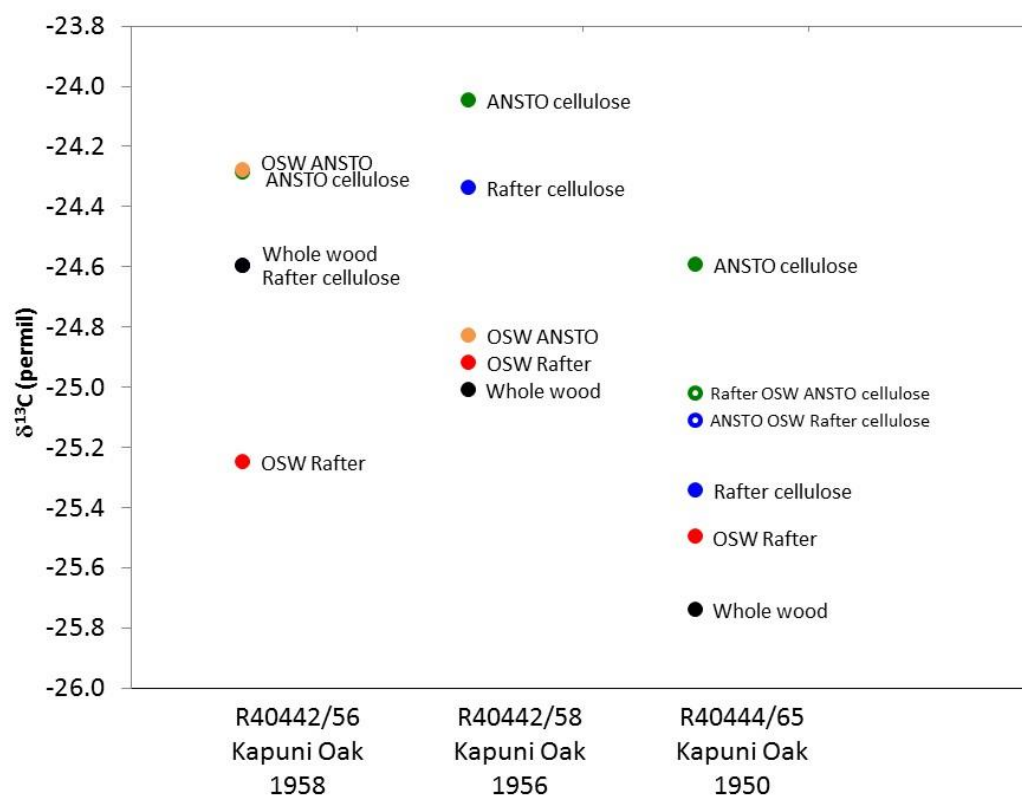
Figure 3.1 δ^{13}C results for Kapuni Oak tree cores.

3.6   Cellulose testing: F^{14}C Results
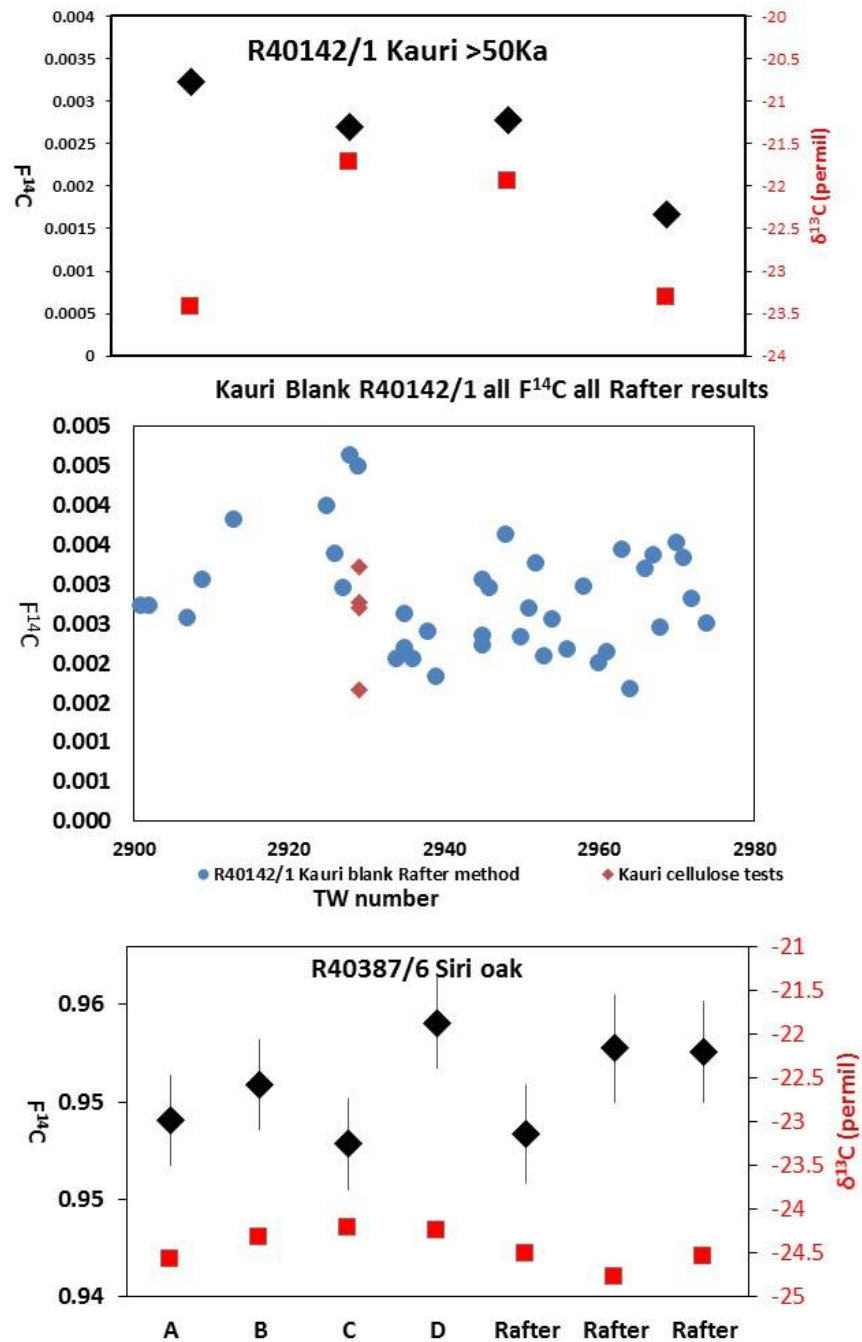
From top to bottom:

Figure 3.2   Kauri R40142/1 F^{14}C and δ^{13}C results.

Figure 3.3   Kauri R40142/1 F^{14}C cellulose results.

Figure 3.4   R40387/6 SIRI Oak F^{14}C and δ^{13}C.
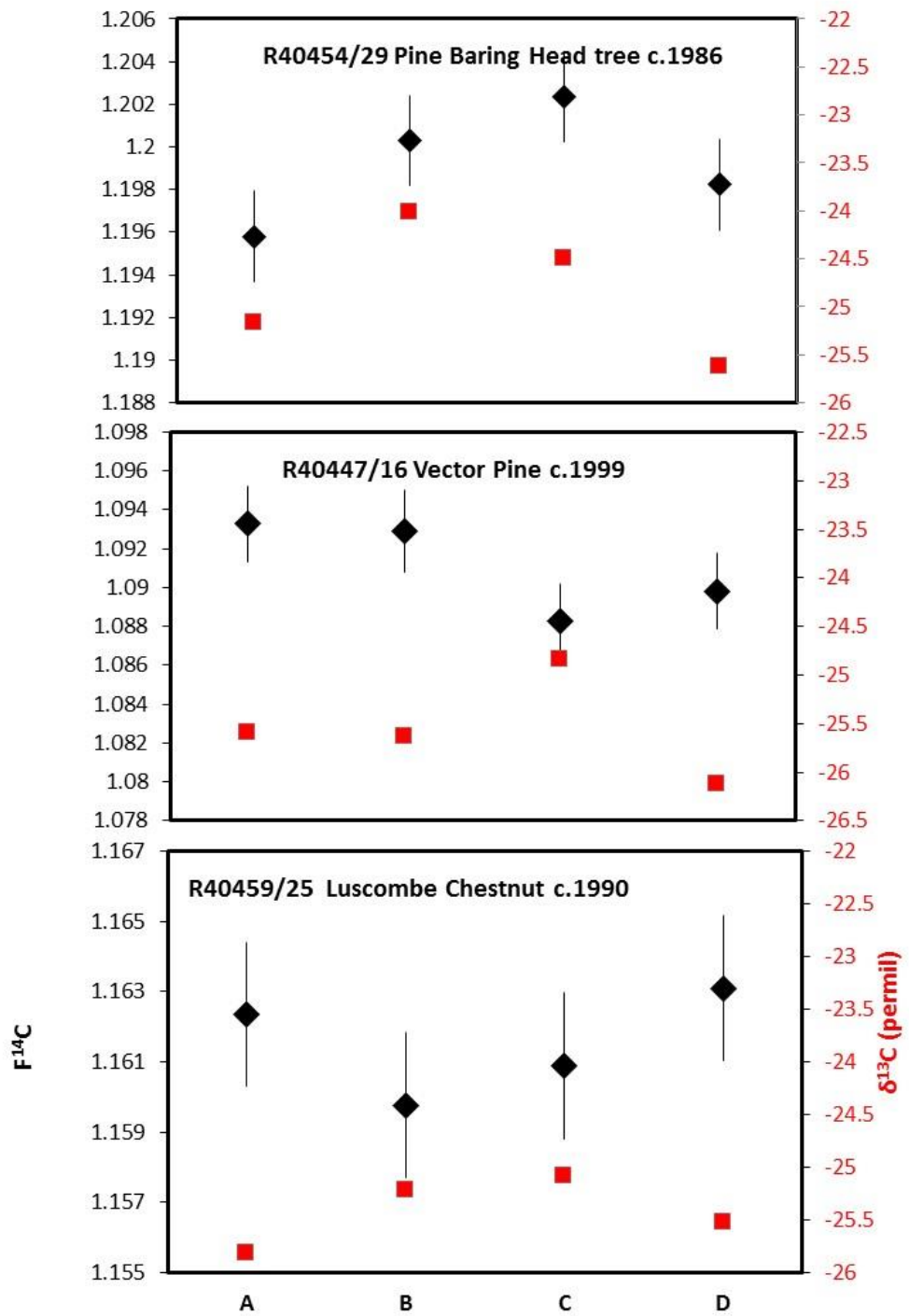
From top to bottom:

Figure 3.5　　F^{14}C and δ^{13}C results Baring Head tree R40454/29.

Figure 3.6　　F^{14}C and δ^{13}C results Vector pine R40447/16.

Figure 3.7　　F^{14}C and δ^{13}C results Luscombe chestnut R40459/25.
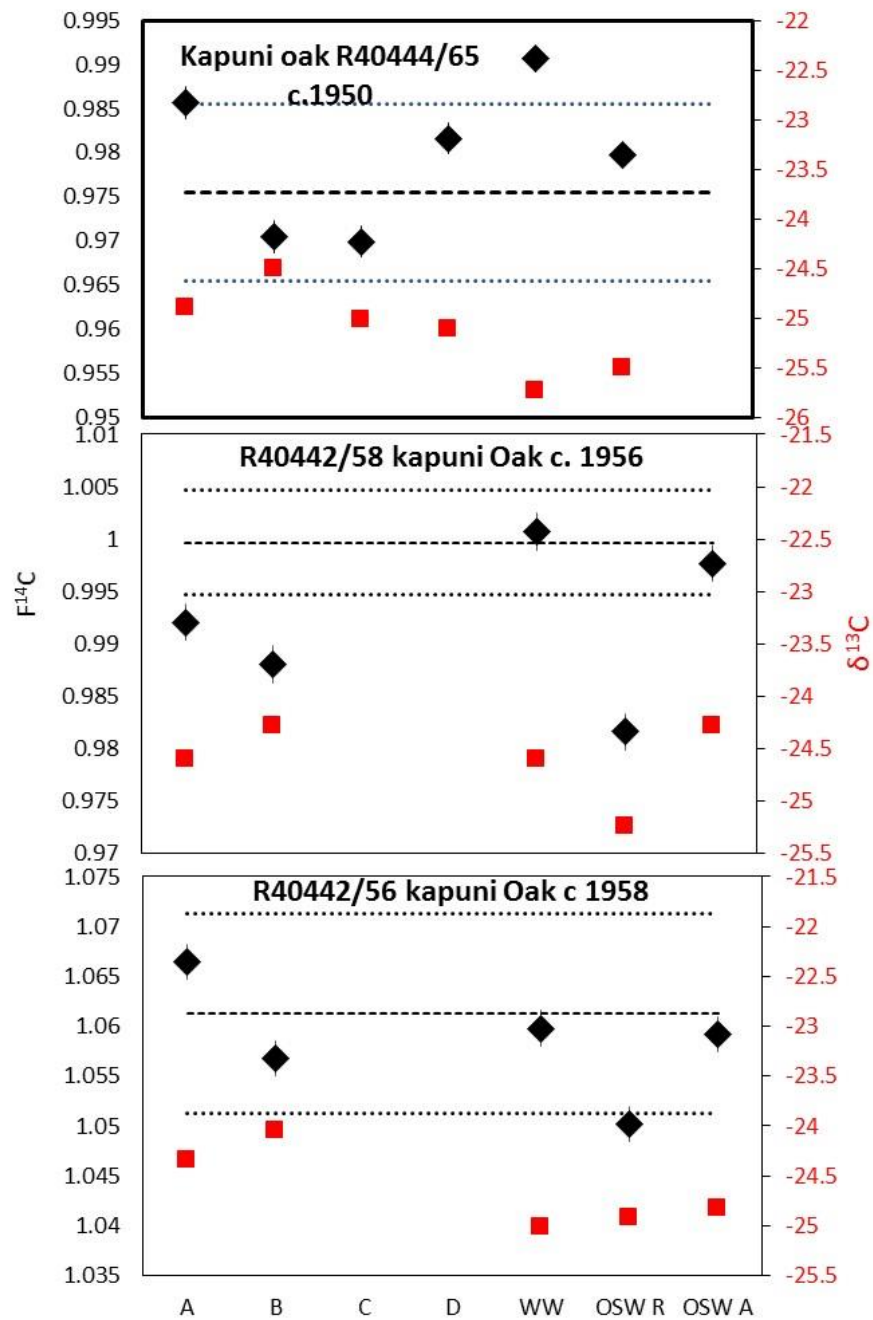
From top to bottom:

Figure 3.8   Kapuni Oak F^{14}C and δ^{13}C results R40444/65.

Figure 3.9   Kapuni Oak F^{14}C and δ^{13}C results R40442/58.

Figure 3.10   Kapuni Oak F^{14}C and δ^{13}C results R40442/56.

Results were compared using a chi square test, to give an indication of whether the results from the four methods were statistically different. Where appropriate the tree ring ^{14}C data is compared with the $^{14}CO_2$ atmospheric curve for the same calendar year to act as truth for the ^{14}C results. The following paragraphs will describe in details the results of the known age samples and unknown modern woods.

3.6.1   Kauri blank material

Due to its age this wood material contains no ^{14}C and is routinely used in our laboratory as a test of sample pre-treatment and combustion (Table 3.2, Figure 3.2). In principle we want to get the lowest possible radiocarbon age from blank materials for two reasons; it is used as control for sample preparation process and it is used to correct the ages of the other unknown samples in the measurement run. In materials of this age there should be no ^{14}C left, but in practice when producing a radiocarbon measurement using infinitely old material it is impossible to produce a radiocarbon age with no ^{14}C activity. The result that is obtained is a reflection of tiny amounts of modern contamination introduced into the sample by the laboratory sample preparation steps. Some of the uncertainty in the age is produced by the measurement process, and the inherent difficulty of detecting very few ^{14}C atoms. There is no evidence the different methods caused any influence on the ^{14}C results, so we can conclude that neither contaminates the sample with modern ^{14}C, but there is a relatively large ~1.5‰ bias in δ^{13}C with Rafter cellulose more depleted than ANSTO cellulose. The F^{14}C results from this study and are consistent with previous results obtained by the laboratory using the Rafter method (Figure 3.3).

3.6.2   Siri Oak Radiocarbon inter-comparison sample

Oak wood R40387/6 from the Sixth international Radiocarbon Inter-comparison (SIRI) (Table 3.2, Figure 3.4). This sample is part of a series of materials submitted to the laboratory for the purposes of participation in an international inter-lab radiocarbon comparison. The Oak has an expected age of approximately 350 years BP, (F^{14}C =0.96). The plot shows results obtained in the cellulose testing and previous results obtained using the standard Rafter method. Results from the 4 fractions show acceptable agreement statistically, with a chi square statistic of 2.3, the chi square test results

scatter slightly more than expected and should be equal to 1 if they agree very well. This scatter is likely due to an underestimate of uncertainties on ancient materials, which the Rafter lab is currently working to rectify (Turnbull et al. 2015). There appears to be no bias in the ^{14}C produced by the two cellulose methods which suggests for this sample the age is independent of the method used. There is very little if any offset between the ANSTO and Rafter δ^{13}C data for the SIRI sample likely because Oak wood is relatively easy to pre-treat relative to other species (Hoper et al. 1998).

3.6.3   Baring Head background tree

The results from the 4 methods scatter slightly more than expected statistically, with a chi square statistic of 1.7 (Table 3.2, Figure 3.5). ANSTO cellulose fractions have higher but not statistically significant F^{14}C result compared to Rafter cellulose. A comparison of the δ^{13}C results in the 4 fractions reveals a ~1‰ bias with Rafter cellulose more depleted than the ANSTO cellulose (Table 3.2, Figure 3.5). The F^{14}C results for the 4 fractions are all low relative to the expected value from $^{14}CO_2$ data, but ANSTO cellulose fractions demonstrate better agreement.

A ring counting error was considered possible based on an overall tendency for the Baring Head tree ring data set to be slightly lower than the $^{14}CO_2$ data and this is investigated and is discussed in the tree ring results chapter. This analysis showed the ring counting assigned to this tree core is reasonable and the overall tendency for the ^{14}C results to be lower than $^{14}CO_2$ data appears to be unrelated to ring counting problems. Since ring counting errors have been discounted, methodological problems in these samples are discussed next.

A likely mechanism for the better agreement of ANSTO results with $^{14}CO_2$ data is the incomplete removal of the extractible and lignin components by the Rafter method. In 1986 the ^{14}C content of the atmosphere was trending downwards therefore the ^{14}C content of the cellulose will be expected to be higher than the ^{14}C content of the younger extractible component. Rafter fractions have lower F^{14}C, than ANSTO, which suggests an incomplete removal of "older" mobile extractive substances by the Rafter cellulose method in this sample.

3.6.4 Vector Pine tree Kapuni

^{14}C results from the 4 methods show slightly more scatter than expected with a chi square statistic of 1.5 (Table 3.2, Figure 3.6). Although a significant difference between the two methods cannot be seen in this sample this can be explained by a relatively slow rate of change in ^{14}C content in the atmosphere around 1999 therefore ^{14}C in cellulose and extractible material in tree rings should be similar. An incomplete removal of contaminants would be difficult to detect using ^{14}C analysis alone in this case. In terms of δ^{13}C results it also hard to see any bias between the methods in this particular sample.

3.6.5 Luscombe Chestnut tree

F^{14}C results from the 4 methods show agreement statistically, with a chi square statistic of 0.5. ANSTO cellulose fractions appear to have slightly lower ^{14}C than Rafter fractions although they are still within statistical agreement with each other (Table 3.2, Figure 3.7). Agreement of F^{14}C in results is likely to be because of a relatively slow rate of change in ^{14}C content in the atmosphere around 1990 therefore ^{14}C in cellulose and extractible material in tree rings should be similar. An incomplete removal of contaminants would be difficult to detect using ^{14}C analysis alone. The δ^{13}C results have a small ~0.6‰ offset with Rafter ^{13}C more depleted than ANSTO cellulose, which suggests greater amounts of non-cellulosic material in the Rafter cellulose.

An assessment of agreement with the atmospheric ^{14}CO$_2$ record in the Vector pine and Luscombe chestnut samples is not possible as the tree rings have been affected by CO$_{2ff}$ pollution from the Kapuni site.

3.6.6 Kapuni Oak tree R40444/65

F^{14}C results from ANSTO cellulose method have lower F^{14}C than Rafter cellulose (Table 3.2, Figure 3.8). This annual ring was produced in 1950 at a time of rapid increase in ^{14}CO$_2$, therefore the ^{14}C content of the cellulose is expected to be lower than the ^{14}C content of the extractible component. Results for the 4 fractions were compared and show a distinct difference statistically with chi square statistic of 19.8.

To confirm the difference between the two methods Rafter and ANSTO Cellulose fractions were repeated using the pre-treated material, as well as whole (untreated)

wood and Rafter OSW. (Table 3.2, Figure 3.8). Ideally this test should have included ANSTO OSW treated wood but there was insufficient material to allow for a radiocarbon measurement. Results from the second combustion and ^{14}C measurement of Rafter A and B ANSTO method confirm the difference between the original results are reproducible. Results from the whole wood (untreated material) have a higher $F^{14}C$ than any of the treated fractions, this illustrates that untreated wood contains modern contaminants that both pre-treatment methods remove.

When results are compared to $^{14}CO_2$ data ANSTO fractions are closer to the average $^{14}CO_2$ value in 1950 than Rafter fractions (Figure 3.8). In this tree core other early tree ring samples have showed variable agreement with $^{14}CO_2$ data and this is thought to be because of the very rapid increases in $^{14}CO_2$ so tree ring ^{14}C and $^{14}CO_2$ data may not agree exactly. This effect may have been replicated by other tree rings in this same core (section 4.2 Kapuni Oak tree ring results), but the difference observed here is thought to be as a result of incomplete removal of contaminants by the Rafter method. Lower $F^{14}C$ in the ANSTO fractions suggests the ANSTO method is removing modern ^{14}C contamination more effectively than the Rafter method. As the solvent extraction methods for ANSTO cellulose methods B and C are different but the $F^{14}C$ results are similar the solvent method chosen appears to be immaterial to the result, and it is the cellulose extraction that is the key determinant of the ^{14}C result.

$F^{14}C$ results from the Rafter OSW (Table 3.2, Figure 3.8) demonstrate that while solvent washes appear to remove some modern contaminants other components remain that solvents are unable to remove, and a solvent only treatment for wood analysis is insufficient. Ideally this test should have included ANSTO OSW treated wood but there was insufficient material to allow for a radiocarbon measurement.

The Rafter OSW result is indeterminate when compared to the ANSTO and Rafter cellulose method results, as it straddles both sets of results. It is lower in ^{14}C than the Rafter cellulose method results, but higher than the ANSTO cellulose results. It is likely that this is caused by contamination of the sample by traces of the (^{14}C dead) organic solvents used in the Rafter OSW that remain after drying.

3.6.7 Kapuni Oak tree 1956 annual ring

Results from Rafter method and ANSTO method show reasonable agreement statistically with a chi square statistic of 1.50 (Table 3.2, Figure 3.9) This was unexpected but not an improbable outcome, based on the 1950 tree ring a significant difference in $F^{14}C$ was expected between the two methods in this ring too. To gauge agreement of cellulose results with the atmospheric record the average $^{14}CO_2$ value for 1956 and its confidence limits were added to the plot, in this sample Rafter cellulose results appear to provide better agreement with the atmospheric values. In 1956 there was a very sharp increase in $^{14}CO_2$ content of the atmosphere and therefore significant difference between cellulose and other wood components is expected with extractives and lignin having higher ^{14}C content than the cellulose. If the ratio of extractives or lignin vary throughout the ring the sample could be rather inhomogeneous, in this instance if the Rafter sample fraction received more of the modern material than the ANSTO fraction, and it seems to have a poorer ability to remove contamination overall, this could explain why the Rafter sample appears higher. The unusually low ^{14}C result for the Rafter OSW is again suspected to be as a result of residual traces of ^{14}C dead solvents in the OSW sample not removed by drying which have been removed after the subsequent cellulose extraction.

3.6.8 Kapuni Oak tree 1958 annual ring

Results from the two cellulose methods show poor agreement with a chi square statistic of 7.7, but this appears to be a reflection of the high result obtained for Rafter cellulose (Table 3.2, Figure 3.10). To assess agreement of cellulose results with the $^{14}CO_2$ record the average $^{14}CO_2$ value for 1958 and its confidence limits were added to the plot, ANSTO cellulose appears provides the best agreement with atmospheric data in this sample. $F^{14}C$ result of the Rafter treatments do not follow a logical sequence, with the cellulose result higher in $F^{14}C$ than the whole wood. It is thought this is because the 1958 sample formed not long before the bomb peak could contain a mixture of ^{14}C components that represents years before and after the bomb peak. If the Rafter method was efficient at removing some of the resins with higher ^{14}C than the cellulose but not the lignin (with possibly even higher ^{14}C), the remaining contaminants in the sample could represent early 1960's, the highest point in the bomb peak and have caused the

Rafter cellulose to effectively appear younger than the whole wood sample. The $F^{14}C$ result of the ANSTO treatments whole wood, ANSTO OSW and ANSTO cellulose follows a logical sequence and shows removal of modern contaminants in the solvent washes and cellulose.

In all the OSW tests traces of Rafter solvents appear to remain in the samples causing the Rafter $F^{14}C$ results to be too low, this is not observed in the ANSTO OSW. The difference between the two methods is that ANSTO method uses a dead radiocarbon solvent cyclohexane/ethanol as the first wash and finishes with a modern organic solvent, ethanol. All the Rafter solvents contain no ^{14}C and are tested before use to confirm they are radiocarbon "dead." The Rafter solvents were chosen by the laboratory in order not to add modern contamination to samples. Ethanol used in the ANSTO method is modern and was confirmed by testing before use. This is a deliberate choice by the ANSTO lab for modern wood samples because any traces of modern solvent left in the sample should not affect the ^{14}C of the wood (Quan Hua pers comm).

Overall the ANSTO method performs consistently better than the Rafter method based on the visual appearance, and $\delta^{13}C$ evidence. It also outperforms the Rafter method in $F^{14}C$ comparisons which is particularly evident in the modern Oak samples because it removes post-modern ^{14}C contamination more efficiently than the Rafter method. Depending on the sample year the difference between the methods is more or less obvious. For older samples where there is little change in $^{14}CO_2$ content of the atmosphere, thus little difference occurs between extractible component and cellulose no difference can be detected in $F^{14}C$ between the two methods.

3.7 Discussion

3.7.1 Comparison of ^{14}C observed in cellulose method

Cellulose testing was carried out to test two cellulose extraction methods and two variants of the methods on 8 wood samples consisting of a variety of species of wood including conifers (softwood) and angiosperm (hardwood). Ages of the samples ranged from post bomb → mediaeval →infinitely old wood blank. The samples were prepared using the ANSTO and Rafter method and two variants of the methods, at least 4 fractions were measured for ^{14}C and δ^{13}C each sample.

A hypothesis was proposed that poor agreement was expected in ^{14}C results for the two cellulose methods in samples formed around the bomb peak. Results of cellulose testing produced statistically different ^{14}C results in the Kapuni Oak c.1950 with observable differences in ^{14}C between the Rafter and ANSTO method. Two more Oak rings (1956, 1958) from an additional core from the same tree were tested to see if this could be replicated again. Comparisons of the ^{14}C cellulose results from the 1956 ring produced a statistically similar result which was unexpected, but comparison of the 1958 results were again statistically different. The inconsistent differences observed are likely due to inhomogeneity of deposits of extractives and lignin throughout the rings. In both cases it is thought that the Rafter method did not effectively remove the contaminants. Overall the ANSTO samples performed better than the Rafter samples in this time period, based on comparison with the ^{14}CO$_2$ record.

Statistically similar ^{14}C results were produced in the Baring Head pine and Luscombe chestnut tree. Comparison of the Baring Head tree ring results with ^{14}CO$_2$ for 1986 were confounded by an overall poor comparison with atmospheric data, however in both trees the ANSTO results more closely reflects levels of atmospheric ^{14}CO$_2$ than the Rafter method. The suggested mechanism for the difference between the ^{14}C results is due to the incomplete removal of younger lignin and/or extractible material by the Rafter method based on evidence of better agreement of F^{14}C values for ANSTO treated samples with the atmospheric ^{14}CO$_2$ data for the same calendar year, and the enriched δ^{13}C results for the ANSTO fractions (that reflect a cleaner cellulose fraction) relative to the Rafter δ^{13}C results.

In the older samples SIRI Oak, Kauri blank and Vector pine sample no significant differences in $F^{14}C$ were observed in cellulose produced by the two cellulose extraction methods, which is proposed to be because there were only small changes in ^{14}C in the atmosphere when these samples were formed, so if there any differences between ^{14}C in cellulose and other wood components they were not detectable using ^{14}C measurements. Samples of this age can be treated using either method.

The hypothesis appears to be confirmed that tree ring samples that contain annual rings affected by mobile post-modern extractible material require a strong oxidation to remove contamination (regardless of whether the mobile fraction has higher or lower ^{14}C than the cellulose) and the ANSTO cellulose method appears to more effective than the Rafter method for this purpose. I propose the difference in ANSTO and Rafter cellulose methods is caused by the more aggressive oxidation action of $NaClO_2$ as opposed to the milder Rafter H_2O_2/NaOH. The strong NaOH washes applied to the ANSTO sample after the oxidation removes the unwanted polysaccharides (hemicellulose portion) that may have residual lignin bound to hemicellulose. The Rafter method does not include another NaOH wash after the oxidation which might improve the overall effectiveness of the method.

Because of the requirement to produce cellulose from tree ring samples from before and after the bomb peak we will adopt the ANSTO method in combination with the Rafter OSW organic solvent washes to prepare the tree ring samples for the masters project.

3.7.2   Purity of cellulose/efficacy of OSW

To test the efficacy of the OSW methods and assess whether they confer any advantage to the cellulose methods whole wood and OSW fractions were tested for the Oak samples that contained excess modern ^{14}C contamination. Both Organic solvent wash methods remove some extractives. There was an obvious offset between ^{14}C results from the OSW fractions from the ANSTO and Rafter method with the Rafter OSW fractions appearing to be too low in ^{14}C. The low ^{14}C was assessed to be contamination of the Rafter OSW fraction by traces of 'dead' ^{14}C solvent, which was removed during the subsequent cellulose extraction. A final water rinsing step has since been added to the sample protocol of the Rafter OSW treatment. This was not observed in ANSTO OSW

fractions as the final wash ethanol is a ^{14}C modern solvent. Agreement between the ^{14}C results for fractions B and C and A and D cellulose fraction for each tree ring sample was similar so no clear enhancement of the cellulose extraction methods or final ^{14}C result was conveyed by using the Rafter or ANSTO OSW methods, so neither solvent wash method could be considered superior. Thus we continue to use the Rafter OSW procedure for modern wood samples for reasons of economy and convenience.

3.8   Difference in Isotopic signatures

3.8.1   Method and species differences

Evidence from δ^{13}C data from the cellulose method comparisons show a fairly consistent pattern of enrichment of δ^{13}C cellulose relative to whole wood using both methods but there is a lesser degree of enrichment in Rafter fractions versus ANSTO fractions (Figure 3.1). The change in δ^{13}C is consistent with a process of enrichment of cellulose relative to OSW fractions and whole wood, in both methods which likely reflects removal of extractives and lignin (Sheu and Chiu 1995, Gaudinski et al. 2005). It is proposed the greater degree of enrichment of the ANSTO fractions is a result of a purer cellulose product that contains less extraneous material.

In terms of differences caused by tree species an observable bias was detected between ANSTO and Rafter cellulose for δ^{13}C results for the Kauri and Baring Head pine samples but the Vector pine, (same species as the Baring Head tree) had indistinct δ^{13}C differences. It is proposed that this is due to resistance to bleaching by the softwood species which results in retention of larger amounts of lignin and resin that is depleted relative to cellulose (Dixon et al. 2001). Small, consistent differences in δ^{13}C between the ANSTO and Rafter cellulose samples in the other tree species are observed but in all cases the Rafter fractions are more depleted than ANSTO cellulose fractions.

3.9   Conclusions

Experimental study of cellulose methods has demonstrated that either the Rafter or ANSTO solvent method is satisfactory for use in most cases, but ANSTO cellulose is a more effective treatment than Rafter cellulose because it removes more contaminating

material, this is evident by visual appearance, δ^{13}C results and in some samples also F^{14}C results.

Proper rinsing of the Rafter soxhlet washed samples to remove acetone is really important. This may be equally as important after the final ANSTO solvent wash too, but as the final solvent is ethanol which has a modern ^{14}C level, traces remaining in modern tree rings would not be obvious. For the infinitely old Kauri and Siri Oak samples it was be just as important to remove traces of the modern ethanol used in the ANSTO solvent washes, however as it is followed by a hot deionised water wash this is unlikely.

For treatment of the tree rings in the project I recommend that we use Rafter OSW solvents method, and the ANSTO cellulose method for modern wood samples where small amounts of contamination may affect the ^{14}C data. For paleo or archaeological samples the Rafter method is sufficient and offers advantages over the ANSTO method because it is faster and uses less toxic and corrosive reagents.

4.0   Tree Ring Results and Analysis

4.1   Background trees: Baring Head tree ring data

The Baring Head atmospheric $^{14}CO_2$ record (hereafter referred to as $^{14}CO_2$ record) is used as "truth" for the project as it is a long term peer reviewed $^{14}CO_2$ data set which is used here to test ^{14}C results from the tree rings. Studies have established that trees incorporate $^{14}CO_2$ into their cellulose reliably thus capturing records of past $^{14}CO_2$ levels (Hua et al. 2013). For this study it is important to establish whether trees sampled for this project sample the atmosphere in a reproducible manner before applying the tree ring method to trees at the test location at Kapuni. A hypothesis is proposed that ^{14}C results from tree rings sampled at the clean air location at Baring Head Wellington should be equivalent to $^{14}CO_2$ level of the Baring Head atmospheric record in the same calendar year. To test this hypothesis a tree was sampled at Baring Head and ^{14}C measured in the annual tree rings. ^{14}C results from tree ring samples are overlaid on the $^{14}CO_2$ curve to demonstrate the agreement of tree ring results to the $^{14}CO_2$ atmospheric record (Figure 4.1). Each point represents a single ^{14}C result from one annual tree ring, two tree cores were sampled and measured from the same tree as a check on sample reproducibility and measurement accuracy. Visually the tree ring data agrees well with the $^{14}CO_2$ data, although there is a tendency for the tree ring data to be slightly lower than the $^{14}CO_2$ record, most points agree reasonably well. A student's paired t-test was then used to statistically compare the two data sets (Figure 4.1, Table 4.1). Statistical agreement is indicated by an average t value equal to 0 with a standard deviation equal to 1. The plots and t-test (Figure 4.1, Table 4.1) demonstrate that the Baring Head tree ^{14}C is consistently slightly lower than $^{14}CO_2$ data.

Two possible explanations are considered here; a bias in the atmospheric record and tree ring counting errors. There is a period in the $^{14}CO_2$ record from 1995–2005 where it is believed there is a bias because the AMS measurements appear to be biased high (J. Turnbull pers comm). The possibility of a bias in the $^{14}CO_2$ data set is under investigation by Turnbull et al. (in preparation) and could explain the observed offset, and two areas in the atmospheric record relevant to the tree ring samples are discussed here. An earlier version of the $^{14}CO_2$ data set (Currie et al. 2011) had a period of anomalously high

^{14}C values between 1990–1993 noted by Currie et al. (2011), which has been revised lower by Turnbull et al. (in preparation) using evidence from new measurements of archived flask samples. The tree rings analysed here confirm the lower values for the 1990–1993 period. Additionally new XCAMS measurements for the time period 1996–2005 tend to be lower than the data used in the previously published version of the atmospheric record (Currie et al. 2011). The tree ring results support the XCAMS data and this data may also be revised lower as a result (J. Turnbull pers comm).

Alternatively the Baring Head tree ring data could be slightly low as a result of ring counting errors. Correlation of rings from the cores extracted from this tree were complicated due to a lack of cohesion between patterns of ring widths but the allocation of rings to calendar years gave a consistent result. The confidence in ring counting in this tree based on this analysis is acceptable (M. Trimble Baring Head pine correlation A6.14).

In an attempt to answer this question and test for possible ring counting errors calendar dates assigned to the tree rings were increased by 1 year then plotted against $^{14}CO_2$ data again (Figure 4.3, Table 4.2). This correction does not seem to improve the agreement of the data, it appears to make the ^{14}C tree ring data too high relative to the $^{14}CO_2$ atmospheric record, and poor agreement of the two data sets is reflected by the negative t statistic average of -1.4. Conversely if the calendar dates are decreased by 1 year the tree ring data appears too low relative to the atmospheric record (Figure 4.3, Table 4.2) again poor agreement of the two data sets is found, reflected by the positive t statistic average of 3.5. This testing of Baring Head tree data set for ring counting errors by moving the assigned calendar dates shows that neither correction improves the data. In conclusion it appears that the original ring counting assigned to this tree is reasonable.

Despite evidence that suggests the Baring Head tree ring data is low relative to the $^{14}CO_2$ record these initial results illustrate two important points; trees sample $^{14}CO_2$ from air in a representative manner, and the agreement of the $F^{14}C$ results from the Baring Head tree with the $^{14}CO_2$ atmospheric record suggests that ^{14}C measurements in tree rings is a valid method to reconstruct $^{14}CO_2$ at the Kapuni site.

Baring Head ^{14}C tree ring results both cores

Baring Head tree all cores 1986-2013
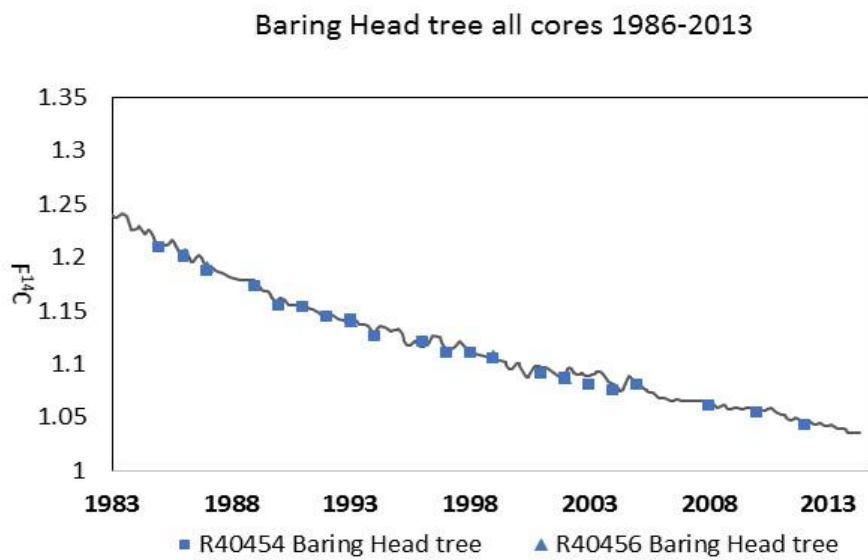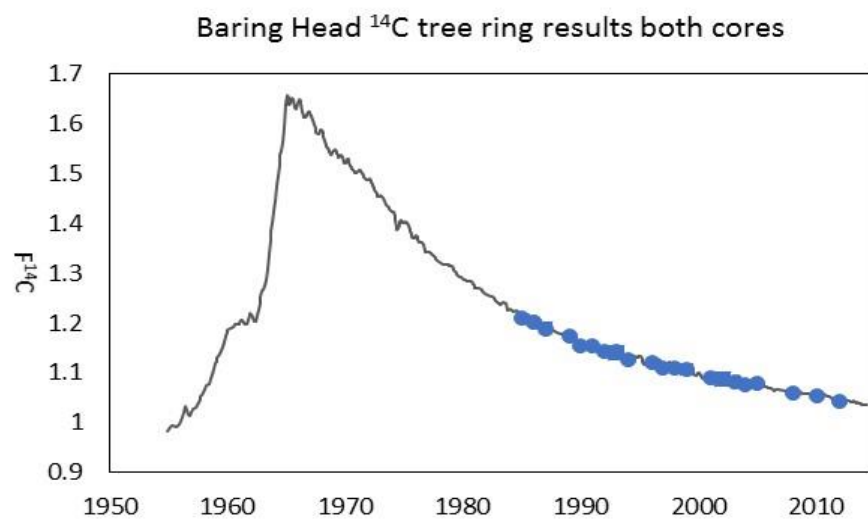
From top to bottom:

Figure 4.1   Baring Head tree ring F^{14}C data overlaid on atmospheric $^{14}CO_2$ smoothed data.

Table 4.1   t-test data Baring Head $^{14}CO_2$ data and Baring Head tree ring data.

R number	Data being compared	Average of T test values	Standard deviation T test values	Number of analyses
BHD tree R40454	BHD $^{14}CO_2$-R40454	1.01	1.65	22
BHD tree R40456	BHD $^{14}CO_2$-R40456	-0.24	0.85	4

Table 4.2   t-test data calendar corrections Baring Head tree ring data.

R number	Data being compared	Adjustment to Baring Head tree data	Average of T test values	Standard deviation T test	Number of analyses
BHD tree R40454	BHD $^{14}CO_2$-R40454	Minus 1 calendar year	3.5	2.3	22
BHD tree R40456	BHD $^{14}CO_2$-R40456	Minus 1 calendar year	3.4	2.1	4
BHD tree R40454	BHD $^{14}CO_2$-R40454	Plus 1 calendar year	-1.4	2.0	22
BHD tree R40456	BHD $^{14}CO_2$-R40456	Plus 1 calendar year	-1.5	2.2	4

t-statistic $^{14}CO_2$ -Baring Head tree R40454 & R40456

■ 14CO2- Baring Head tree R40454 ▲ 14CO2 -Baring Head tree R40456

Baring Head tree all cores calendar dates adjusted by 1 year

♦ Baring Head tree R40454 minus 1 calendar year
● Baring head tree R40456 plus 1 calendar year
♦ Baring Head tree R40454 plus 1 calendar year
● Baring Head tree R40456 minus 1 calendar year
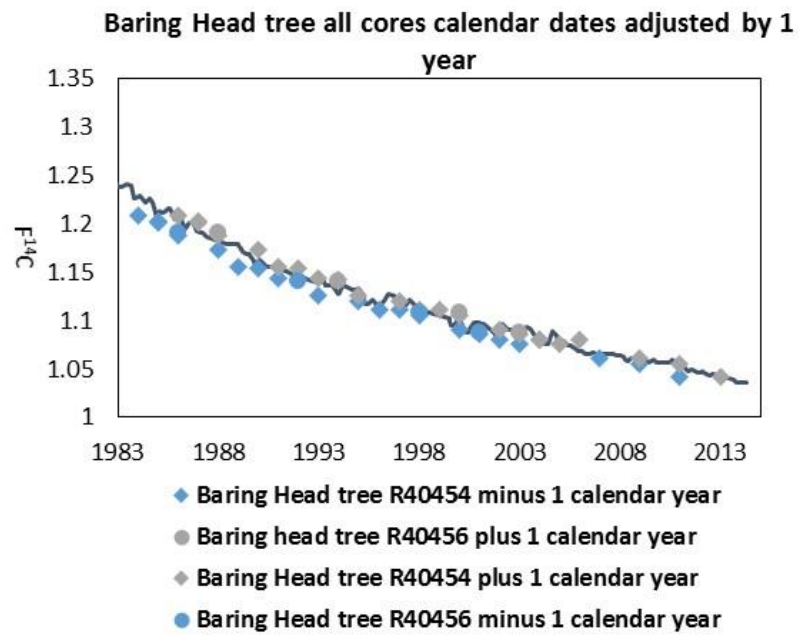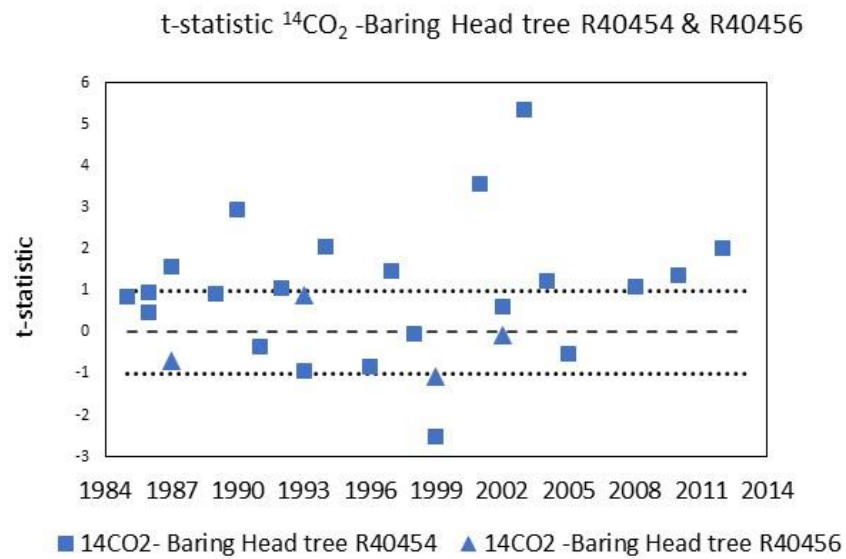
From top to bottom:

Figure 4.2   Students t- test Baring head $^{14}CO_2$ data and Baring Head tree.

Figure 4.3   Calendar corrections applied to Baring Head tree ring data.

4.2   Background Oak Tree at Kapuni

After establishing that the Baring Head tree was a reasonable proxy for the $^{14}CO_2$ record an Oak tree was sampled in a background location in Taranaki ~3 km upwind of the pollution sources at the Kapuni site (Figure 2.2, 4.4 & 4.6). The rationale for sampling the Kapuni background Oak (hereafter referred to as Kapuni Oak) is because it is expected that it should represent background $^{14}CO_2$ at Kapuni and also be comparable with the $^{14}CO_2$ record, but this needed to be tested in the same way as the Baring Head tree to see if this was true. If the Kapuni Oak is representative of $^{14}CO_2$ record it can be used to provide tree ring ^{14}C values for background in Taranaki for the CO_{2ff} calculations.

There are several points for discussion in the Kapuni Oak data, pre 1980 data where poor agreement was found, and post 1980 data where agreement with $^{14}CO_2$ data was good (Figure 4.4, 4.6). The 1978 ring for both cores is anomalous, a ring counting error was suspected as the cause of the poor agreement, ring correlation photographs were investigated for evidence of correlation or counting errors. A series of very narrow, close together rings with difficult to discern boundaries was observed for the period between 1975 and 1980 in the Kapuni Oak tree cores (Figure 4.7, 4.8). It is proposed that the anomalous results for 1978 are due to a related issue; cutting of the core into rings resulted in ring boundaries not being sampled properly and material from more than one annual ring incorporated into the sample.

Kapuni oak tree both cores R40444 and R40442

R40442 core
Kapuni Oak

Kapuni oak tree both cores R40444 and R40442
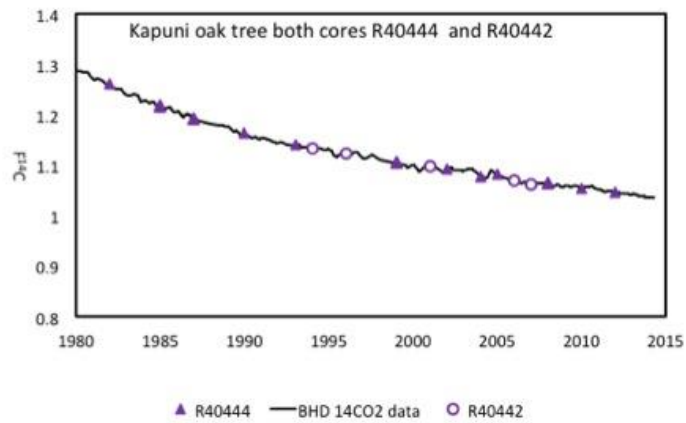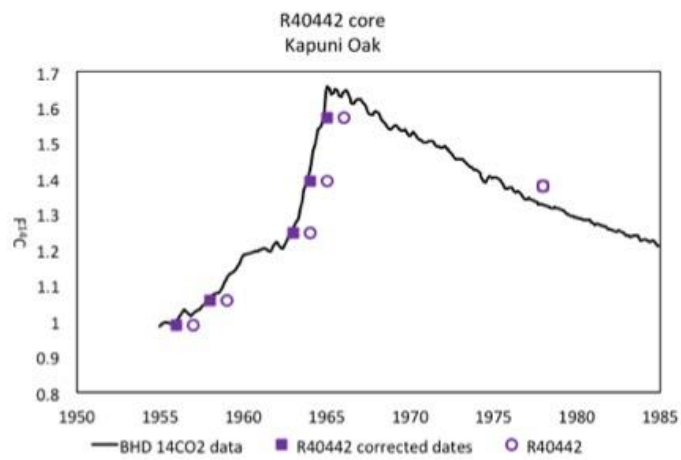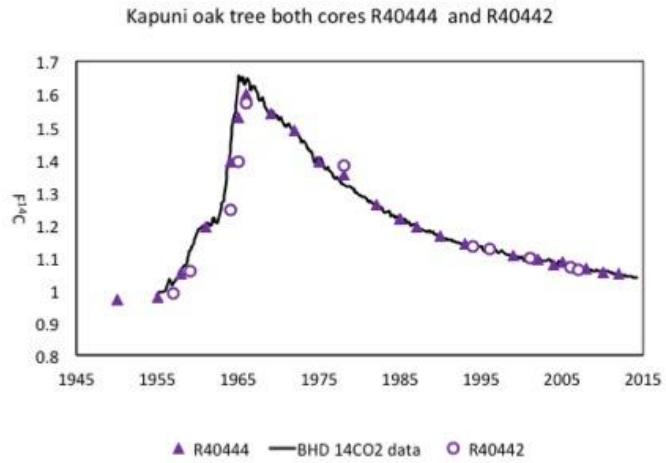
From top to bottom:

Figure 4.4   Kapuni background Oak tree ring $F^{14}C$ data overlaid on the $^{14}CO_2$ data.

Figure 4.5   Calendar correction applied to R40442 core data.

Figure 4.6   Kapuni background Oak $F^{14}C$ post 1980 data zoomed x scale.

.
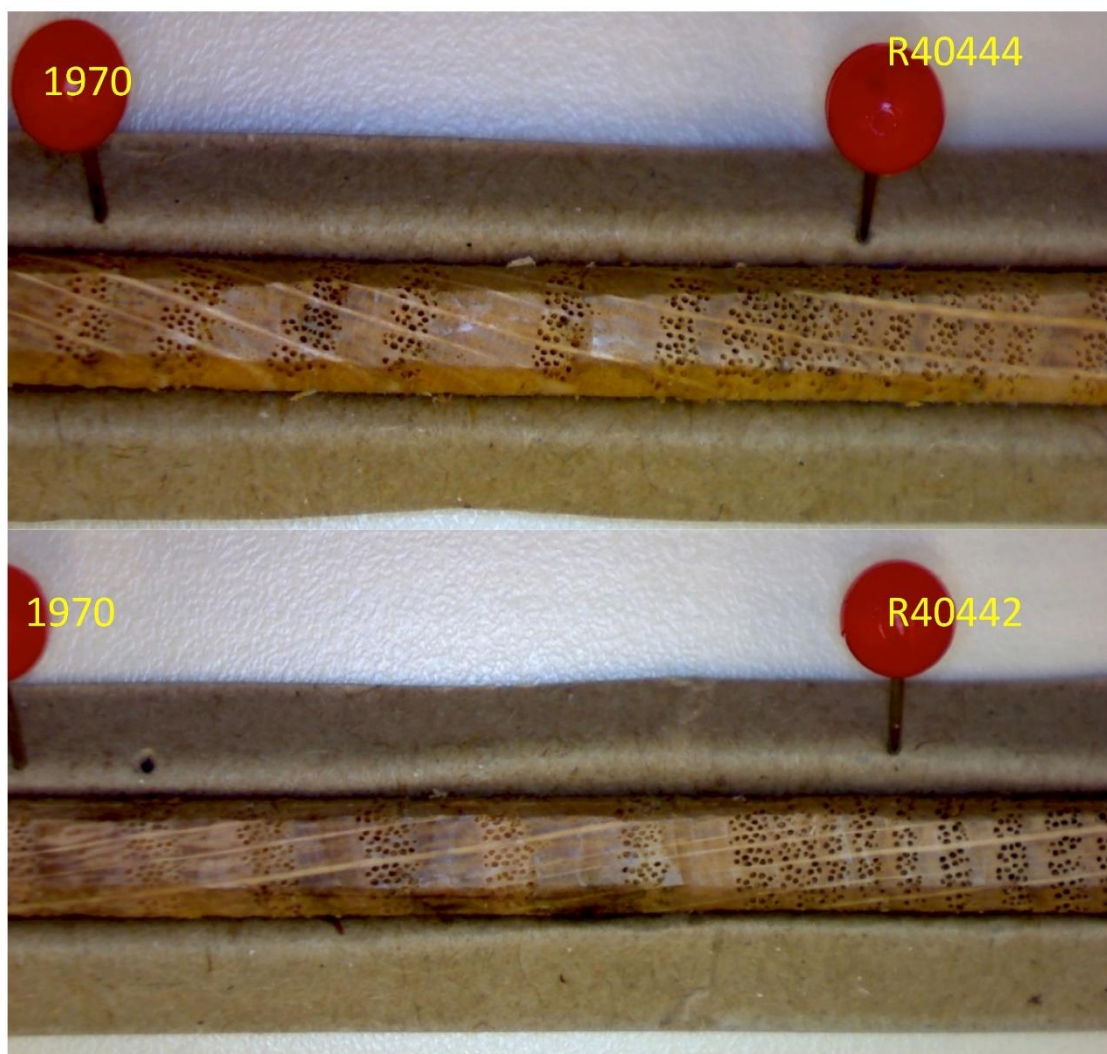
From top to bottom:

Figure 4.7   1970–1985 annual rings from R40444 core.

Figure 4.8   1970–1985 annual rings from R40442 core.

Early tree rings in both cores show poor agreement with the $^{14}CO_2$ data. R40442 core samples show a consistent lower offset from the $^{14}CO_2$ record but data from the R40444 core shows variable agreement with the atmospheric data. In the Oak core R40442 the offset from the atmospheric curve suggests an apparent ring counting error prior to 1978 (Figure 4.4). The offset suggests the rings have been assigned to a calendar year higher than it ought to be.

To test that decreasing the R40442 data by 1 calendar year would result in an improvement in agreement between tree rings and $^{14}CO_2$ data, a 1 year "correction" was applied to the data for 1955–1966, the corrected and uncorrected data was plotted against $^{14}CO_2$ data (Figure 4.5). A student's paired-t test was then used to statistically compare the two data sets (Table 4.3, Figure 4.9). The "correction" of 1 calendar year applied to R40442 core data greatly improves the agreement with $^{14}CO_2$ data with the t-statistic improving from 2.6 (uncorrected) to 0.4 corrected. This offset in early tree rings of the R40442 core suggests the result of a missing ring; which has the effect of rings being assigned to a later year than truth. The correlation photos were examined for evidence of a locally missing ring in the R40442 core, but this could not be established. After 1978 the next ring measured was 1994, from this point on results compare well to $^{14}CO_2$ atmospheric record, with a t-statistic of -0.1 (Table 4.4, Figure 4.10). It is very rare for Oak to produce missing rings (Baillie 1973, English Heritage 1998) so the possibility of a missing ring in the Kapuni Oak tree seems low unless the tree was subject to storm damage or attack. It is more probable that the error is a result of a locally absent growth ring in the R40442 core that was not replicated in the R40444 core. However, the most likely possibility is a misinterpretation of a large ring in the core which should have been identified as two separate rings. The last two scenarios would both result in a one year counting error with the ring assigned a calendar date one year later than it should have been and would explain the offset of the data from the curve.

t- statistic $^{14}CO_2$-Kapuni Oak tree both cores all years

▲ 14CO2 -Oak R40444   ● 14CO2 - Oak R40442
○ 14CO2-Oak R40442 corrected

t-statistic $^{14}CO_2$ -Kapuni Oak tree both cores data after 1980

▲ 14CO2 -Oak R40444   ● 14CO2 - Oak R40442
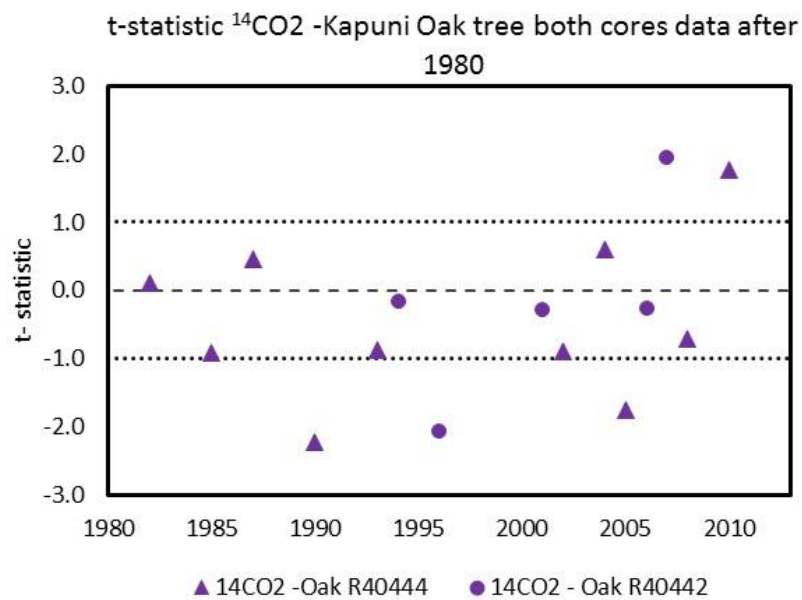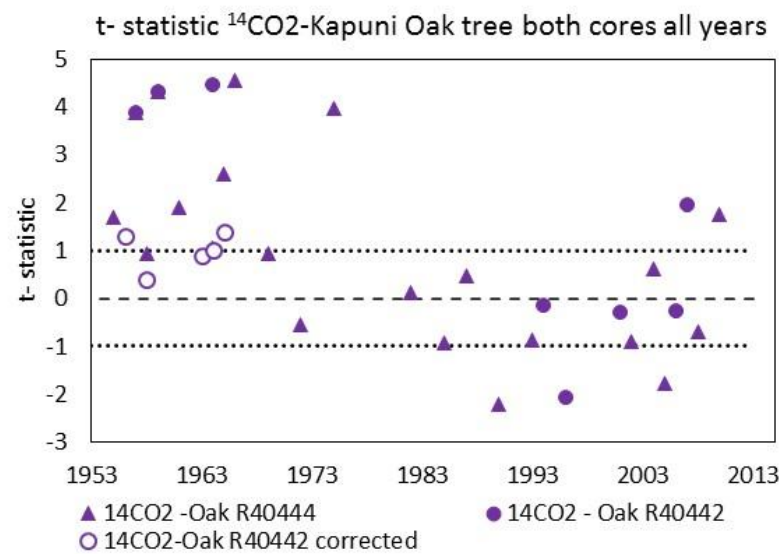
From top to bottom:

Figure 4.9   t-test $^{14}CO_2$ atmospheric data and Kapuni Oak tree.

Figure 4.10   t-test $^{14}CO_2$ atmospheric data and Kapuni Oak tree data after 1980.

Table 4.3   t-test of Kapuni Oak tree data R40442 core and $^{14}CO_2$ data.

R numbers	Data being compared	Average T test value	Standard deviation T test	Number of analyses
R40442 uncorrected	BHD $^{14}CO_2$ – Oak tree	2.6	3.3	10
R40442 corrected	BHD $^{14}CO_2$ – Oak tree	0.4	1.2	10
R40444	BHD $^{14}CO_2$ – Oak tree	1.0	2.0	21

Table 4.4   t-test of Kapuni Oak tree data R40442 core and $^{14}CO_2$ data post 1980.

R Numbers	Post 1980 Data	Average T test value	Standard deviation T test	Number of analyses
R40444 (1982–2010)	BHD $^{14}CO_2$ – Oak tree	-0.5	1.2	10
R40442 (1994–2007)	BHD $^{14}CO_2$ – Oak tree	-0.2	1.4	5

Early tree ring results from the R40444 core have more variable agreement with $^{14}CO_2$ data and it is hard to discern whether any ring counting errors have been made, but with no evidence of a consistent bias ring counting errors are not likely. The t-statistic for the complete R40444 core is 0.99, and as agreement with $^{14}CO_2$ data is variable a correction to assigned calendar years could not be justified. Rings after 1980 for R40444 correlate well with $^{14}CO_2$ atmospheric data, with the t-statistic -0.5 (Table 4.3). The much better correlation of post 1980 data supports the assessment that an error was made in the counting of the early rings of core R40442 and an unidentified problem with the R40444 core is causing poor agreement with the $^{14}CO_2$ record. Overall confidence in the ring counting analysis of the Kapuni Oak tree was high due to a reasonable degree of correlation between ring width patterns and the visible nature of the ring boundaries (M. Trimble Oak tree correlation A6.11).

Two possible scenarios exist for unsatisfactory agreement with $^{14}CO_2$ data by the R40444 core. A bias could be created between the atmospheric data and the tree ring data due to a difference in averaging of ^{14}C content of the atmosphere and the tree rings. $^{14}CO_2$ increased sharply by ~120‰ from 1957–1959, with large oscillations near the bomb peak and it is possible that an offset between the two data sets is produced.

The $^{14}CO_2$ record is based on CO_2 absorbed from air discrete air samples collected continuously over a period of several weeks with several data points being produced per year (and some un-sampled periods), so as a result $^{14}CO_2$ is averaged across day and night. Tree ring ^{14}C results represent a whole year of growth of photosynthetic material with an average of 8 months of assumed sampling time, with trees effectively averaging $^{14}CO_2$ only during daylight periods (Bozhinova et al. 2013). To try to minimise differences between the data sets the $^{14}CO_2$ data was averaged for the same 8 month period as the trees are assumed to be photosynthesising. Despite the best efforts to align the two data sets it is possible, and even likely, during this period of high $^{14}CO_2$ variability some differences will become apparent.

The second possibility is recycling of stored nutrients by the tree in the early spring growth. This has only been reported for Oak trees and is an important consideration for stable isotope analysis because the $\delta^{13}C$ of the early-wood tends to be more closely correlated with the late-wood of the year before. Often the early-wood is removed to

avoid biasing data (Hill et al. 1995, McCarroll and Loader 2004, Switsur et al. 1995). This may be of little consequence for radiocarbon analysis generally, but the change in ^{14}C in the post bomb years is very large and therefore annual rings could contain ^{14}C from a wide variety of time stamps. If portions of the tree ring were inhomogeneous and received more of the early-wood than other years or in some years this was more noticeable, this could potentially explain some of the variability of the Oak sample.

4.3   Comparison of the Kapuni Oak and the Baring Head tree

The ^{14}C data from the Kapuni Oak tree was compared to the ^{14}C of the Baring Head tree to assess the agreement between the two data sets, both tree represent background conditions so ^{14}C should be similar, comparison is possible for where the data sets overlap 1985–2012 (Figure 4.11).

The statistical difference between the two data sets is tested with a student's t test (Table 4.5, Figure 4.12). The average t-statistic of 1.7 for the Kapuni Oak/Baring Head tree ring results shows that the Kapuni Oak tree ring results are consistently slightly higher than the Baring Head tree ring results. Although both of these trees agree reasonably well with the atmospheric record and the ring counting for both trees seems reasonable, causes for poor agreement between the Baring Head tree and the Kapuni Oak could be due to differences caused by the species of the tree and climatic factors. Oak and Pine trees may have different periods of dormancy, and possible climate differences between Baring Head and Taranaki could feasibly create a difference in the effective time period that the trees photosynthesize and thus sample the atmosphere.

Table 4.5   t- test of Kapuni Oak both cores and Baring head tree ring data.

R numbers	Tree being compared	Average T test value	Standard deviation T test	Number of analyses
R40442-R40454	Oak-Baring Head tree	2.6	1.0	3
R40444-R40454	Oak-Baring Head tree	1.9	1.6	10
R40444-R40456	Oak- Baring head tree	0.7	1.7	4

Kapuni Oak and Baring Head tree corresponding year

t -Test of Kapuni Oak-Baring Head tree
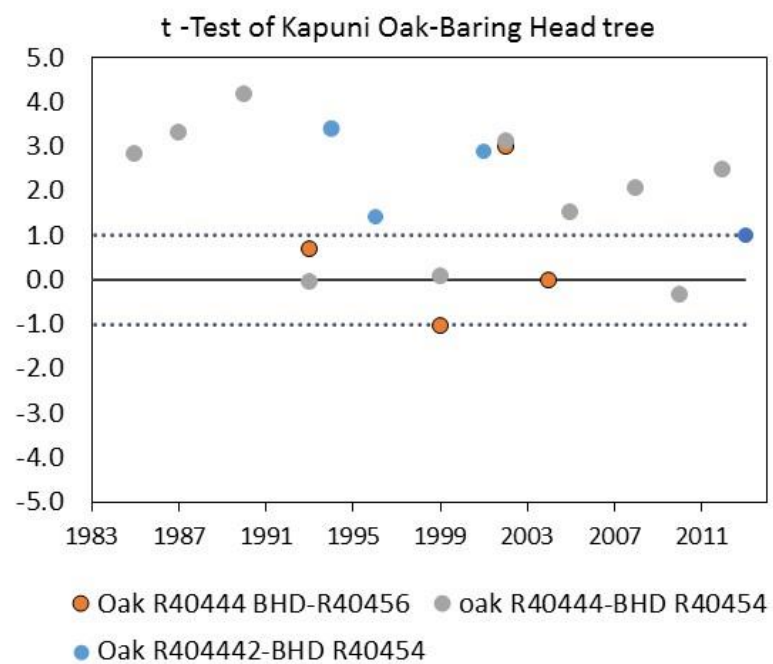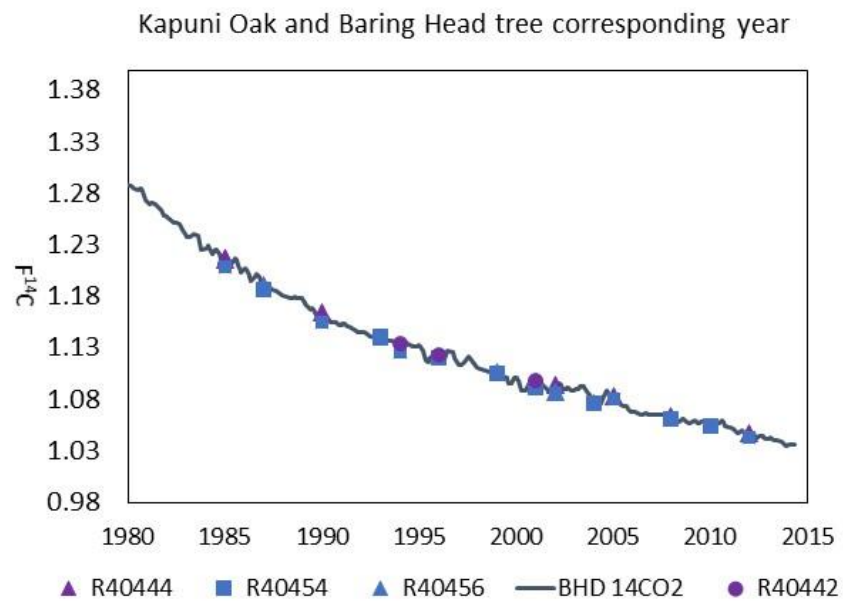
From top to bottom:

Figure 4.11   F^{14}C Kapuni Oak and Baring Head tree rings.

Figure 4.12   t test Kapuni Oak tree data with Baring Head tree.

4.3.1 Choice of data set to provide the Δ_{bg} term for the project calculations

Based on ^{14}C results it can be concluded that background conditions at Kapuni are similar to Baring Head, and that either location could be used to provide background ^{14}C information. In addition the testing of the Baring Head tree and the Kapuni Oak tree demonstrate that trees sample the atmosphere is a representative manner and both trees represent background clean air conditions.

In order to calculate CO_{2ff} for the polluted trees data is required for background levels of ^{14}C for the Δ_{bg} term of the equation. The Baring Head atmospheric [14]CO_2 data set was adopted as it is a well-established accurate record that consists of hundreds of samples consisting of air, flask and static absorption over NaOH and the record is correlated with other peer reviewed international [14]CO_2 records. The Baring Head tree ring data supports the Baring Head atmospheric data, agreement of the two data sets suggests that the atmospheric [14]CO_2 record will be a good proxy for the background conditions at Kapuni.

The Kapuni Oak tree was sampled because it was reasoned that it would make a suitable local background for the polluted Kapuni trees as it is subject to similar conditions but without influence of CO_{2ff}. However as the early tree ring dates for the Oak are questionable, the cause of which is interpreted as being caused by ring counting and sampling errors. Unfortunately the questionable dates cast doubt over the entire Oak data set thus we consider the Oak tree data set to be unreliable and reject it for use as the background.

4.4   Polluted trees

4.4.1   Luscombe Chestnut tree ring data

Luscombe chestnut F^{14}C tree ring results
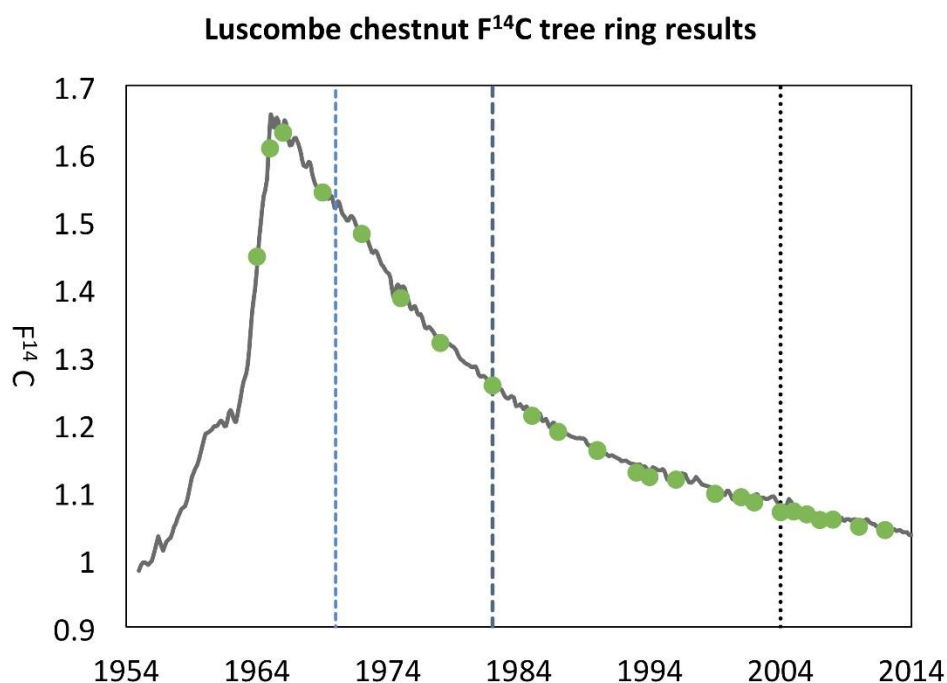
Figure 4.13   F^{14}C results from Luscombe chestnut tree ring.

Having established that tree ring method works and measurements of ^{14}C can reproduce historic $^{14}CO_2$ values, the method is now applied to trees growing in a polluted location at the Kapuni site. The Luscombe chestnut tree is located ~850m in a secondary downwind location from the Vector and Ballance sites. Its position relative to the sites means that it should receive CO_{2ff} emissions from both sites particularly in Northerly conditions but little from the West (Figure 2.2).

Correlation between two of the four cores extracted from the Luscombe chestnut tree were problematic, and thus two cores were rejected based on difficulty of correlating patterns between the rings. However two further cores were able to be correlated successfully (M. Trimble Luscombe chestnut correlation A6.12). Based on the excellent agreement of the Luscombe chestnut tree ^{14}C results with the atmospheric curve prior to 1970 (Figure 4.13), it appears the correlation and counting of the rings was very accurate, and a high level of confidence can be placed in these results.

Luscombe chestnut tree ring results are presented in (Figure 4.13). Each data point represents a ^{14}C result from a single annual tree ring, data is overlaid on the $^{14}CO_2$ atmospheric curve. The data shows excellent agreement with the Baring Head curve until 1970 when emissions from the Vector Plant begin. After 1970 Luscombe F^{14}C values decrease because of CO_{2ff} influence from the Vector plant which contains no ^{14}C, the decrease in F^{14}C is indirectly related to the amount of CO_{2ff} added (Table A6.1 Appendices).

The Luscombe chestnut tree represents early post bomb data 1960–1965 more successfully than the Kapuni Oak sample for the same time period. The earlier opinion that there is a difference in atmospheric averaging of the Kapuni Oak tree versus the $^{14}CO_2$ record while possible, are not replicated by the Chestnut tree perhaps because of differences in Oak and chestnut growth periods.

4.5   Vector Pine tree
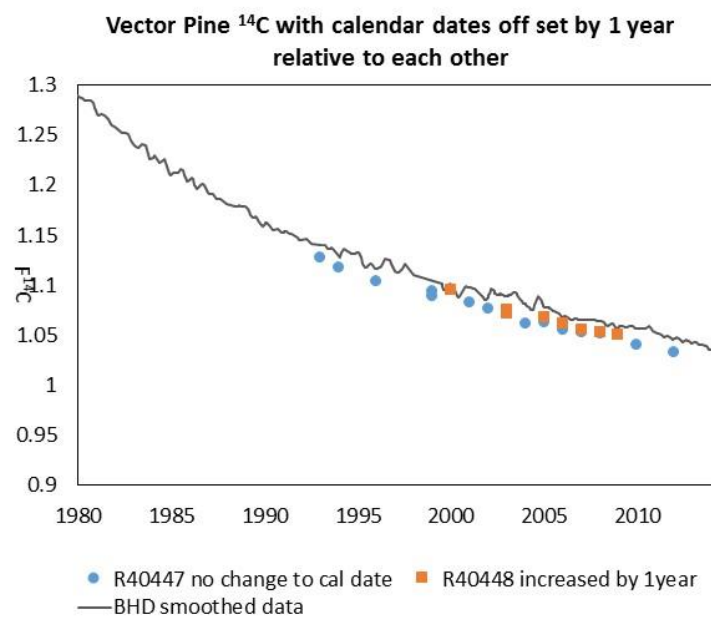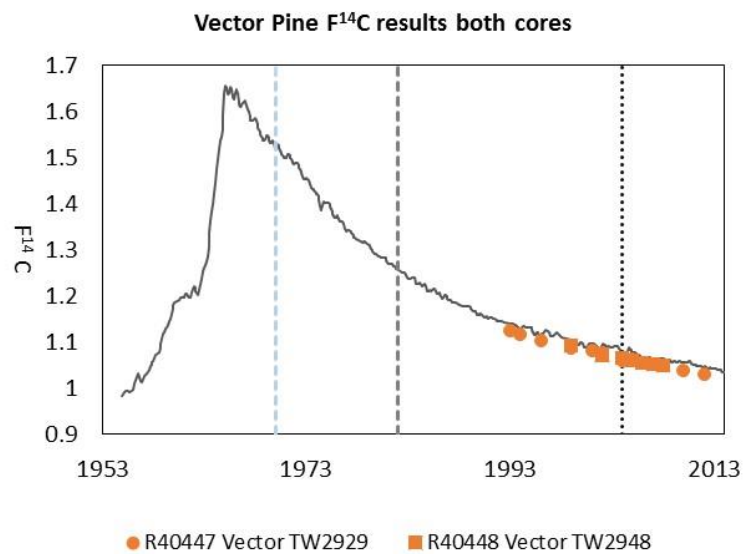
From top to bottom:

Figure 4.14   F^{14}C results Vector pine tree.

Figure 4.15   Correlation test of Vector pine F^{14}C data.

The Vector pine (Monterey pine *Pinus radiata,* same species as the Baring Head tree), is expected to receive a large CO_{2ff} signal from both sites because of its close proximity to the sources (Figure 2.2). It is a relatively young tree, the earliest ring where a good correlation between the different cores was able to be made is 1992 therefore emissions from the plant can only be assessed starting in the early 90's. Overall confidence in correlation and counting for this tree is low due to difficulty caused by variances in patterns and clarity of ring boundaries but the overall the allocation of calendar years is expected to be ± 1–2 year at most (M. Trimble Vector pine correlation A6.13). To test the correlation of the Vector tree the assigned calendar dates from one core were moved relative to the other core and $F^{14}C$ plotted with the adjusted calendar scale. The data which was clustered together in the original plot (Figure 4.14) was spread apart by this correlation test and no longer agreed (Figure 4.15) this confirms that the correlation of the cores is consistent and most likely correct.

Vector pine tree results plotted on the $^{14}CO_2$ atmospheric curve (Figure 4.14). Each data point represents a $F^{14}C$ result from a single annual tree ring from two cores sampled from the same tree as a check on sample reproducibility and counting errors. The tree ring data shows that CO_{2ff} emissions devoid of ^{14}C are detected in the tree ring results. The ^{14}C results for the tree ring samples are consistently lower than the ^{14}C atmospheric results and which are indirectly related to the amount of CO_{2ff} added. The Vector pine contains lower $F^{14}C$ relative to the Luscombe tree and the degree of deviation of the Vector pine from the $^{14}CO_2$ curve demonstrates that the tree sees higher levels of CO_{2ff} than the Luscombe tree (Table A6.2 and Table A6.3 Appendices).

4.6 Calculation of CO_{2ff} from ^{14}C data

4.6.1 Record of historic CO_2 concentrations for the project

CO_2 concentration data is required to make CO_{2ff} calculations. There is an established record of CO_2 concentration data measured at Baring Head Wellington from 1970 (Brailsford et al. 2012, Stephens et al. 2013). As the Baring Head record $^{14}CO_2$ is used to provide a basis for background conditions at Kapuni it is reasonable to apply the Baring Head CO_2 concentration record as a proxy for CO_2 concentrations at Kapuni as well. To apply the Baring Head CO_2 concentration data to calculate CO_{2ff} it was averaged over an

8 month period from September to April to replicate CO_2 concentrations during photosynthesis. An uncertainty was calculated for the 'averaged' data by taking the standard deviation of the individual measurements (Table A6.5 Appendices).

4.6.2 Baring Head $^{14}CO_2$ data

Baring Head $^{14}CO_2$ data was averaged for the 8 month period September to April to calculate an annual value for the Δbg term of the mass balance equation. The uncertainty for the annual Baring Head $Δ^{14}C$ was calculated by taking a standard deviation of the individual measurements. Results for the years 1955–1965 were subject to large variability in ^{14}C concentration and lower precision and are often based on relatively few data points. In the original $^{14}CO_2$ data set there were no $^{14}CO_2$ measurements in 1999 (Currie et al. 2011). In the new data set a smooth curve fit analysis has gap-filled missing 1999 $^{14}CO_2$ data (Turnbull et al. 2015) (Table A6.4 Appendices).

4.6.3 Emissions data

Monthly (2004–2013) and annual emissions (1991–2004) from the Vector plant were provided by P Stephenson (Vector). Emissions are assumed to be constant with reported variability of 3% within a 24 hour period (Turnbull et al. 2014). Monthly emissions for the months of April–September (2004–2013) were tabulated and averaged to represent the 8 months of the year when trees are assumed to be photosynthesising. Detailed emission information prior to 2004 could not be obtained and data is based on an average annual figures recorded from the months from July–June. The pre 2004 data is subject to higher errors due to changes in the way emissions were calculated at the plant (P. Stephenson pers comm) and because of the disparity between the values produced for 2004 calculated using monthly figures versus annual data (Table A6.6, Table 4.6).

Ballance emissions for the years 1990–2013 were obtained from the biennial monitoring report produced by Taranaki Regional Council (2013 b). Ballance reports both CO_2 emissions and tonnes of urea produced per annum.

1. Using annual urea production figures CO_{2ff} emissions were calculated using a factor that estimates CO_2 production based on lifecycle analysis produced by Ledgard et al. (2011).

2. Annual CO_2 emission figures were used to estimate a monthly total CO_{2ff} emission rate then the calculated totals CO_2 versus the urea CO_2 emissions were compared. The two estimates of CO_2 are in good agreement (Table 4.6).

It was assumed that both emission sources produce simultaneous and near constant emissions which reach both of the polluted trees depending on wind conditions. Emissions data from Vector and Ballance CO_2 data were summed and the total plotted against CO_{2ff} values for the Luscombe chestnut and Vector pine tree using a different colour to denote pre 2004 emissions and post 2004 emissions (Table 4.7, Figure 4.16 and 4.17).

Table 4.6 CO_2 emissions and urea production from Ballance agri-nutrients ammonia urea plant.

Year from 1 July to 30 June	Ballance Annual emissions CO_2 Tonnes/yr	Tg C yr^{-1} calculated from CO_2 emissions	Tonnes of Urea per annum	Tg C yr^{-1} calculated from urea production
1999/2000	171100	0.05	218034	0.06
2000/2001	179000	0.06	247575	0.06
2001/2002	186900	0.06	235755	0.06
2002/2003	183170	0.06	260316	0.07
2003/2004	190000	0.06	262674	0.07
2004/2005	182202	0.06	263703	0.07
2005/2006	185046	0.06	256281	0.07
2006/2007	199636	0.06	256519	0.07
2007/2008	187905	0.06	245163	0.06
2008/2009	156486	0.05	222047	0.06
2009/2010	189731	0.06	251269	0.06
2010/2011	194521	0.06	252140	0.06
2011/2012	102209 **+**	0.03	107391	0.03
2012/2013	170650	0.05	243841	0.06

Calculation from tonnes of urea utilises a factor from lifecycle analysis 0.936 (Ledgard et al. 2011 and the resulting CO_2 is converted into TgC.

Tonnes urea x 0.936/1000000/(44.01/12.01) TgC

+ Ballance plant production was low in 2011 because of a fire which shut production down for several months.

Table 4.7   Combined Ballance and Vector CO_{2ff} emissions.

Year	Combined Vector CO_2 and Ballance CO_2 data gCS^{-1} *	Combined Vector CO_2 and Ballance Urea CO_2 data gCS^{-1}	Tg C yr^{-1} Vector and Ballance
1999/2000	3611	3656	0.13
2000/2001	3732	3915	0.14
2001/2002	4394	4426	0.16
2002/2003	3888	4125	0.14
2003/2004	5776	5970	0.21
2004/2005	6907	7175	0.25
2005/2006	7310	7503	0.27
2006/2007	7442	7510	0.27
2007/2008	6237	6326	0.23
2008/2009	6324	6254	0.23
2009/2010	7295	7412	0.27
2010/2011	7121	7202	0.26
2011/2012	6184	6051	0.23
2012/2013	6113	6343	0.22

* used for CO_{2ff} plots

4.6.4 CO_{2ff} Calculations

CO_{2ff} calculations were made for the polluted trees using the mass balance equation 1.1 described in section 1.3, using CO_2 concentration information and $^{14}CO_2$ data from Baring Head described above section 4.61 and 4.62.

4.7 CO$_{2ff}$ results
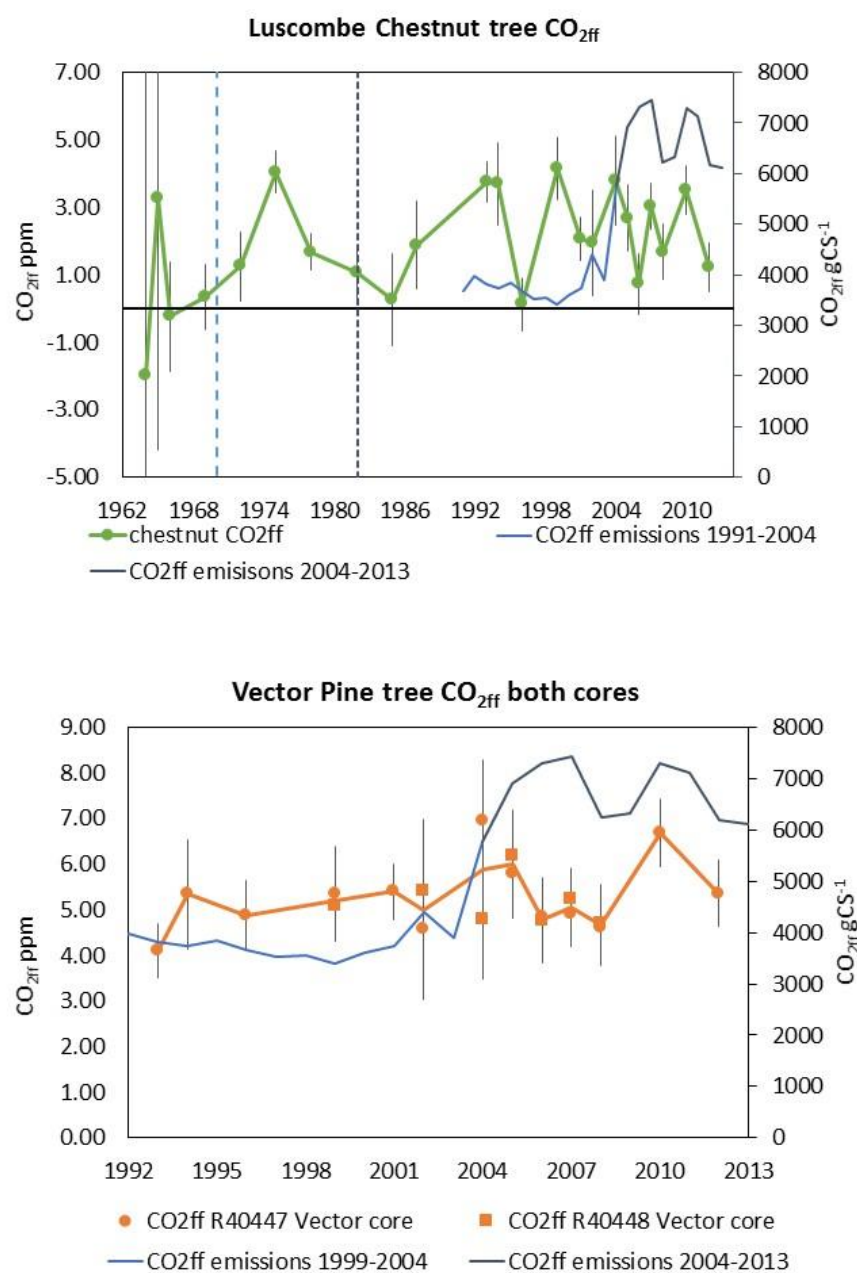
From top to bottom:

Figure 4.16   Calculated CO$_{2ff}$ data plotted with uncertainties Luscombe chestnut tree.

Figure 4.17   Calculated CO$_{2ff}$ data plotted with uncertainties Vector pine tree.

4.7.1 Luscombe chestnut

Observed CO_{2ff} emissions in the Luscombe chestnut tree are presented in (Figure 4.16). The years 1970 and 1982 are denoted by dotted lines. CO_{2ff} was calculated for four years prior to 1970 to demonstrate that pre 1970 emissions are indistinguishable from zero with a weighted mean of 0.2 ppm ± 0.8 ppm (Table 4.8). After 1970 CO_{2ff} values in the Luscombe chestnut are 1–4 ppm with a weighted mean of 2.3 ± 0.2 ppm (1972–2012). There is quite a lot of variability displayed by the CO_{2ff} results that is investigated later by comparison with the meteorological information section 4.81.

Table 4.8   Trends in CO_{2ff} data Luscombe chestnut tree.

Time period	Weighted mean CO_{2ff}	Combined emissions Vector and Ballance Tg yr^{-1}
1964–1969 (pre 1970)	0.2 ± 0.8 ppm	nil
1972–2012	2.3 ± 0.2 ppm	N/A
1972–1982	2.2 ± 0.3 ppm	N/A
1982–2003	2.3 ± 0.3 ppm	0.14 (2003)
2004–2012	2.3 ± 0.3 ppm	0.23

4.7.2 Vector Pine tree

Observed CO_{2ff} emissions in the Vector pine tree are between 4–7 ppm with a weighted mean of 5.2 ± 0.2ppm (1972–2012) (Figure 4.17, Table 4.9). Results from the two cores agree within the uncertainty limits. Higher CO_{2ff} values are observed in the Vector Pine than in the Luscombe Chestnut tree caused by an increased input of CO_{2ff} related to the closer proximity and orientation of tree relative to the emission sources, as a result the Vector pine tree receives a larger CO_2 signal overall.

Table 4.9   Trends in CO_{2ff} data in Vector Pine.

Time period	R40447 core CO_{2ff} weighted mean	R40448 core CO_{2ff} weighted mean	Combined emissions Vector and Ballance Tg yr^{-1}
1993–2012	5.2 ± 0.2pppm	N/A	N/A
1993–2003	5.0 ± 0.3ppm	N/A	0.14 (2003)
2004–2012	5.5 ± 0.3ppm	N/A	0.23
1999–2008	N/A	5.1 ± 0.7ppm	N/A

4.8   Assessment of results using Meteorological data

Meteorological information comprising wind strength and direction was analysed and information relevant to the growth season of the trees was selected from the data set to represent conditions that the trees experience during photosynthesis. There is no meteorological station located at Kapuni so wind data was collected from the Hawera AWS weather station ~20km away to act as a proxy for conditions at Kapuni (Cliflo 2014). A temporary meteorological station was installed at the Kapuni site during 2013 that was provided some data for Turnbull et al. (2014). There is a short period of time (1 month) where the temporary meteorological station data can be compared to Hawera data. An analysis of correlation between Hawera meteorological station and the temporary meteorological station installed at the Kapuni site was provided by Liz Keller. The correlation was reasonable and thus it is reckoned to be a reasonable proxy for conditions at Kapuni (Keller et al. in preparation).

Hourly wind information was sorted for daylight hours 08:00–16:00 local time between September April for the years 2004–2012 to construct wind roses which illustrate in graphical format wind speed, direction and frequency (Figure 4.18). Meteorological data was analysed to create the wind roses by Liz Keller for the project.
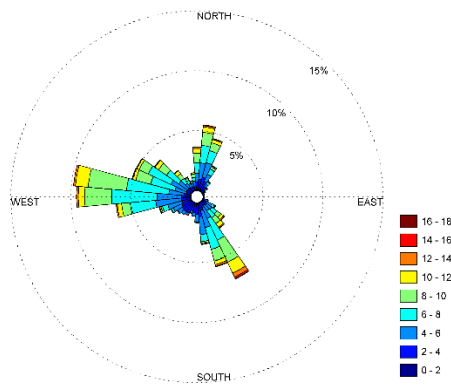
Figure 4.18   Wind rose for Hawera averaged data for 2004–2012.

4.8.1   Qualitative analysis of contribution of Ballance and Vector sources to Luscombe chestnut and Vector pine in different wind conditions

The dominant prevailing wind condition at the Kapuni site is Westerly, winds from the South and North East occur less often. To assess how wind patterns affect atmospheric transport the wind information was sorted and plotted to create histograms of wind speed for the wind 3 types on an annual basis (Table A6.7 Appendices). The wind types were grouped based on their trajectories, Westerly >230 and <330 degrees, South Easterly >100 and <220 and North Easterly >330 and <80 (Figures 4.19 and 4.20 and 4.21 and 4.22) show representative histograms. Only 2 small sectors of wind directions were not included (80–100 and 220–230) and on average this excluded about 100 observations in 1 calendar year or 4% of the data. Only a tiny proportion of the data has wind speeds of <2 meters per second. Removal of low wind speeds did not affect the overall frequency of wind types so all wind speeds were retained.

Figure: 200405 all wind directions

Figure: 2004_05 Westerly winds

Figure: 2004_05 South East winds

Figure: 2004_05 North East winds
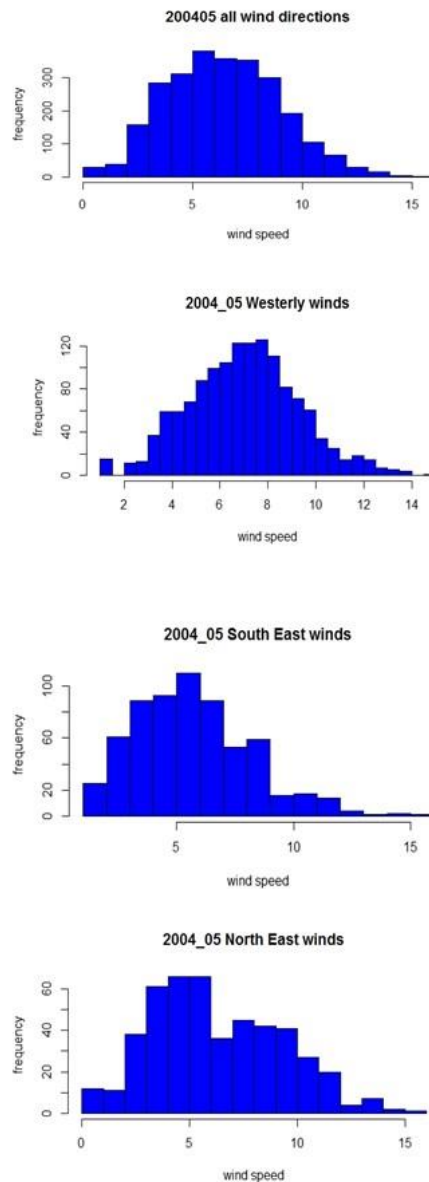
From top to bottom:

Figure 4.19   Histogram September to April 2004–2005 all wind speeds and directions.

Figure 4.20   Histogram September to April 2004–2005 Westerly winds.

Figure 4.21   Histogram September to April 2004–2005 South East winds.

Figure 4.22   Histogram September to April 2004–2005 North East winds.

A qualitative assessment was made of the possible trajectory of the plume from both of the CO_{2ff} sources under the three different weather patterns and how this might influence CO_{2ff} at the trees location. Coordinates of trees and sources were determined from a distance and bearing calculator ([http://www.moveable-type.co.uk/scripts/latlong.html)](http://www.moveable-type.co.uk/scripts/latlong.html) (Tables 4.10, 4.11, Figure 2.2).

Table 4.10   Qualitative assessment of signal of CO_{2ff} at Vector tree.

Source	Compass Bearing	Distance source to tree	Wind conditions NE <80 >330	Wind conditions SE >100 and <220	Wind conditions W >230 and <330
Vector	172	0.28km	Large signal	No signal	Significant signal due to proximity
Ballance	120	0.72km	Unlikely	No signal	Large signal

Table 4.11   Qualitative assessment of signal of CO_{2ff} at Luscombe chestnut tree.

Source	Compass Bearing source to tree	Distance of source to tree	Wind conditions NE <80 >330	Wind conditions SE >100 and <220	Wind conditions W >230 and <330
Vector	203	0.87km	Small signal	No signal	Signal unlikely
Ballance	164	0.92km	Large signal	No signal	Signal unlikely if wind direction constant

The Vector tree is closer to the Vector source than the Ballance source and in a primary downwind location (Figure 2.2, Table 4.10). Qualitative analysis suggest that in North East conditions the Vector pine sees a large signal from Vector but is not likely to get a signal from Ballance. In Westerly conditions the Vector pine sees a significant signal from Vector (due to the proximity of the source to the tree) and a large signal from Ballance. In South Easterly conditions the plume is blown away from the tree and there should be no signal.

The Luscombe Chestnut tree is located in a more distant secondary downwind location (Table 4.11, Figure 2.2). Analysis suggests that in North Easterly conditions the tree sees a small signal from Vector and a large signal from Ballance. In Westerly conditions the Luscombe chestnut is unlikely to see the plume from the Vector plant and possibly gets a small signal from the Ballance plant especially if the wind is not constantly from the West. In South Easterly conditions the plume is pushed away from the trees. This implies that in years when the frequency of wind patterns change one or other of the sources exerts a more dominant influence on the trees, and as wind strength and magnitudes of the sources also vary this creates quite a complicated pattern that must be a significant factor in the variability of the observed CO_{2ff} data.

Further qualitative analysis can be made using the metrological data, this time comparing frequency of the three different wind types with observed CO_{2ff} data. The Hawera meteorological data (2004–2012) was sorted into three wind direction groups and frequency and mean wind speed calculated for each wind type for each year (Table A6.7 Appendices). Westerly winds have the highest mean speed winds, whereas winds from South and North East tend to have somewhat lower wind speeds and there is significant temporal variation in the frequency of the wind directions observed. To see if any associations can be made between the frequency of the wind types and CO_{2ff} data, a plot was constructed of frequency of wind types for comparison with the observed CO_{2ff} in the Vector tree and Luscombe chestnut tree. Comparisons are restricted to the years where meteorological data is available 2004–2013 (Table A6.7, Figures 4.23, 4.24 & 4.25).
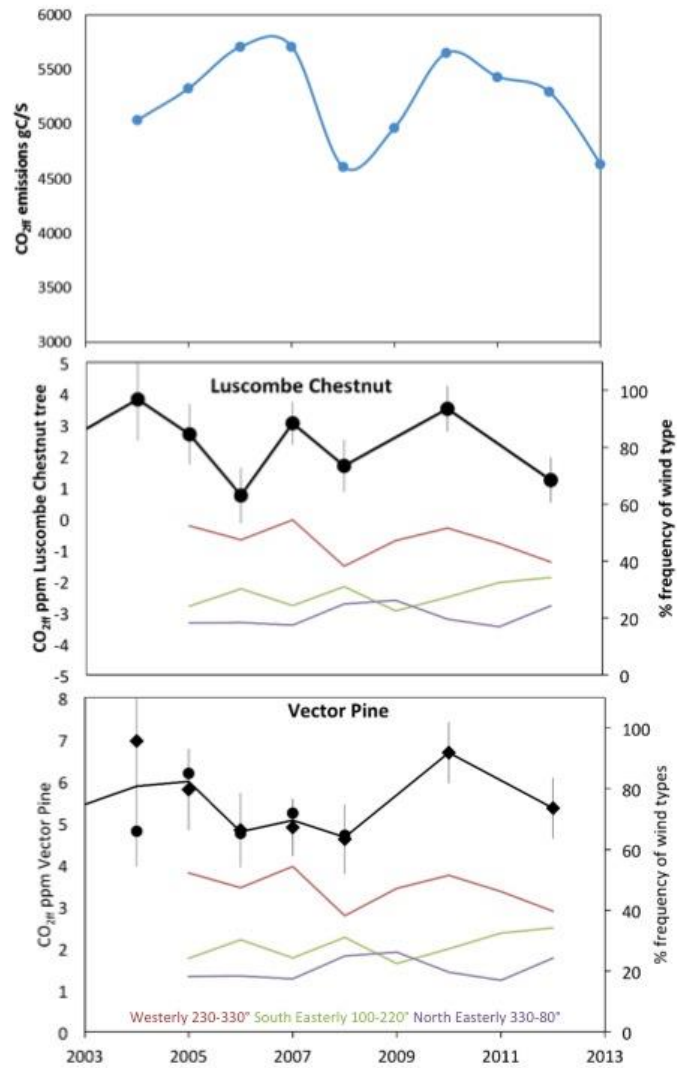
From top to bottom:

Figure 4.23   Combined CO_{2ff} emissions data from Vector and Ballance plants.

Figure 4.24 CO_{2ff} data from Luscombe chestnut plotted with frequency wind types.

Figure 4.25 CO_{2ff} data from Vector pine plotted with frequency wind types.

Analysis of (Figures 4.24, 4.25) suggests a correlation between an increase in CO_{2ff} and frequency of Westerly winds as shown by the agreement of the frequency of Westerly wind patterns and increased CO_{2ff} in both trees while there appears to be a negative correlation for frequency of South Easterly conditions and observed CO_{2ff}. An increase in North Easterly conditions appear to have little influence on CO_{2ff} concentrations. The other thing notable in the plots is a correlation appears to exist with CO_{2ff} increasing between 2008–2010 and decreasing between 2010–2012 in both trees consistent with an increase rise and fall in total emissions in the same years (Figures 4.23, 4.24, 4.25, Table 4.7).

An association between Westerly wind patterns and an increase in CO_{2ff} is easily explained in the Vector tree and is consistent with the tree seeing emissions of CO_{2ff} from Ballance and Vector, but is harder to reconcile the pattern of increased CO_{2ff} emissions at the Luscombe chestnut tree. The previous assessment suggests that it is unlikely that either source provides CO_{2ff} to the Luscombe chestnut tree in Westerly conditions because of the distance and relative location of the tree, so the apparent association between Westerly winds and increased CO_{2ff} in the Luscombe chestnut tree may well be anomalous or is likely due to other factors. There is a possibility that the topography of the area has some influence on the distribution of CO_{2ff}. The area at the site is pretty flat but it is not inconceivable that there is some turbulence created by a band of trees to the South of Ballance and west of Vector (Figure 2.2). The Kapuni stream running North-South could funnel some Vector CO_{2ff} from Vector to the Luscombe chestnut tree as well. The lack of association between increased CO_{2ff} in North Easterly conditions also conflicts with the previous assessment which suggests that the Vector pine tree sees a large plume from Vector and a questionable contribution from Ballance whereas the Luscombe chestnut is reckoned to receive a signal from Ballance so Northerly conditions ought to result in higher CO_{2ff} levels in the trees too. The association between decreased CO_{2ff} in both the trees in years with an increased frequency of South Easterly winds is completely reasonable because Southerly winds push the plume away from the trees.

4.9   Discussion CO$_{2ff}$ observations

Calculated CO$_{2ff}$ values for both trees were compared with reported emissions from the Kapuni site, a large increase in emissions from the Vector plant 2004–2012 results in an increase in total emissions from ~0.14Tg to ~0.23Tg on average ~64% above pre-2004 levels. When this is compared to CO$_{2ff}$ values for the same time period no increase can be detected in the Luscombe tree, this is likely to be because emissions from both sources only reach the tree in Northerly conditions and Ballance emissions are likely the largest influence on the Luscombe chestnut which have remained fairly constant (Table 4.10, Table 4.11).

If this large increase in emissions was reflected by the tree there should be a much larger change in CO$_{2ff}$. If we observe changes in CO$_{2ff}$ over short periods of time we would probably consider them fairly insignificant but regard long term consistent changes as indicators of real change. The period of increased emissions started in 2004 continues to the present day, and we would expect to see trends in this time frame.

Results from the wind trajectory analysis of the Vector pine suggested the Vector plant ought to be a large source to the Vector tree in Northerly and Westerly conditions. The increase in Vector emissions should be apparent in the Vector pine over this period whereas the increase in CO$_{2ff}$ in the Vector pine is only ~10%. I propose that the relatively small increase seen by the Vector pine is a reflection of near constant emissions from the Ballance plant and a minor contribution made by the Vector plant to the Vector pine, with few of Vectors emissions reaching the tree. This is possible because westerly winds have the highest mean wind speed, therefore emissions from Vector are likely driven away from the tree but equally this increases the likelihood of emissions from Ballance reaching the tree.

4.10   Conclusions

The project's main aim was to recreate historic CO_{2ff} emissions from the Kapuni site from the Vector gas processing plant from the period 1970 to 2013 and the Ballance ammonia urea plant from 1982–2013 using radiocarbon measurements in tree rings to quantify CO_{2ff} using a mass balance equation. This has been achieved through the sampling of trees in polluted locations at Kapuni to provide plant material for cellulose extraction and ^{14}C measurement. Two other trees sampled in clean air locations, Baring Head pine and Kapuni Oak tree ^{14}C results were in general agreement with the Baring Head atmospheric record demonstrating that trees reliably track atmospheric $^{14}CO_2$ levels.

This study has provided some unique data about past levels of CO_{2ff} emissions at the Kapuni site not previously reported elsewhere, and a record of historic CO_{2ff} is reported for two polluted Kapuni trees. Between 1–3 ppm CO_{2ff} was measured in the Luscombe chestnut tree for the years 1970–2013. Between 4–7 ppm CO_{2ff} was measured in the Vector pine tree for the years 1992–2013. These results are consistent with Turnbull et al. (2014) with reported results of 2–5ppm CO_{2ff} in grass material 650m downwind of the Vector Plant.

Calculated CO_{2ff} values were compared to reported emissions from the Kapuni site, a large increase in emissions from the Vector plant 2004–2012 results in an emission increase from ~0.14 Tg to ~0.23Tg total emissions on average ~64% above pre-2004 levels which are not seen in the CO_{2ff} observations. The Vector pine tree does demonstrate a~10% increase for this time period. It is thought that the majority of emissions from Vector are removed by predominant westerly winds so Vector only makes a minor contribution to the increase in CO_{2ff} in the tree and the majority of CO_{2ff} observed is contributed by the Ballance plant. No increase in CO_{2ff} could be detected in the Luscombe tree in the same time period but CO_{2ff} levels are lower at that distance so increases may be hard to distinguish from natural variation.

Two qualitative assessments were carried out using the meteorological data, the first assessed the likely trajectory of the plume from both sources under different wind patterns and how this influences CO_{2ff} at the trees location, with the implication that when frequency of weather patterns change the dominance of sources also varies. As

the dominance of the sources change it implies that the magnitude of emissions reaching the tree also change and very likely explains the variability seen in the CO_{2ff} data.

The second assessment looked at frequency of wind directions and calculated CO_{2ff} emissions. A correlation was seen between higher CO_{2ff} emissions with an increased frequency of Westerly winds at the site. This apparent increase in emissions in Westerly conditions is reasonable in the Vector tree but increased emissions in the Luscombe tree are hard to explain because it is proposed that only minor emissions reach the Luscombe tree in Westerly conditions with Northerly conditions providing most of the CO_{2ff}. There appears to be a negative correlation in frequency of South Easterly winds and increased emissions, consistent with plumes being pushed away from the trees. A relationship between increased emissions with an increased frequency of North Easterly conditions could not be established. The trees both show an increase in CO_{2ff} in 2008–2010 and a decrease in 2010–2012 consistent with a rise and fall in total emissions in the same time period (Table 4.7).

The tree ring method appears to be a valid and useful technique that could be applied to other point sources in conjunction with other techniques such as CO_2 collection by absorption over NaOH solution with the additional benefit that the use of tree rings allows historic emissions to be evaluated which cannot be achieved by other methods.

An assessment of the ability of the method to quantify the emissions from the Vector and Ballance sites will be made after a modelling study using WindTrax a Lagrangian stochastic particle dispersion model (Thunder Beach Scientific, Nanaimo, Canada www.thunderbeachscientific.com) (Keller et al. 2015. in preparation). The model analysis will be used to predict the dispersion and magnitude of the emissions at the Kapuni site, and to assess whether the observed variability in CO_{2ff} in the tree ring results is an artefact of variability in atmospheric transport and meteorology or corresponds to actual changes in CO_{2ff} observations. Modelled observations will be compared with the observed CO_{2ff} data to assess the ability of the method to determine the magnitude of the emissions, and to determine what size of changes in emissions could be detected using the tree ring method (Keller et al. in preparation).

5.0 References

Allen, M. R., D. J. Frame, C. Huntingford, C. D. Jones, J. A. Lowe, M. Meinshausen, and N. Meinshausen (2009), Warming caused by cumulative carbon emissions towards the trillionth tonne, *Nature*, *458*(7242), 1163–1166.

Anchukaitis, K. J., M. N. Evans, T. Lange, D. R. Smith, S. W. Leavitt, and D. P. Schrag (2008), Consequences of a rapid cellulose extraction technique for oxygen isotope and radiocarbon analyses, *Analytical Chemistry*, *80*(6) 2035–2041.

Baisden, W. T., C. A. Prior, D. Chambers, S. Canessa, A. Phillips, C. Bertrand, A. Zondervan, J. C. Turnbull, J. Kaiser, and F. Bruhn (2013), Rafter radiocarbon sample preparation and data flow: Accommodating enhanced throughput and precision, *Nuclear Instruments and Methods in Physics Research Section B: Beam Interactions with Materials and Atoms*, *294*(0), 194–198.

Ballantyne, A. P., C. B. Alden, J. B. Miller, P. P. Tans, and J. W. C. White (2012), Increase in observed net carbon dioxide uptake by land and oceans during the past 50 years, *Nature*, *488*(7409), 70–72.

Barbour, M. M., A. S. Walcroft, and G. D. Farquhar (2002), Seasonal variation in $\delta^{13}C$ and $\delta^{18}O$ of cellulose from growth rings of Pinus radiata, *Plant, Cell & Environment*, *25*(11), 1483–1499.

Barnett, J. R. (1973), Seasonal Variation in the Ultrastructure of the Cambium in New Zealand Grown Pinus radiata D. Don, *Annals of Botany*, *37*(5), 1005–1011.

Bates, N. R., Best, M. H. P. Neely, K. Garley, R. Dickson, A. G. and Johnson, R. J. (2012). Detecting anthropogenic carbon dioxide uptake and ocean acidification in the North Atlantic Ocean. *Biogeosciences,* 9(7): 2509–2522.

Baxter, M. S., and J. G. Farmer (1973), Glasgow University radiocarbon measurements VII, *Radiocarbon*, *15*(3), 488–492.

Becker, B. (1993), An 11,000-year German Oak and pine dendrochronology for radiocarbon calibration, *Radiocarbon*, *35*(1), 201–213.

Benner, R., M. L. Fogel, E. K. Sprague, and R. E. Hodson (1987), Depletion of ^{13}C in lignin and its implications for stable carbon isotope studies, *Nature*, *329*(6141), 708–710.

Boettger, T., et al. (2007), Wood Cellulose Preparation Methods and Mass Spectrometric Analyses of $\delta^{13}C$, $\delta^{18}O$, and Nonexchangeable δ2H Values in Cellulose, Sugar, and Starch: An Inter-laboratory Comparison, *Analytical Chemistry*, *79*(12), 4603–4612.

Boettger, T., A. Hiller, and K. Kremenetski (2003), Mid-Holocene warming in the northwest Kola Peninsula, Russia: northern pine-limit movement and stable isotope evidence, *The Holocene*, *13*(3), 403–410.

Borella, S., M. Leuenberger, M. Saurer, and R. Siegwolf (1998), Reducing uncertainties in $\delta^{13}C$ analysis of tree rings: Pooling, milling, and cellulose extraction, *Journal of Geophysical Research: Atmospheres*, *103*(D16), 19519–19526.

Bozhinova, D., M. Combe, S. W. L. Palstra, H. A. J. Meijer, M. C. Krol, and W. Peters (2013), The importance of crop growth modelling to interpret the $\Delta^{14}CO_2$ signature of annual plants, *Global Biogeochemical Cycles*, *27*(3), 792–803.

Brailsford, G., B. Stephens, A. Gomez, K. Riedel, S. Mikaloff Fletcher, S. Nichol, and M. Manning (2012), Long-term continuous atmospheric CO_2 measurements at Baring Head, New Zealand, *Atmospheric Measurement Techniques*, *5*(12), 3109–3117.

Braziunas, T. F., I. Y. Fung, and M. Stuiver (1995), The preindustrial atmospheric $^{14}CO_2$ latitudinal gradient as related to exchanges among atmospheric, oceanic, and terrestrial reservoirs, *Global Biogeochemical Cycles*, *9*(4), 565–584.

Brendel, O., P. P. M. Iannetta, and D. Stewart (2000), A rapid and simple method to isolate pure alpha cellulose, *Phytochemical Analysis*, *11*(1), 7–10.

Briffa, K. R. (2000), Annual climate variability in the Holocene: interpreting the message of ancient trees, *Quaternary Science Reviews*, *19*(1–5), 87–105.

Broecker, W. S., T. H. Peng, G. Ostlund, and M. Stuiver (1985), The distribution of bomb radiocarbon in the ocean *Journal of Geophysical Research-Oceans*, *90*(NC4), 6953–6970.

Brookman, T., and T. Whittaker (2012), Experimental assessment of the purity of α-cellulose produced by variations of the Brendel method: Implications for stable isotope ($\delta^{13}C$, $\delta^{18}O$) dendroclimatology, *Geochemistry, Geophysics, Geosystems*, *13*(9) Q0AI01.

Cain, W. F., and H. E. Suess (1976), Carbon 14 in tree rings, *Journal of Geophysical Research*, *81*(21), 3688–3694.

Canadell, J. G., C. Le Quere, M. R. Raupach, C. B. Field, E. T. Buitenhuis, P. Ciais, T. J. Conway, N. P. Gillett, R. A. Houghton, and G. Marland (2007), Contributions to accelerating atmospheric CO_2 growth from economic activity, carbon intensity, and efficiency of natural sinks, *Proceedings of the National Academy of Sciences of the United States of America*, *104*(47), 18866–18870.

Church, J. A., et al. (2013), Sea Level Change, in *Climate Change 2013: The Physical Science Basis. Contribution of Working Group I to the Fifth Assessment Report of the Intergovernmental Panel on Climate Change*, edited by T. F. Stocker, D. Qin, G.-K. Plattner, M. Tignor, S. K. Allen, J. Boschung, A. Nauels, Y. Xia, V. Bex and P. M. Midgley, pp. 1137–1216, Cambridge University Press, Cambridge, United Kingdom and New York, NY, USA, doi:10.1017/CBO9781107415324.026.

CliFlo: NIWA's National Climate Database on the Web: http://cliflo.niwa.co.nz/ , last access: 4 November 2014.

Cooper, J. C. (2000), Comparison of two bleaching agents for cellulose extraction method for radiocarbon dating, BSc Thesis, pp. 40.

Craig, H. (1954), Carbon-13 variations in sequoia rings and the atmosphere *Science*, *119*(3083), 141–143.

Crampton, E. W., and L. A. Maynard (1938), The Relation of Cellulose and Lignin Content to the Nutritive Value of Animal Feeds, *The Journal of Nutrition*, *15*(4), 383–395.

Cropper, J. P. (1979), Tree-ring skeleton plotting by computer, *Tree-Ring Bulletin*, *39*, 47–59.

Cullen, L. E., and C. MacFarlane (2005), Comparison of cellulose extraction methods for analysis of stable isotope ratios of carbon and oxygen in plant material, *Tree Physiology*, *25*(5), 563–569.

Currie, K. I., G. Brailsford, S. Nichol, A. Gomez, R. Sparks, K. R. Lassey, and K. Riedel (2011), Tropospheric $^{14}CO_2$ at Wellington, New Zealand: the world's longest record, *Biogeochemistry*, *104*(1–3), 5–22.

Davis, S. J., and K. Caldeira (2010), Consumption-based accounting of CO_2 emissions, *Proceedings of the National Academy of Sciences of the United States of America*, *107*(12), 5687–5692.

De Vries, H. L., and G. W. Barendsen (1954), Measurements of Age by the Carbon-14 Technique, *Nature*, *174*(4442), 1138–1141.

Dixon, R. A., F. Chen, D. Guo, and K. Parvathi (2001), The biosynthesis of monolignols: a "metabolic grid", or independent pathways to guaiacyl and syringyl units? *Phytochemistry*, *57*(7), 1069–1084.

Ed Dlugokencky and Pieter Tans, N. E. (2014), Trends in atmospheric carbon dioxide: Recent global CO_2, edited, National Oceanic and atmospheric administration, and Earth System Research Laboratory (NOAA/ESRL).

English heritage (1998), Dendrochronology guidelines on producing and interpreting dendrochronological dates Available at http://www.helm.org.uk/guidance-library/dendrochronology-guidelines/dendrochronology.pdf.

Farmer, J. G., and M. S. Baxter (1974), Atmospheric carbon dioxide levels as indicated by the stable isotope record in wood, *Nature*, *247*(5439), 273–275.

Freyer, H. D., and N. Belacy (1983), $^{13}C/^{12}C$ records in northern hemispheric trees during the past 500 years—Anthropogenic impact and climatic superpositions, *Journal of Geophysical Research: Oceans*, *88*(C11), 6844–6852.

Friedlingstein, P., et al. (2014), Persistent growth of CO_2 emissions and implications for reaching climate targets, *Nature Geoscience*, *7*(10), 709–715.

Friedlingstein, P., R. A. Houghton, G. Marland, J. Hackler, T. A. Boden, T. J. Conway, J. G. Canadell, M. R. Raupach, P. Ciais, and C. Le Quere (2010), Update on CO_2 emissions, *Nature Geoscience*, *3*(12), 811–812.

Friedrich, M., S. Remmele, B. Kromer, J. Hofmann, M. Spurk, K. F. Kauser, C. Orcel, and M. Kuppers (2004), The 12,460-year Hohenheim Oak and pine tree-ring chronology from Central Europe; a unique annual record for radiocarbon calibration and paleoenvironment reconstructions, *Radiocarbon*, *46*(3), 1111–1122.

Fritts, H. C. (1976), *Tree Rings and Climate*, 567 pp, academic press Inc New York.

Fuss, S., J.G. Canadell, G.P. Peters, M Tavoni, R. M. Andrew, P. Ciais, R. B Jackson, C. D. Jones, F. Kraxner, N. Nakicenovic, C. Le Quéré M. R. Raupach, A. Sharifi P. Smith Y. Yamagata. (2014). "Betting on negative emissions. *Nature Clim. Change*, 4(10), 850–853.

Gaudinski, J. B., T. E. Dawson, S. Quideau, E. A. G. Schuur, J. S. Roden, S. E. Trumbore, D. R. Sandquist, S. W. Oh, and R. E. Wasylishen (2005), Comparative analysis of cellulose preparation techniques for use with C-13, C-14, and O-18 isotopic measurements, *Analytical Chemistry*, *77*(22), 7212–7224.

Gaudinski, J. B., M. S. Torn, W. J. Riley, C. Swanston, S. E. Trumbore, J. D. Joslin, H. Majdi, T. E. Dawson, and P. J. Hanson (2009), Use of stored carbon reserves in growth of temperate tree roots and leaf buds: Analyses using radiocarbon measurements and modelling, *Global Change Biology*, *15*(4), 992–1014.

Godwin, H. (1962), Radiocarbon Dating: Fifth International Conference, *Nature*, *195*(4845), 943–945.

Goldstein; I. S (2004), Wood formation and properties/Chemical properties of wood, in *Encyclopedia of Forest Sciences*, edited by J. Y. Burley, J; Evans, J, pp. 1835–1839, Elsevier, Oxford.

Graven, H. D., T. P. Guilderson, and R. F. Keeling (2012), Observations of radiocarbon in CO_2 at seven global sampling sites in the Scripps flask network: Analysis of spatial gradients and seasonal cycles, *Journal of Geophysical Research: Atmospheres*, *117*(D2), D02303.

Green, J. W. (1963), *Wood cellulose, In Methods of Carbohydrate Chemistry*, Vol III R. L Whistler ed, Academic Press, New York pp 9–21.

Gregg, J. S., R. J. Andres, and G. Marland (2008), China: Emissions pattern of the world leader in CO_2 emissions from fossil fuel consumption and cement production, *Geophysical Research Letters*, *35*(8) L08806.

Guan, D., Z. Liu, Y. Geng, S. Lindner, and K. Hubacek (2012), The Gigatonne gap in China's carbon dioxide inventories, *Nature Clim. Change*, *2*(9), 672–675.

Haneca, K., Č. Katarina, and H. Beeckman (2009), Oaks, tree-rings and wooden cultural heritage: a review of the main characteristics and applications of Oak dendrochronology in Europe, *Journal of Archaeological Science*, *36*(1), 1–11.

Harlow, B. A., J. D. Marshall, and A. P. Robinson (2006), A multi-species comparison of $\delta^{13}C$ from whole wood, extractive-free wood and holocellulose, *Tree Physiology*, *26*(6), 767–774.

Hedges, R. E. M. (1992), Sample Treatment Strategies in Radiocarbon Dating, in *Radiocarbon After Four Decades*, edited by R. E. Taylor, A. Long and R. Kra, pp. 165–183, Springer New York.

Hill, S. A., J. S. Waterhouse, E. M. Field, V. R. Switsur, and T. A Rees (1995), Rapid recycling of triose phosphates in Oak stem tissue, *Plant, Cell & Environment*, *18*(8), 931–936.

Hoffer, M., and J. C. Tardif (2009), False rings in jack pine and black spruce trees from eastern Manitoba as indicators of dry summers, *Canadian journal of forest research*, *39*(9), 1722–1736.

Hogg, A., C. Turney, J. Palmer, E. Cook, and B. Buckley (2013), Is there any evidence for regional atmospheric ^{14}C offsets in the Southern Hemisphere?, *Radiocarbon*, *55*(4), 2029–2034.

Hogg, A. G., L. K. Fifield, C. S. M. Turney, J. G. Palmer, R. Galbraith, and M. G. K. Baillie (2006), Dating ancient wood by high-sensitivity liquid scintillation counting and accelerator mass spectrometry-Pushing the boundaries, *Quaternary Geochronology*, *1*(4), 241–248.

Hogg, A. G., et al. (2013), Shcal13 Southern Hemisphere calibration, 0-50,000 years cal BP, *Radiocarbon*, *55*(4), 1889–1903.

Hoper, S. T., F. G. McCormac, A. G. Hogg, T. F. G. Higham, and M. J. Head (1998), Evaluation of wood pretreatments on Oak and cedar, *Radiocarbon*, *40*(1), 45–50.

Houghton, R. A., J. I. House, J. Pongratz, G. R. van der Werf, R. S. DeFries, M. C. Hansen, C. Le Quéré, and N. Ramankutty (2012), Carbon emissions from land use and land-cover change, *Biogeosciences*, *9*(12), 5125–5142.

Hsueh, D. Y., N. Y. Krakauer, J. T. Randerson, X. Xiaomei, S. E. Trumbore, and J. R. Southern (2007), Regional patterns of radiocarbon and fossil fuel-derived CO_2 in surface air across North America, *Geophysical Research Letters*, *34*(2), 1–6.

Hua, Q., M. Barbetti, G. E. Jacobsen, U. Zoppi, and E. M. Lawson (2000), Bomb radiocarbon in annual tree rings from Thailand and Australia, *Nuclear Instruments & Methods in Physics Research Section B-Beam Interactions with Materials and Atoms*, *172*, 359–365.

Hua, Q., M. Barbetti, V. A. Levchenko, R. D. D'Arrigo, B. M. Buckley, and A. M. Smith (2012), Monsoonal influence on Southern Hemisphere $^{14}CO_2$, *Geophysical Research Letters*, *39(19) L19806*.

Hua, Q., M. Barbetti, and A. Z. Rakowski (2013), Atmospheric radiocarbon for the period 1950–2010, *Radiocarbon*, *55*(4), 2059–2072.

Hua, Q., M. Barbetti, and U. Zoppi (2004), Radiocarbon in annual tree rings from Thailand during the pre-bomb period, AD 1938–1954, *Radiocarbon*, *46*(2), 925–932.

IPCC (2006). IPCC Guidelines for National Greenhouse Gas Inventories, Prepared by the National Greenhouse Gas Inventories Programme. B. L. Eggleston H.S., Miwa K., Ngara T. and Tanabe K. (eds). Published: IGES, Japan. Published by the Institute for Global Environmental Strategies (IGES), Hayama, Japan on behalf of the IPCC. Available at http://www.ipcc-nggip.iges.or.jp/public/2006gl/

IPCC (2013), *Climate Change 2013: The Physical Science Basis. Contribution of Working Group I to the Fifth Assessment Report of the Intergovernmental Panel on Climate Change*, 1535 pp., Cambridge University Press, Cambridge, United Kingdom and New York, NY, USA, doi:10.1017/CBO9781107415324.

Jansen, H. S. (1970), Secular variations of radiocarbon in New Zealand and Australian trees., in *Radiocarbon variations and absolute chronology, Nobel Symposium 12th Proceedings, Stockholm.*, edited by I. U. Olsson, pp. 264–274, John Wiley and Sons, Almqvist and Wiksell Stockholm.

Keller, K. M., Joos, F. Raible, C.C. (2014). Time of emergence of trends in ocean biogeochemistry. Biogeosciences 11(13): 3647–3659.

Keller, E. D., J. C. Turnbull, and M. W. Norris, Detecting long-term changes in point source fossil CO_2 emissions with tree ring archives, in preparation.

Le Quéré, C., et al. (2014), Global carbon budget 2013, *Earth Syst. Sci. Data*, *6*(1), 235–263, doi:10.5194/essd-6-235-2014.

Le Quere, C., et al. (2009), Trends in the sources and sinks of carbon dioxide, *Nature Geoscience*, *2*(12), 831–836.

Le Quere, C., et al. (2007), Saturation of the Southern Ocean CO_2 sink due to recent climate change, *Science*, *316*(5832), 1735–1738.

Leavitt, S. W., and S. R. Danzer (1993), Method for batch processing small wood samples to holocellulose for stable-carbon isotope analysis, *Analytical Chemistry*, *65*(1), 87–89.

Ledgard, S. F., M. Boyes, and F. Brentrup (2011), Life cycle assessment of local and imported fertilisers used on New Zealand farms, *In adding to the knowledge base for the nutrient manager.* Currie, L.D, Christensen, C.L. eds, Fertiliser and Lime Research Centre Massey University Palmerston North, Occasional report No 24.

Levin, I., S. Hammer, E. Eichelmann, and F. R. Vogel (2011), Verification of greenhouse gas emission reductions: the prospect of atmospheric monitoring in polluted areas, *Philosophical Transactions of the Royal Society a-Mathematical Physical and Engineering Sciences*, *369*(1943), 1906–1924.

Levin, I., S. Hammer, B. Kromer, and F. Meinhardt (2008), Radiocarbon observations in atmospheric CO_2: Determining fossil fuel CO_2 over Europe using Jungfraujoch observations as background, *Science of the Total Environment*, *391*(2–3), 211–216.

Levin, I., and V. Hesshaimer (2000), Radiocarbon – A unique tracer of global carbon cycle dynamics, *Radiocarbon*, *42*(1), 69–80.

Levin, I., and U. T. E. Karstens (2007), Inferring high-resolution fossil fuel CO_2 records at continental sites from combined $^{14}CO_2$ and CO observations, *Tellus B*, *59*(2), 245–250.

Levin, I., B. Kromer, M. Schmidt, and H. Sartorius (2003), A novel approach for independent budgeting of fossil fuel CO_2 over Europe by $^{14}CO_2$ observations, *Geophysical Research Letters*, *30*(23) 2194.

Levin, I., T. Naegler, B. Kromer, M. Diehl, R. J. Francey, A. J. Gomez-Pelaez, L. P. Steele, D. Wagenbach, R. Weller, and D. E. Worthy (2010), Observations and modelling of the global distribution and long-term trend of atmospheric $^{14}CO_2$, *Tellus Series B-Chemical and Physical Meteorology*, *62*(1), 26–46.

Levin, I., and C. Roedenbeck (2007), Can the envisaged reductions of fossil fuel CO_2 emissions be detected by atmospheric observations? *Naturwissenschaften*, *95*(3), 203–208.

Li, Q., and Y. Liu (2013), A simple and rapid preparation of pure cellulose confirmed by monosaccharide compositions, $\delta^{13}C$, yields and C%, *Dendrochronologia*, *31*(4), 273–278.

Libby, L. M., and L. J. Pandolfi (1974), Temperature-dependence of isotope ratios in tree rings *Proceedings of the National Academy of Sciences of the United States of America*, *71*(6), 2482–2486.

Loader, N. J., I. Robertson, and D. McCarroll (2003), Comparison of stable carbon isotope ratios in the whole wood, cellulose and lignin of Oak tree-rings, *Palaeogeography Palaeoclimatology Palaeoecology*, *196*(3–4), 395–407.

Loh, Z., R. Leuning, S. Zegelin, D. Etheridge, M. Bai, T. Naylor, and D. Griffith (2009), Testing Lagrangian atmospheric dispersion modelling to monitor CO_2 and CH_4 leakage from geosequestration, *Atmospheric Environment*, *43*(16), 2602–2611.

Long, A., Arnold, L. D, Damon, P.E, Ferguson, C.W, Lerman, J.C, Wilson, A.T (1979), Radial translocation in bristlecone pine, paper presented at Radiocarbon Dating: Proceedings of the Ninth International Conference, Los Angeles and La Jolla, 1976 Univ of California Press, Berkeley California, 1979.

Lyu, K., X. Zhang, J. A. Church, A. B. A. Slangen, and J. Hu (2014), Time of emergence for regional sea-level change, *Nature Climate Change*, *4*(11), 1006–1010.

Macfarlane, C., C. R. Warren, D. A. White, and M. A. Adams (1999), A rapid and simple method for processing wood to crude cellulose for analysis of stable carbon isotopes in tree rings, *Tree Physiology*, *19*(12), 831–835.

Manning, M. R., D. C. Lowe, W. H. Melhuish, R. J. Sparks, G. Wallace, C. M. Brenninkmeijer, and R. C. McGill (1990), The use of radiocarbon measurements in atmospheric studies, *Radiocarbon*, *32*(1), 37–58.

Marland, G. (2012), Emissions accounting: China's uncertain CO_2 emissions, *Nature Climate. Change*, *2*(9), 645–646.

Marra, M. J., B. V. Alloway, and R. M. Newnham (2006), Paleoenvironmental reconstruction of a well-preserved Stage 7 forest sequence catastrophically buried by basaltic eruptive deposits, northern New Zealand, *Quaternary Science Reviews*, *25*(17–18), 2143–2161.

Matthews, H. D., S. Solomon, and R. Pierrehumbert (2012), Cumulative carbon as a policy framework for achieving climate stabilization, *Philosophical Transactions of the Royal Society A: Mathematical, Physical and Engineering Sciences*, *370*(1974), 4365–4379.

McCarroll, D., and N. J. Loader (2004), Stable isotopes in tree rings, *Quaternary Science Reviews*, *23*(7–8), 771–801.

Meijer, H. A. J., H. M. Smid, E. Perez, and M. G. Keizer (1996), Isotopic characterisation of anthropogenic CO_2 emissions using isotopic and radiocarbon analysis, *Physics and Chemistry of the Earth*, *21*(5–6), 483–487.

Meijer, H. J., J. van der Plicht, J. S. Gislefoss, and R. Nydal (1995), Comparing long-term atmospheric ^{14}C and ^{3}H records near Groningen, the Netherlands with Fruholmen, Norway and Izana, Canary Islands ^{14}C stations, *Radiocarbon*, *37*(1), 39–50.

Meinshausen, M., N. Meinshausen, W. Hare, S. C. B. Raper, K. Frieler, R. Knutti, D. J. Frame, and M. R. Allen (2009), Greenhouse-gas emission targets for limiting global warming to 2°C, *Nature*, *458*(7242), 1158–1162.

Miller, B. R., R. F. Weiss, P. K. Salameh, T. Tanhua, B. R. Greally, J. Mühle, and P. G. Simmonds (2008), Medusa: A Sample preconcentration and GC/MS Detector System for in Situ Measurements of Atmospheric Trace Halocarbons, Hydrocarbons, and Sulfur Compounds, *Analytical Chemistry*, *80*(5), 1536–1545.

Nisbet, E., and R. Weiss (2010), Top-Down versus Bottom-Up, *Science*, *328*(5983), 1241–1243.

Nydal, R., and J. S. Gislefoss (1996), Further application of bomb ^{14}C as a tracer in the atmosphere and ocean, *Radiocarbon*, *38*(3), 389–406.

Nydal, R., and K. Lövseth (1983), Tracing bomb ^{14}C in the atmosphere 1962–1980, *Journal of Geophysical Research: Oceans*, *88*(C6), 3621–3642.

Olsson, I. U. (1980), ^{14}C in extractives from wood, *Radiocarbon*, *22*(2), 515–524.

Olsson, I. U., and G. Possnert (1992), ^{14}C activity in different sections and chemical-fractions of Oak tree rings, AD 1938–1981, *Radiocarbon*, *34*(3), 757–767.

Palstra, S. W. L., U. Karstens, H.-J. Streurman, and H. A. J. Meijer (2008), Wine ethanol ^{14}C as a tracer for fossil fuel CO_2 emissions in Europe: Measurements and model comparison, *Journal of Geophysical Research-Atmospheres*, *113*(D21) D21305.

Park, R., and S. Epstein (1961), Metabolic Fractionation of C13 & C12 in Plants, *Plant Physiology*, *36*(2), 133–138.

Pearl, I.A., (1967) The Chemistry of lignin, Dekker New York, 355pp.

Peters, G. P., R. M. Andrew, T. Boden, J. G. Canadell, P. Ciais, C. Le Quere, G. Marland, M. R. Raupach, and C. Wilson (2013), The challenge to keep global warming below 2 [deg]C, *Nature Climate Change*, *3*(1), 4–6.

Peters, G. P., J. C. Minx, C. L. Weber, and O. Edenhofer (2011), Growth in emission transfers via international trade from 1990 to 2008, *Proceedings of the National Academy of Sciences*, *108*(21), 8903–8908.

Pettersen, R. C. (1984), The chemical composition of wood, *In the chemistry of solid wood*, Vol *207*, 57–126.

Prinn, R. G., et al. (2000), A history of chemically and radiatively important gases in air deduced from ALE/GAGE/AGAGE, *Journal of Geophysical Research: Atmospheres*, *105*(D14), 17751–17792.

Rafter, T. (1955), ^{14}C variations in nature and the effect on radiocarbon dating, *New Zealand Journal of Science and Technology B 37(1)*, 20–38.

Rafter, T. A., and G. J. Fergusson (1957), "Atom Bomb Effect" – Recent Increase of Carbon-14 Content of the Atmosphere and Biosphere, *Science*, *126*(3273), 557–558.

Rakowski, A. (2011), Radiocarbon method in monitoring of fossil fuel emission, *Geochronometria*, *38*(4), 314–324.

Rakowski, A. Z., M.-J. Nadeau, T. Nakamura, A. Pazdur, S. Pawelczyk, and N. Piotrowska (2013), Radiocarbon method in environmental monitoring of CO_2 emission, *Nuclear Instruments & Methods in Physics Research Section B-Beam Interactions with Materials and Atoms*, *294*, 503–507.

Randerson, J. T., I. G. Enting, E. A. G. Schuur, K. Caldeira, and I. Y. Fung (2002), Seasonal and latitudinal variability of troposphere $\Delta^{14}CO_2$: Post bomb contributions from fossil fuels, oceans, the stratosphere, and the terrestrial biosphere, *Global Biogeochemical Cycles*, *16*(4) 1112.

Raupach, M. R., S. J. Davis, G. P. Peters, R. M. Andrew, J. G. Canadell, P. Ciais, P. Friedlingstein, F. Jotzo, D. P. van Vuuren, and C. Le Quere (2014), Sharing a quota on cumulative carbon emissions, *Nature Climate Change*, *4*(10), 873–879.

Reimer, P. J., T. A. Brown, and R. W. Reimer (2004), Discussion: Reporting and Calibration of Post-Bomb ^{14}C Data, *Radiocarbon*, *51*(4), 1299–1304.

Rinne, K. T., T. Boettger, N. J. Loader, I. Robertson, V. R. Switsur, and J. S. Waterhouse (2005), On the purification of alpha-cellulose from resinous wood for stable isotope (H, C and O) analysis, *Chemical Geology*, *222*(1–2), 75–82.

Rocha, A. V., M. L. Goulden, A. L. Dunn, and S. C. Wofsy (2006), On linking interannual tree ring variability with observations of whole-forest CO_2 flux, *Global Change Biology*, *12*(8), 1378–1389.

Scheller, H. V., and P. Ulvskov (2010), Hemicelluloses, *Annual Review of Plant Biology*, *61*(1), 263–289.

Scott, E. M. (2003), Section 1: The Fourth International Radiocarbon Intercomparison (FIRI), *Radiocarbon*, *45*(2), 135–150.

Sjöstrom, E. (1993) Wood chemistry Fundamentals and applications 2nd Edn, 293pp. Academic Press San Diego.

Sheu, D. D., and C. H. Chiu (1995), Evaluation of Cellulose Extraction Procedures for Stable Carbon Isotope Measurement in Tree Ring Research, *International Journal of Environmental Analytical Chemistry*, *59*(1), 59–67.

Sitch, S., et al. (2015). Recent trends and drivers of regional sources and sinks of carbon dioxide. *Biogeosciences* 12(3): 653–679.

Smith, J. B., et al. (2009), Assessing dangerous climate change through an update of the Intergovernmental Panel on Climate Change (IPCC) "reasons for concern", *Proceedings of the National Academy of Sciences*, *106*(11), 4133–4137.

Solomon, S., G.-K. Plattner, R. Knutti, and P. Friedlingstein (2009), Irreversible climate change due to carbon dioxide emissions, *Proceedings of the National Academy of Sciences*, *106*(6), 1704–1709.

Southon, J. R., and A. L. Magana (2010), A Comparison of Cellulose Extraction and ABA Pretreatment Methods for AMS ^{14}C Dating of Ancient Wood, *Radiocarbon*, *52*(3) 1371–1379.

Speer, J. H. (2010), *Fundamentals of tree-ring research*, University of Arizona Press 333pp.

Stokes, M., and T. Smiley (1968), An introduction to tree-ring dating, Univ. Chicago Press: Chicago 73pp.

Striebly S. (2013), Comparing conifers and deciduous trees. Washington Native Plant Society Blog, Botanical Rambles Blog. Available at http://www.wnps.org/blog/conifers-deciduous-trees/.

Stuiver, M., B. Kromer, B. Becker, and C. W. Ferguson (1986), Radiocarbon age calibration back to 13,300 years BP and the ^{14}C age matching of the German Oak and United States bristlecone-pine chronologies, *Radiocarbon*, *28*(2B), 969–979.

Stuiver, M., and G. W. Pearson (1993), High precision bidecadal calibration of the radiocarbon time scale, AD 1950–500 BC and 2500–6000 BC, *Radiocarbon*, *35*(1), 1–23.

Stuiver, M., and H. A. Polach (1977), Discussion; reporting of ^{14}C data, *Radiocarbon*, *19*(3), 355–363.

Stuiver, M., and P. D. Quay (1981), Atmospheric ^{14}C changes resulting from fossil fuel CO_2 release and cosmic ray flux variability, *Earth and Planetary Science Letters*, *53*(3), 349–362.

Stuiver, M., and P. J. Reimer (1993), Extended ^{14}C data-base and revised calib 3.0 ^{14}C age calibration program, *Radiocarbon*, *35*(1), 215–230.

Suess, H. E. (1955), Radiocarbon concentration in modern wood, *Science*, *122*(3166), 415–417.

Suess, H. E. (1970), Bristle-cone pine calibration of the radiocarbon time-scale, 5200 BC To the present, in *Radiocarbon variations and absolute chronology, Nobel Symposium, 12th proceedings.*, edited by I. Olsson, pp. 303–311, Wiley, Chichester and New York.

Switsur, V. R., Waterhouse, J.S., Field, E.M., Carter, A.H.C, Loader, N.J., (1995), Stable isotopes in tree rings from Oak-techniques and some preliminary results, *Palaoklimaforschung*, *15*, 129–140.

Tans, P. P., A. F. M. De Jong, and W. G. Mook (1978), Chemical pretreatment and radial flow of ^{14}C in tree rings, *Nature*, *271*(5642), 234–235.

Tans, P. P., and D. W. R. Wallace (1999), Carbon cycle research after Kyoto, *Tellus B*, *51*(2), 562–571.

Taranaki Regional Council (2013a) Technical Report 2012–83, 2013. Vector Kapuni GTP Monitoring Programme Biennial Report 2010–2012 Technical Report 2012–83: 126pp. Available at http://www.trc.govt.nz/assets/Publications/technical-reports/oil-and-gas-compliance-monitoring-reports/1176482w2.pdf.

Taranaki Regional Council (2013b) Technical report 2012-91, 2013. Ballance Agri-Nutrients (Kapuni) Ltd Monitoring Programme Biennial Report 2010-2012 Technical Report 2012–91: 124pp. Available at http://www.trc.govt.nz/assets/Publications/technical-reports/industry-compliance-monitoring-reports/1001898w2.pdf

Trumbore, S. (2000), Age of soil organic matter and soil respiration: Radiocarbon constraints on belowground C dynamics, *Ecological Applications*, *10*(2), 399–411.

Turnbull, J. C., J. B. Miller, S. J. Lehman, P. P. Tans, R. J. Sparks, and J. Southon (2006), Comparison of $^{14}CO_2$, CO, and SF_6 as tracers for recently added fossil fuel CO_2 in the atmosphere and implications for biological CO_2 exchange, *Geophysical Research Letters*, *33*(1) L10817.

Turnbull, J., P. Rayner, J. Miller, T. Naegler, P. Ciais, and A. Cozic (2009), On the use of $^{14}CO_2$ as a tracer for fossil fuel CO_2: Quantifying uncertainties using an atmospheric transport model, *Journal of Geophysical Research-Atmospheres*, *114 (D22) D22302*.

Turnbull, J. C., et al. (2011a), Assessment of fossil fuel carbon dioxide and other anthropogenic trace gas emissions from airborne measurements over Sacramento, California in spring 2009, *Atmos. Chem. Phys.*, *11*(2), 705–721.

Turnbull, J. C., P. P. Tans, S. J. Lehman, D. Baker, T. J. Conway, Y. Chung, J. Gregg, J. B. Miller, J. R. Southon, and L. X. Zhou (2011b), Atmospheric observations of carbon monoxide and fossil fuel CO_2 emissions from East Asia, *Journal of Geophysical Research: Atmospheres (1984–2012)*, *116*(D24) D24302.

Turnbull, J. C., E. D. Keller, T. Baisden, G. Brailsford, T. Bromley, M. Norris, and A. Zondervan (2014), Atmospheric measurement of point source fossil CO_2 emissions, *Atmos. Chem. Phys.*, *14*(10), 5001–5014.

Turnbull. J.C., A. Zondervan, J. Kaiser, M. Norris, J. Dahl, W.T Baisden, and S. J. Lehman (2015) High precision atmospheric $^{14}CO_2$ measurement at the Rafter Radiocarbon laboratory, *Radiocarbon,* Vol 57(3) 377–388.

Turney, C. S. M., R. G. Roberts, N. de Jonge, C. Prior, J. M. Wilmshurst, M. S. McGlone, and J. Cooper (2007), Redating the advance of the New Zealand Franz Josef Glacier during the Last Termination: evidence for asynchronous climate change, *Quaternary Science Reviews*, *26*(25–28), 3037–3042.

UNFCCC (1992), Framework: convention on climate change, United Nations Framework Conference on Environment and Development, Rio de Janeiro, Brazil, Available at http://unfccc.int/resource/docs/convkp/conveng.pdf

UNFCCC (2009). Copenhagen Accord, Proposal by the President, document FCCC/CP/2009/L.7. United Nations Framework Convention on Climate Change (UNFCCC). Available at http://unfccc.int/resource/docs/2009/cop15/eng/l07.pdf

UNFCCC (2010). The Cancun Agreements, document FCCC/CP/2010/7/Add.1. United Nations Framework Convention on Climate Change (UNFCCC). Available at http://unfccc.int/resource/docs/2010/cop16/eng/07a01.pdf

Van de Water, P. K. (2002), The effect of chemical processing on the $\delta^{13}C$ value of plant tissue, *Geochimica et Cosmochimica Acta*, *66*(7), 1211–1219.

Van Der Laan, S., U. Karstens, R. E. M. Neubert, I. T. Van Der Laan-Luijkx, and H. A. J. Meijer (2010), Observation-based estimates of fossil fuel-derived CO_2 emissions in the Netherlands using $\Delta^{14}C$, CO and $^{222}Radon$, *Tellus B*, *62*(5), 389–402.

Vogel, F. R., S. Hammer, A. Steinhof, B. Kromer, and I. Levin (2010), Implication of weekly and diurnal ^{14}C calibration on hourly estimates of CO-based fossil fuel CO_2 at a moderately polluted site in south-western Germany, *Tellus B*, *62*(5), 512–520.

Wallis, A. F., Wearne, R.H., Wright, P.J., (1997), New approaches to the rapid analysis of cellulose in wood. Paper presented at Proceedings of the 9th International Symposium of wood and pulping chemistry, Technical association of pulp and paper Industry, Montreal Canada.

Weiss, R. F., and R. G. Prinn (2011), Quantifying greenhouse-gas emissions from atmospheric measurements: a critical reality check for climate legislation, *Philosophical Transactions of the Royal Society a-Mathematical Physical and Engineering Sciences*, *369*(1943), 1925–1942.

Wilson, A. T., and M. J. Grinsted (1977), $^{12}C/^{13}C$ in cellulose and lignin as palaeothermometers, *Nature*, *265*(5590), 133–135.

Wilson, A. T., J. M. Gumbley, and D. J. Spedding (1963), Resin Metabolism in the Sapwood of Pinus radiata, *Nature*, *198*(4879), 500–500.

Zink-Sharp (2004), Wood formation and properties/formation and structure of wood, in *Encylopedia of forest sciences*, edited by J. Y. Burley, J; Evans, J, pp. 1806–1815, Elseivier Oxford.

Zondervan, A. T. Hauser, J. Kaiser, R. Kitchen, J. C. Turnbull, and J.G. West (2015), XCAMS: the compact C-14 accelerator mass spectrometer extended for Be-10 and Al-26 at GNS Science, New Zealand, *Nuclear Instruments and Methods in Physics Research Section B: Beam Interactions with Materials and Atoms, Vol 361,* 25-33*.*

6.0 Appendices

6.1 Correlation of tree cores. Marcus Trimble

6.1.1 Correlation of tree rings Kapuni Oak R40442 and R40444

Correlations for core samples KAP-KAP-T1-C1 through C4 (Kapuni Oak) were done mainly by eye, utilizing the microscope only to determine boundaries that were in question as some boundaries are not readily visible by eye. These boundaries are also not always easily visible in the photographs below, so every attempt has been made to indicate where the boundaries are. In some cases, boundaries have been inferred based on the context of the ring sequence in question and with cross comparison of the other samples. Each inference will be discussed below as it appears.

Due to the clarity of the annual record, thanks to the ring-porous nature of the Oak, confidence in the overall correlations is high. Core C1 (R40444) and C4 (R40442) were used for the research samples.

All pattern interpretations will move from oldest rings to the youngest in a given time block
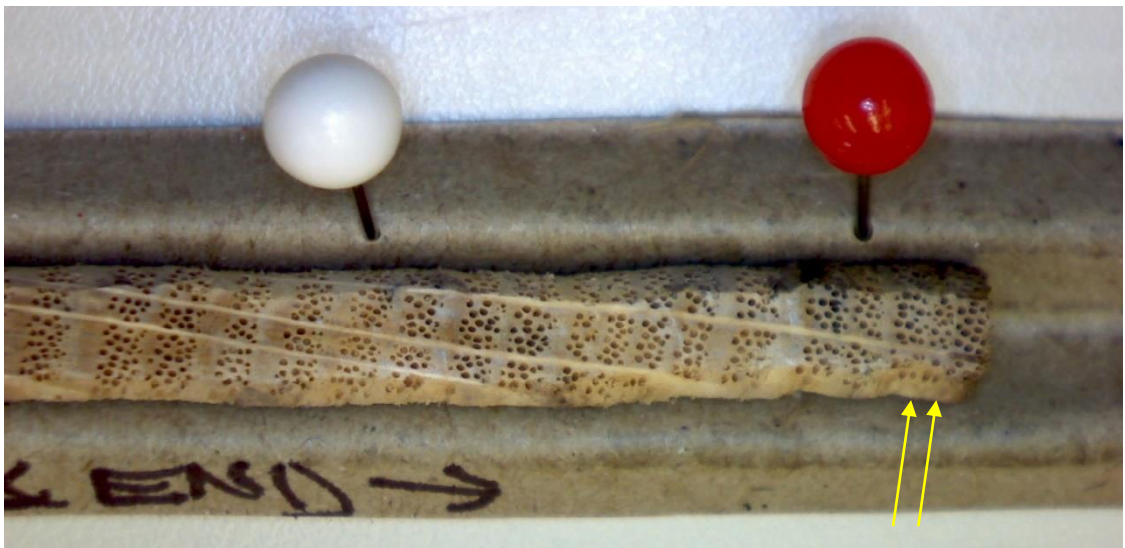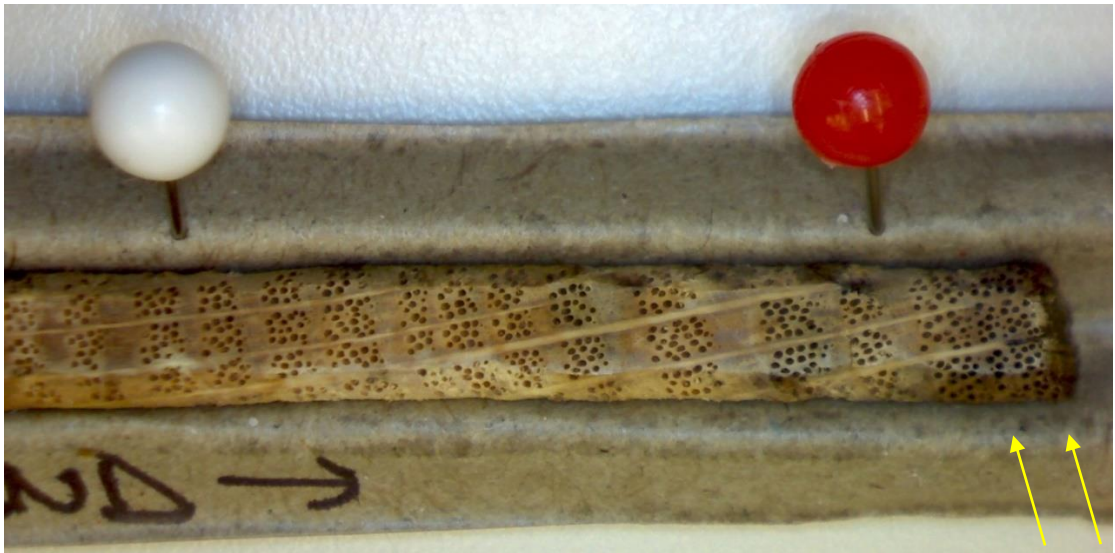
2000–2013

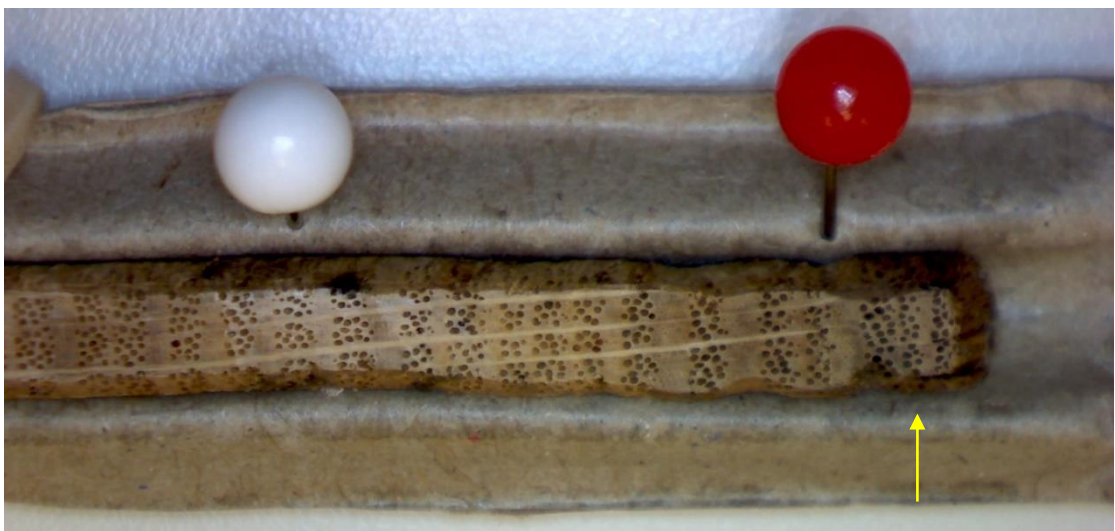Figure A6.1a

Figure A6.1b

Figure A6.1c
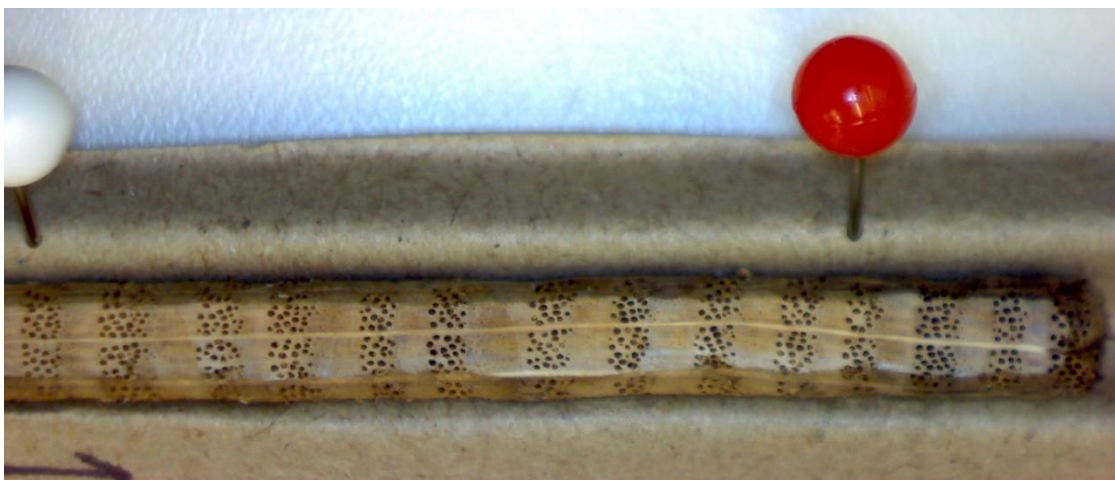
Figure A6.1d

Figure A6.1a-d   Photos Kapuni Oak cores R40442 & R40444 (2000–2013).

The photos in Figure A6.1a-d show cores C1-C4 in order a-d. The white pin marks early-wood beginning 2000, red pin marks early-wood 2010. Yellow arrows indicate hard to identify boundaries. Photos in Figure A6.1, above are used here to show the patterns between the years 2000 and 2013. An explanation of the interpreted patterns is found below:

- For the years 2000–2007, the spacing starts off relatively wide until 2004, where the rings experience narrowing through 2007. This can be seen in samples C1 through C3, with C4 maintaining a more or less regular ring width, with little variance.

- From 2007 to 2008 the rings experience a widening. The ring for 2009 shows a bit of narrowing from the previous two years, which can be seen in samples C1–C3.

- Between 2010 and 2013, the pattern is a bit variable but can be seen in samples C1 to C3 with the ring for 2010 being bigger than the following years which experience tightening. However, sample C3 shows a little more growth for the year 2012. Sample C4 is an outlier in this particular year grouping, showing fairly regular spacing.

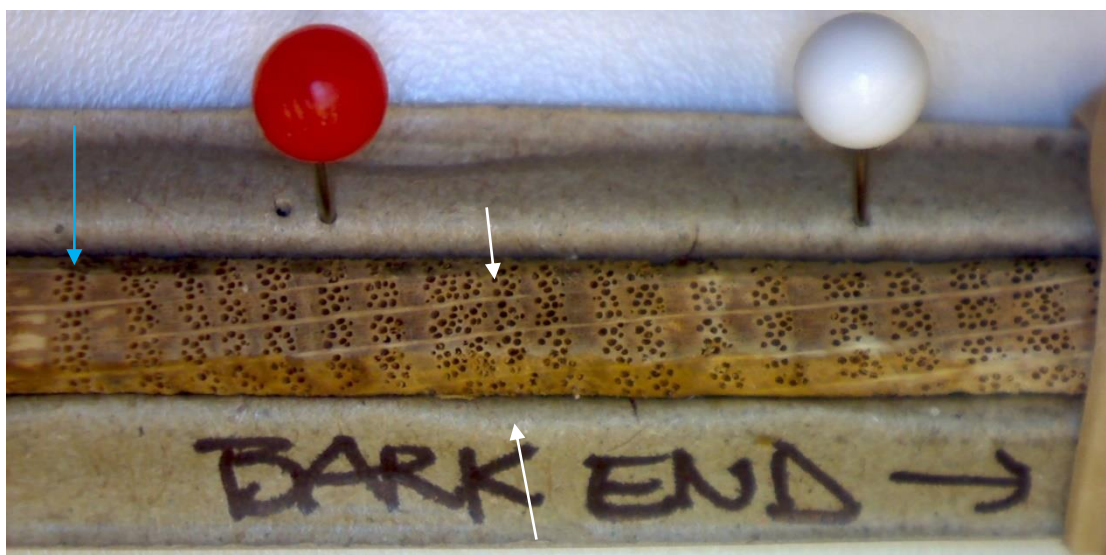**1985–1999**

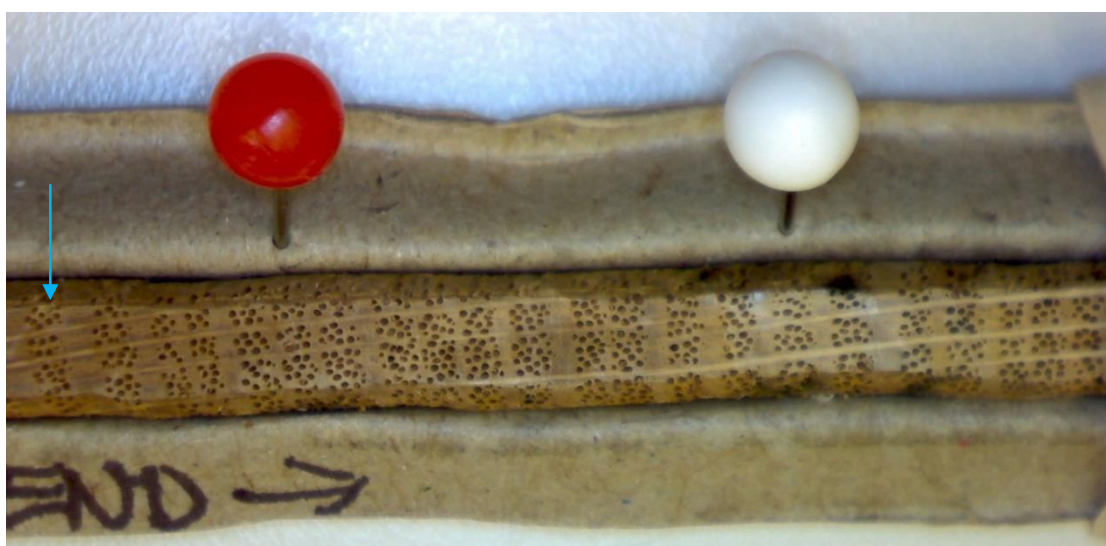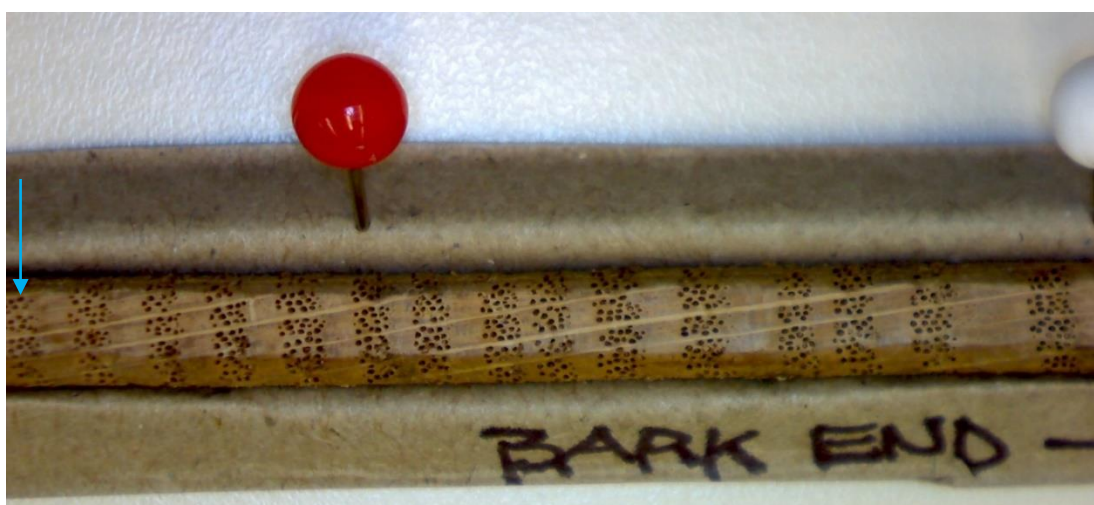
FigureA6.2a

Figure A6.2b

Figure A6.2c

Figure A6.2d

Figure A6.2a-d   Photos Kapuni Oak cores R40442 & R40444 (1985–1999).

The photos in Figure A6.2a-d show cores C1-C4 in order a-d. The red pin indicates 1990 and white pin indicates the year 2000. Blue arrows indicates early-wood for 1985 and white arrow points to an inferred tree ring boundary. In sample C3 there is an inferred boundary. Below the pattern interpretations are explained, as is the reason for the interpreted boundary shown in A6.2b:

- For the years 1985–1987 there is a noticeable progressive narrowing of ring width in the direction of younging for samples C1–C3. The ring for 1986 is narrower than 1985 and the ring for 1987 is narrower than 1986. C4 shows regular spacing over this time period.

- From 1988 to 1989 there is no real correlation between the samples. C1 and C3 the ring for 1988 being wider than the ring for 1989, however, C2 shows the reverse with the ring for 1988 being narrower than for 1989. C4 again shows regular spacing.

- Examining the years 1990 through 1993, there is a distinct patter across all 4 samples, however, C4 shows this pattern a bit more subtly. From 1990 to 1991 there is a widening of ring width. This widening is followed by a pronounced narrowing of rings from 1992–1993. Samples C1–C3 show this explicitly, while in C4 it's slightly more difficult to see at first glance. Sample C2 has an inferred ring boundary, indicated by the white arrows in Figure A6.2b. This boundary has been inferred, because without it, all previous and subsequent correlations with this core will not match. If this boundary were not inferred, it would also represent an abnormally large growth of early-wood for that year and would be the widest band of early-wood in all cores across this time block. While this is possible, considered in the context of the other samples, it seems more likely that late-wood growth was minimal to absent in this area of the tree for that year.

- From 1994 to 1995, there is progressive widening of ring width over the previous years of narrowing. The ring for 1996 shows marked narrowing. The rings for 1997–1999 are wider than the ring for 1996 and the spacing for the 3 years is fairly regular across samples C1–C3 with C4 showing a slightly different pattern over the 3 years, but still wider than 1996.
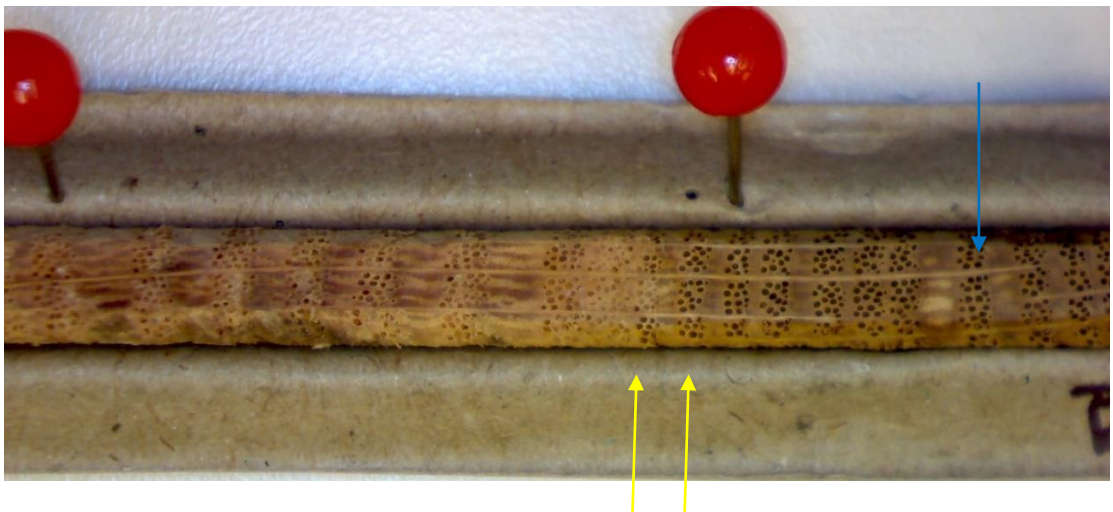
1970–1984

Figure A6.3a

Figure A6.3b

Figure A6.3c

Figure A6.3d

Figure A6.3a–d Photos Kapuni Oak cores R40442 & R40444 (1970–1984).

The photos in Figure A6.3a-d show cores C1-C4 in order a-d. Red pin indicates early-wood for 1970, blue arrow early-wood for 1984, yellow arrows indicate indistinct ring boundaries, and white arrow shows location of an inferred boundary. The patterns for correlation can be seen in the above photos. Please note the existence of an inferred boundary in sample C3, which will be explained along with the points of correlation below:

- The ring growth patterns from 1970–1975 are fairly variable across the 4 cores. However, the rings are all relatively wide across all the samples with variable spacing from year to year in individual samples.

- Significant narrowing occurs in the rings for years 1976 and 1977 across all 4 samples. The narrowing is so strong that it nearly obscures the boundaries, in samples C2 and C3 particularly. Sample C3 has an inferred boundary as even under microscope is was difficult to see any noticeable difference at the inferred boundary. There was a slight change in the pattern of the porous wood to allow for the placement of a boundary, but it may be questionable. The boundary can also be inferred by looking at the rings around the boundary in question and correlating across the other 3 samples, looking at the previous and subsequent years.

- For the years 1978 and 1979 there is a widening over the previous two years. In sample C1, however, the ring for 1978 is only slightly wider and is hard to see in the photo. Samples C1, C2 and C4 show a progressive widening, with 1979 being wider than 1978. Sample C3 is the opposite.

- Looking at the years 1980 and 1981, it can be seen that the ring for 1981 is wider than for 1980 across all 4 cores. There is then a narrowing, sometimes significant, particularly in cores C2 and C3, for the years 1982–1983. This narrowing is very slight in sample C1 and C4.

- 1984 experienced a widening compared with the previous years as shown in samples C1 and C2. It is also evident in samples C3 and C4, but is just slightly out of picture.

1962–1969
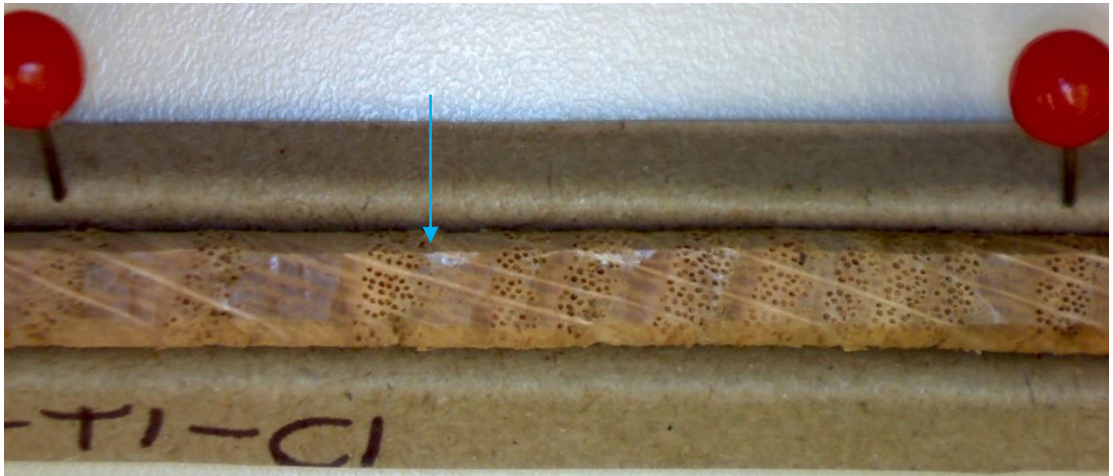
Figure A6.4a

Figure A6.4b

Figure A6.4c

Figure A6.4d

Figure A6.4a-d Photos Kapuni Oak cores R40442 & R40444 (1962–1969).

The photos in Figure A6.4a-d show cores C1-C4 in order a-d. The red pin on far right indicates the year 1970. In Figure A6.4a the left hand red pin indicates the year 1960. The blue arrows indicate early wood for 1962. There is little in the way of discernible patterns that can be tracked across the four core samples. What can be seen is explained below:

- From 1962–1964 there is progressive narrowing of rings as seen in samples C2, C3 and C4. C1 does not show pattern that fits at all with the other 3 cores. In sample C4, the narrowing from 1962 to 1963 is slight.

- The ring for 1965 experiences a widening over the previous year, which is evident in samples C2, C3 and C4.

- The trend from 1962–1969 is that of overall narrowing. This is noticeable across all samples. However, sample C1 shows a wider ring for 1969.

**Early 1950's–1959**
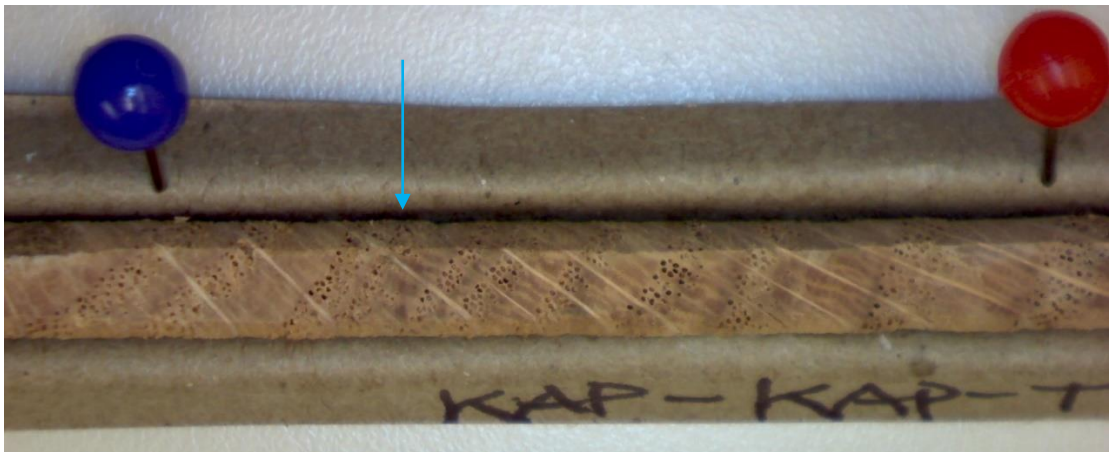
Figure A6.5 a

Figure A6.5b

Figure A6.5c

Figure A6.5d

Figure A6.5a–d Photos Kapuni Oak cores R40442 & R40444 (1950–1959)

The photos in Figure A6.5a-d show cores C1-C4 in order a-d. The red pin on right of core indicates the year 1960. Blue pin in Figure A6.5a, A6.5c indicate the year 1950. The blue arrow points to the year 1953 to provide 2 reference points in each photo. Patterns in the tree rings from the early 1950's until 1959 are not easy to correlate across the 4 samples. Below is the interpreted patterns, if any:

- In samples C2, C3 and C4 there is a narrow ring for 1953, followed by a wider ring in 1954, followed by a narrower ring for 1955. C1 shows a slightly similar pattern that is off by a year, but the other correlations for C1 indicate that the current placement of calendar years is appropriate.

Again, correlation is among the samples C2, C3 and C4 for years 1956–1959. Taken in the context of just the 4 years themselves, the ring for 1956 is the narrowest of the 4, followed by a widening for 1957. The ring for 1958 shows a slight narrowing and this is followed by a wide ring for 1959 which across all 4 core samples, is the widest ring for the time block.

6.1.2   Correlation of tree rings Luscombe chestnut R40459

Four cores were extracted from tree KAP-LUS-T1, (Luscombe chestnut) however, only two of the cores collected have been found useful. Core C3 (R40459) was used to provide research samples. The two cores that have been disregarded can be seen below with an explanation of why they have disregarded.

The remaining two cores have had calendar years allocated to each ring and have been correlated as well as possible. Unfortunately, however, there are very few if any discernible patterns that can be tracked along the two selected core samples. Below are photos and short explanations of a few blocks of time to illustrate the fact that pattern correlation has not been particularly fruitful for the two samples.

2004–2013

Figure A6.6a

Figure A6.6b

Figure A6.6a-b   Photos Luscombe Chestnut cores R40459 (2004–2013).

The photos in Figure A6.6a-d show cores C1 and C3 in order a-b. Red pin indicates the boundary between the growth years 2009-2010. Yellow arrows indicate the boundary between years 2003-2004. A discussion of the patterns above can be found below:

- Examining the rings for the calendar years 2004 through 2006, both samples show ring widths that do not vary greatly. Sample C1 shows an ever so slight increase in ring width over the 3 years. On the other hand, sample C3 shows a little bit of an increase in ring width in 2005 over 2004, with a very slight narrowing, if any change, in the ring for 2006.

- The years 2007–2009 show a noticeable narrowing over the previous years. However, the pattern of narrowing is quite different between the 2 cores. Core sample C1 shows 2007 as being the narrowest of the 3 years and significantly narrower than the previous year's ring. From 2007 to 2009 in sample 1, there is a progressive widening.

- Sample C3 shows that the ring for 2007 is noticeably narrower than for 2006, but not nearly as pronounced as in sample C1. The ring for 2008 is narrower still and the narrowest for the years 2007–2009. The following year, 2009, shows a widening with a ring that is similar in width to the ring for 2007.

- From 2010–2013 sample C1 shows that rings for 2010 and 2011 are quite similar in width with the ring for 2011 possibly being slightly wider. The ring for 2012, however, is narrower than the previous 2 years. Over the same time period, 2010–2013, core C3 shows a progressive narrowing of ring widths.

1994–2000

Figure A6.7a

Figure A6.7b

Figure A6.7a–b Photos Luscombe Chestnut cores R40459 (1994–2000).

The photos in Figure A6.7a-b show cores C1-C3 in order a-b. The white pin indicates the boundary between growth years 1999-2000. The yellow pin points to boundary 1993-1994. The patterns shown in the above photos in Figure A6.7a–b are discussed below:

- In sample C1, the overall pattern for the years 1994 through 2000 is that of narrowing. However, it should be noted that the ring for 1996 experienced widening, bringing it back to approximately the same width as the ring for 1994. This is then followed by a progressive narrowing through the year 2000.

- From 1994 through 2000, in sample C3, the overall pattern is fairly consistent in ring width. There is some minor widening from 1995 to 1996, followed by a slight progressive narrowing.
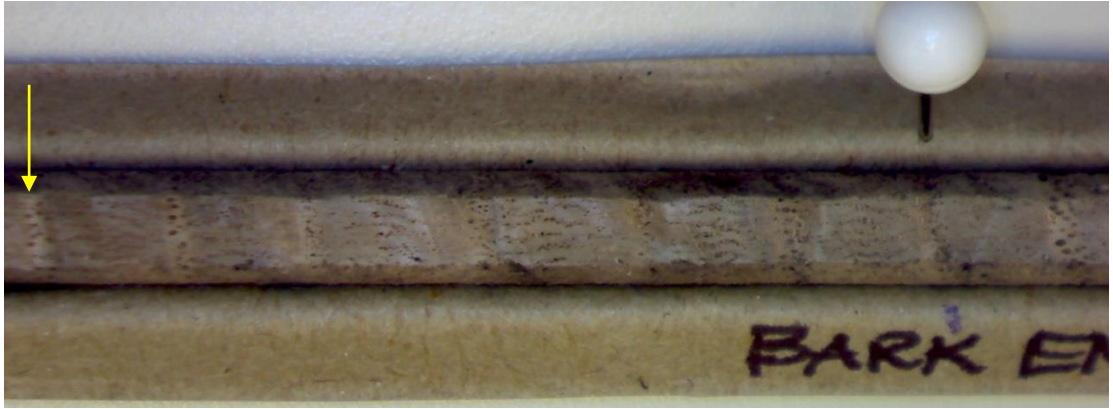
1980–1984

Figure A6.8a
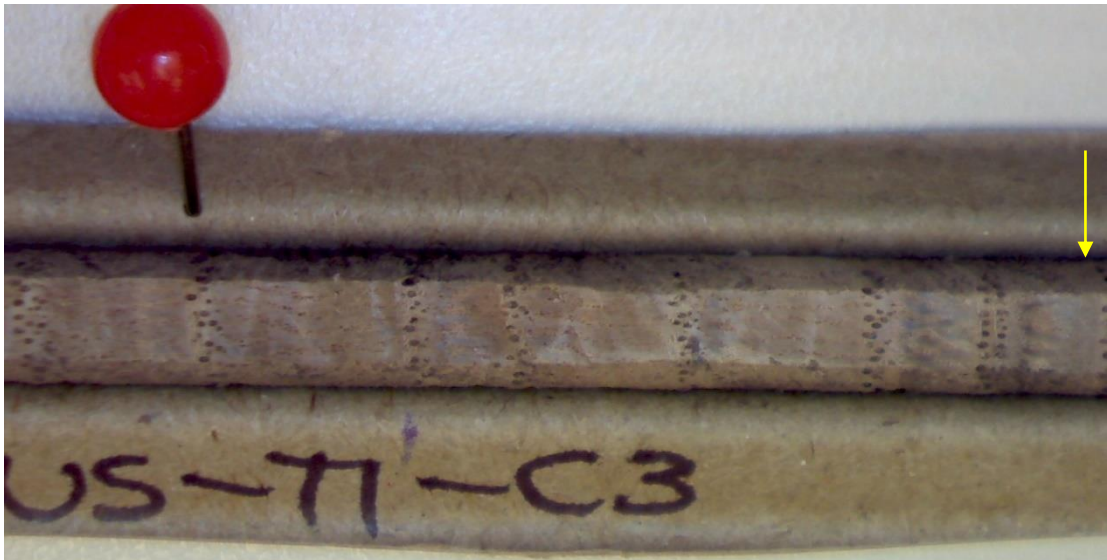
Figure A6.8b

Figure A6.8a–b Photos Luscombe Chestnut cores R40459 (1980–1984).

The photos in Figure A6.8a-b show cores C1 &C3 in order a-b. The red pin indicate the boundary between growth years 1979-1980. The yellow arrows indicate the boundary between 1984-1985. Interpretations of the patterns seen above in Figure A6.8a–b are discussed below:

- In sample C1, the ring for 1980 is significantly wider than the surrounding rings. This wide ring is followed by a noticeably narrower ring in 1981. The ring for 1982 widens out. The rings for 1983 and 1984 are narrower than the ring 1982, with the 1984 ring being slightly wider.

- The pattern for 1980 through 1982 in sample C3 is similar to that in sample C1. As can be seen above in Figure A6.8b, the ring for 1980 is relatively wide followed by a significantly narrower ring in 1981. This is then followed by a noticeable widening for the 1982 ring. This is where the similarities for the two cores end for this time block, however. As the ring for 1983 is wider than the ring for 1982 and is followed by a narrower ring in 1984.

1965–1969

Figure A6.9a

Figure A6.9b

Figure A6.9a–b Photos Luscombe Chestnut cores R40459 (1965–1969).

Figure A6.9a-b photos showing core samples C1 &C3. The red pin indicates boundary between growth years 1969-1970. The yellow arrow indicates boundary between years 1964-1965. The green arrows point to indistinct ring boundaries. Discussion of the interpreted patterns for the years 1965–1969 can be found below:

- Sample C1 shows a break in the ring for 1965 that appears to be due to wood rot. Due to the break, it's a little difficult to compare the ring width for 1965 to the ring for 1966, however, it appears that they are similar in width. The rings for 1967 and 1968 show a progressive widening with the 1968's ring being the widest ring in the time block. This is followed by a narrowing of ring width for 1969.

- As with sample C1, sample C3 also has a break in the 1965 ring that, however, is a bit more difficult to determine the cause of. It may be rot, but that is uncertain. The ring for 1966 is the widest ring in time block for this sample. This is followed by a progressive narrowing through 1969.

6.1.3 Correlation of tree rings Vector pine R40447 and R40448

Tree KAP-VEC-T1, a Radiata Pine, yielded 4 core samples, which have been inspected by eye and microscopy to try and determine the boundaries between calendar years. Cores C1 (R40447) and C2 (R40448) were used to provide samples for the research project. The clarity of tree ring boundaries and ring width patterns vary significantly from core to another. There are also instances of what appear to be slight false/double rings, that is, more than one growth ring within a single year. Most of these are faint, but can be noticed sometimes by a slight change in colour within an area of lighter coloured early-wood. In some instances, however, an interpreted calendar year boundary is not greatly different than what has been interpreted to be an actual ring boundary. Below, in Figures A6.10 and A6.11, are photos showing both an interpreted ring boundary as well as an interpreted false ring.
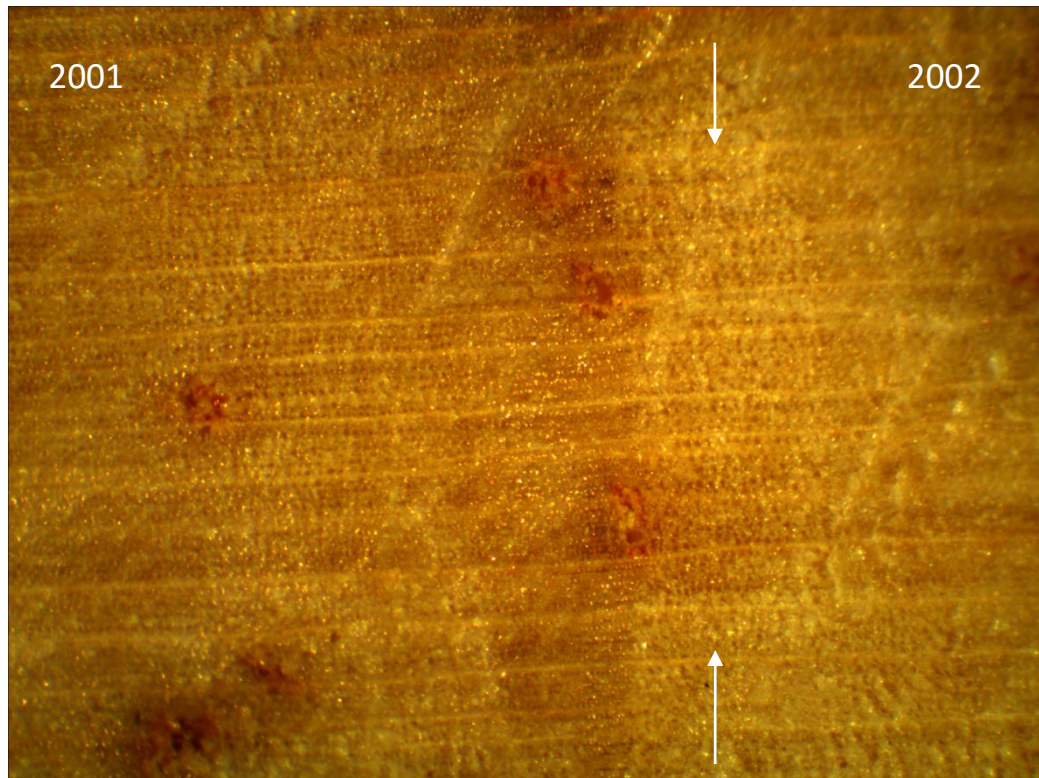
Figure A6.10   Interpreted ring boundary Vector Pine.

Figure A6.10, above, shows the interpreted boundary between the years 2001 and 2002. White arrow point to boundary between years. Looking from left to right, with age decreasing to the right, relatively large pores can be seen gradually tightening and narrowing to a relatively abrupt boundary. To the right of this boundary the immediate return of large pores can be seen, signifying the early-wood growth of the following year. It is these characteristics, along with the general context of the rings to be discussed below, that has allowed this boundary to be inferred.
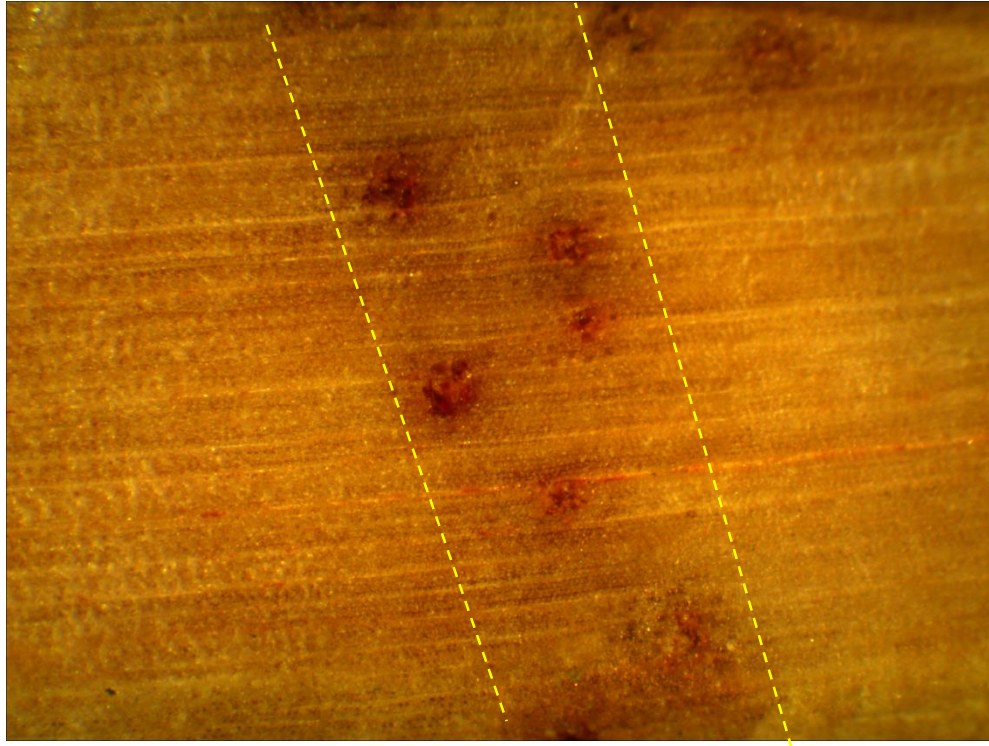
Figure A6.11 Interpreted false ring Vector Pine.

The double ring shown in Figure A6.11 is interpreted as a false ring, mainly due to the lack of an abrupt boundary to mark the end of a growing year. The area within the yellow dashed lines roughly outlines the location of the narrower compact cells of the false ring. Looking from left to right, there is a gradual tightening and narrowing of the pores followed by a gradual widening. This is often characteristic of double rings.

Due to the variance in tree ring patterns between samples and boundary clarity, correlation has been frustrating and difficult. Thus, the level of confidence with which correlations are made in these samples is low. Patterns across cores, if present, are subtle. In many cases the pattern in one core for a given time block does not match the other cores. The figures and explanations below are, therefore, more just showing the variance in ring patterns for specific time periods. The most significant piece of evidence that the allocated calendar years are accurate or are within a year or two at worst, is that for each core sample the last clearly visible ring towards the centre of the tree represents the year 1992.

2008–2013

Figure A6.12a

Figure A6.12b
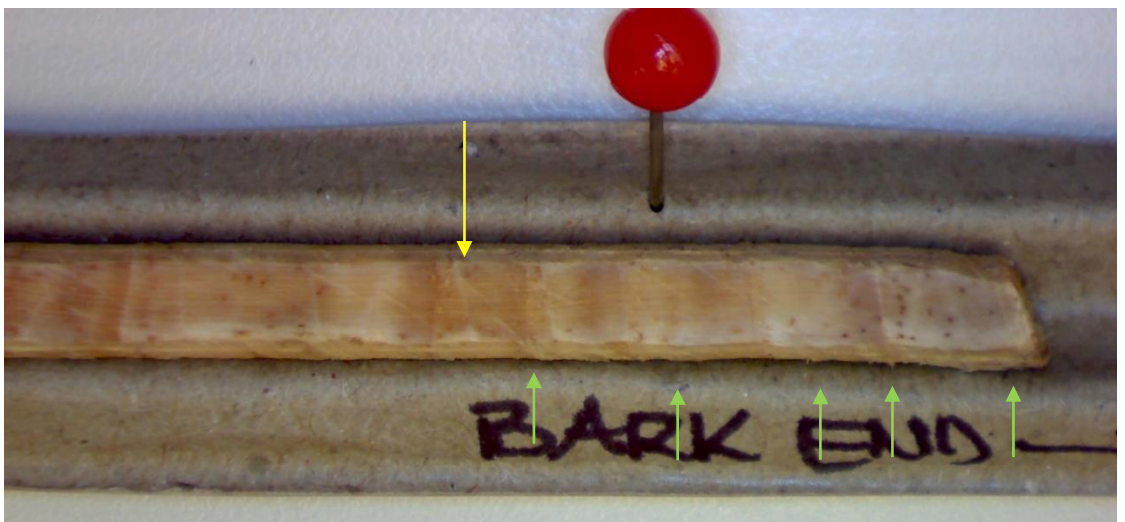
Figure A6.12c
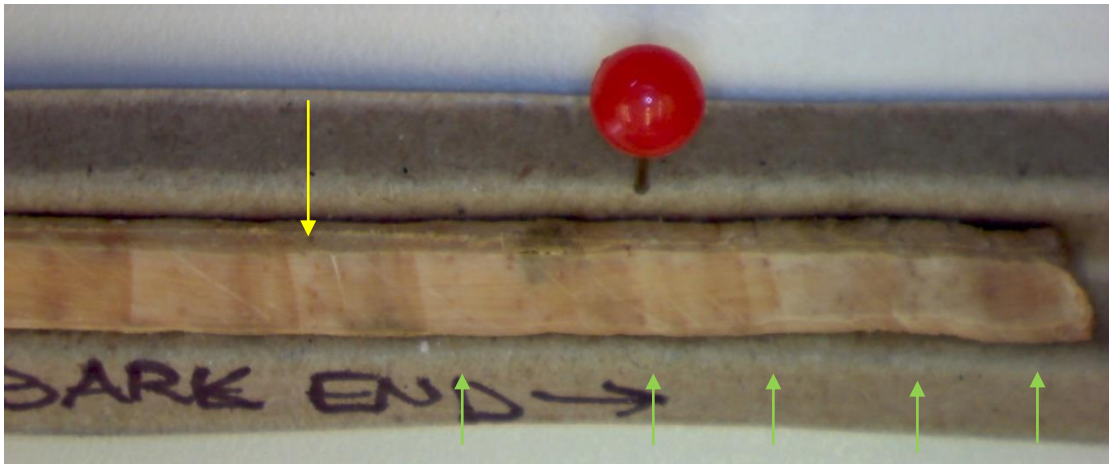
Figure A6.12d

Figure A6.12a–d Photos Vector Pine cores R40447 & R40448 (2008–2013).

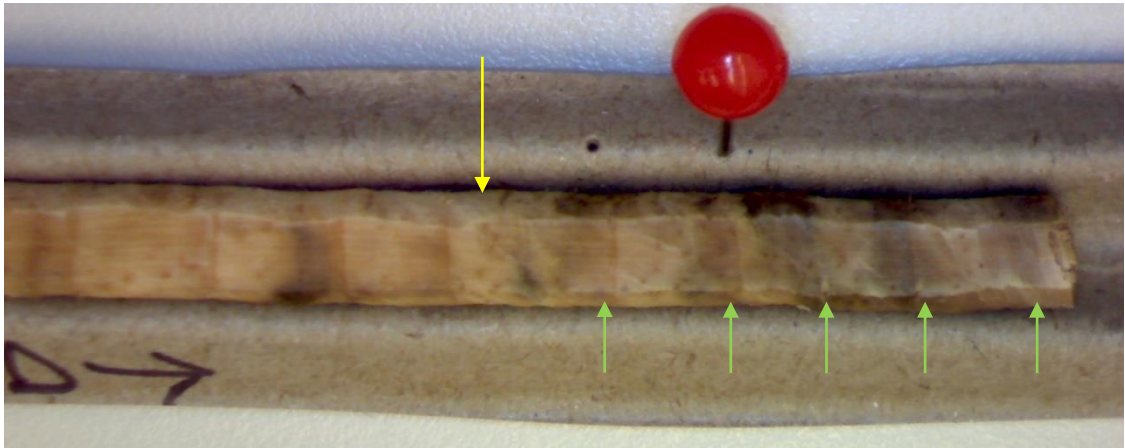The photos in Figure A6.12a-d show cores C1-C4 in order a-d. Red pin indicates early-wood for year 2010. Yellow arrows indicate the boundary between the growth years 2007-2008. Green arrows indicate indistinct boundaries. An explanation of the patterns found in Figure A6.12a–d is below:

Starting with the year 2008, beginning immediately left of the yellow arrows, sample C1 shows a narrow ring followed by a wider ring for 2009. Samples C2 and C3 show a slight widening of rings from 2008 to 2009. Sample C4 shows significant widening from 2008 to 2009 where the ring for 2009 is about twice as wide as the ring for 2008.

For the years 2010 to 2012, samples C1 and C4 both show a progressive widening of rings. However, with sample C4, the widening from 2011 to 2012, is slight the rings may be fairly even in width. Sample C2 shows a narrowing from 2010 to 2011 and the ring for 2012 is approximately the same width as 2011. This seems consistent with the pattern for C4 for years 2011 through 2012, but it doesn't necessarily indicate correlation. Sample C3 shows relatively even ring widths for 2010–2012. This pattern too shows consistency with the patterns for 2011 and 2013 for samples C2 and C4.

The incipient ring for 2013 is relatively consistent in its width across the 4 samples, though is a little hard to see in the photos above.

**2000–2004**

Figure A6.13a
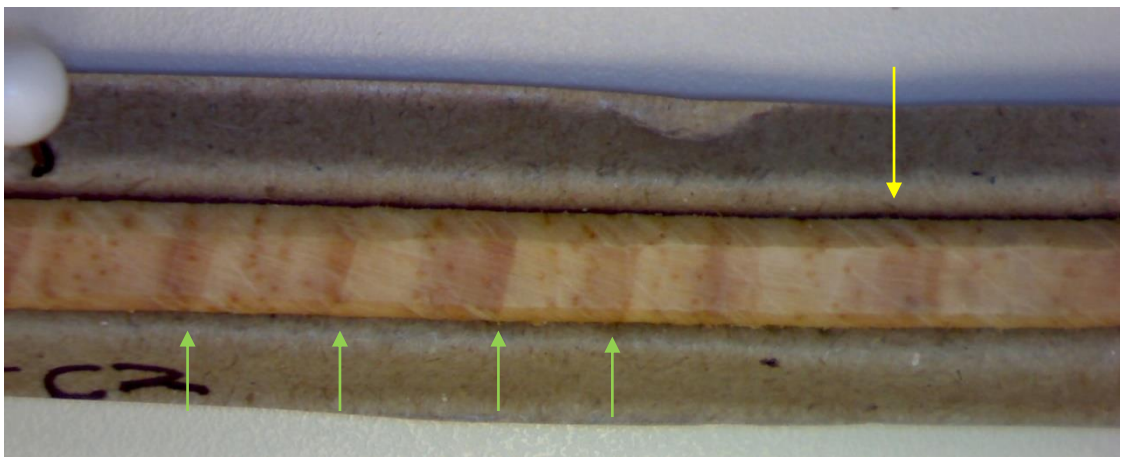
Figure A6.13b

Figure A6.13c

Figure A6.13d

Figure A6.13a–d Photos Vector Pine cores R40447 & R40448 (2000–2004).

The photos in Figure A6.13a-d show cores C1-C4 in order a-d. White pin indicates boundary between years 1999-2000. Yellow arrow indicates 2004-2005 growth year. Green arrows indicate indistinct boundaries. Explanations of interpreted patterns for the years 2000–2004 in Figure A6.13a–d can be found below:

- Sample C1 shows relatively consistent ring widths for the years 2000 to 2004. There, of course, may be slight variations in thickness.

- Core sample C2 shows a narrowing of ring width from 2000 to 2001. The ring for 2002 is wider than for 2001 and then there is a progressive narrowing of rings from 2002 to 2004

- From 2000 through 2003, sample C3 shows a relatively consistent ring width (there may be slight variations in thickness). However, in 2004 the ring width increases dramatically with a ring that is at least 2x wider than the previous years.

- In sample C4, there is a narrowing of ring width from 2000 to 2001, followed by a progressive widening of ring width through 2003. The ring for 2004 is narrower than the previous ring, however.

1996–1999

Figure A6.14a

Figure A6.14b

Figure A6.14c

Figure A6.14d

Figure A6.14a-d   Photos Vector Pine cores R40447 & R40448 (1996–1999).

The photos in Figure A6.14a-d show cores C1-C4 in order a-d. White pin indicates growth year 1999-2000. Yellow arrow points to boundary between years 1995-1996. Pattern interpretations are as below:

- In sample C1, ring widths for the years 1996 through 1999 are fairly consistent. There will, of course, be variances in the width, but it's a little difficult to discern by eye.

- From 1996 to 1998, sample C2 shows a progressive narrowing. This is followed by a wider ring for the year 1999, which is significantly wider than the previous 2 years. Core sample C3 shows a similar pattern to C2. A main point of difference, however, is that the ring for 1998 appears to be only slightly wider than the ring for 1997, but the overall pattern is akin to the pattern in C2.

- Sample C4 shows a narrowing from 1996 to 1997. This narrowing is followed by a significant widening that progresses through 1999.

1992–1996

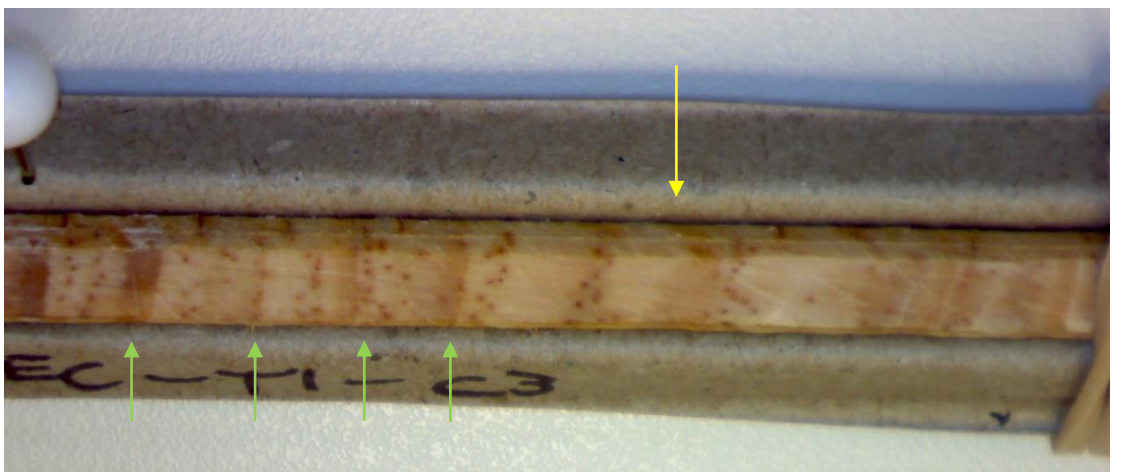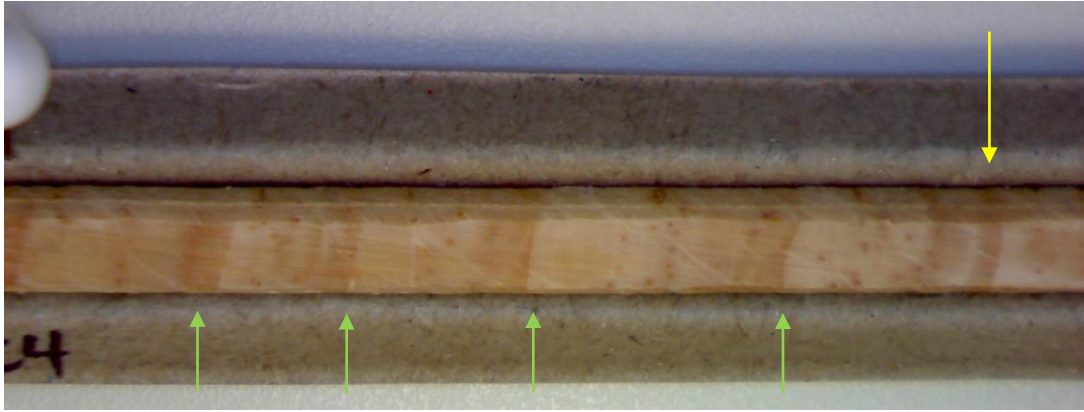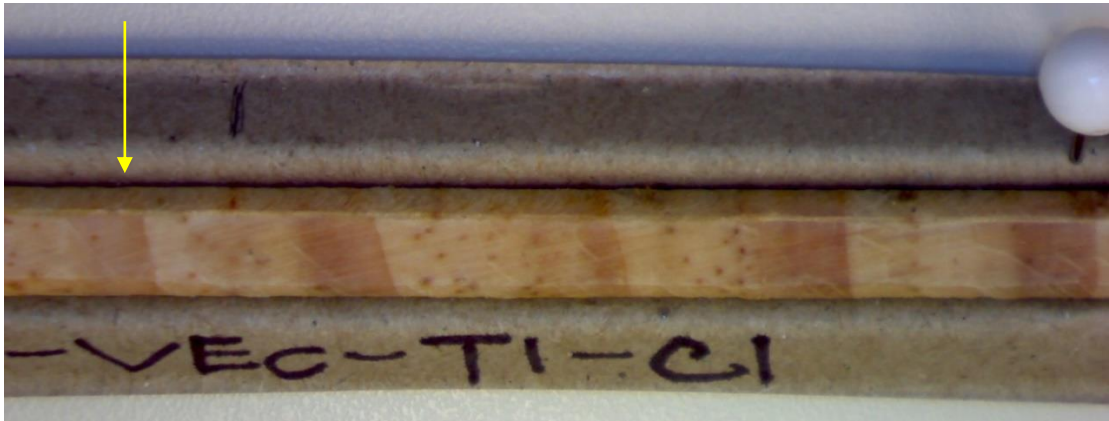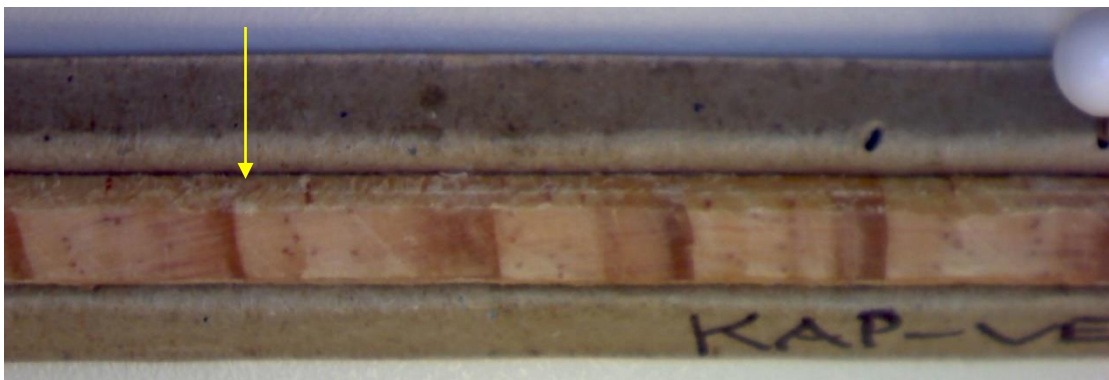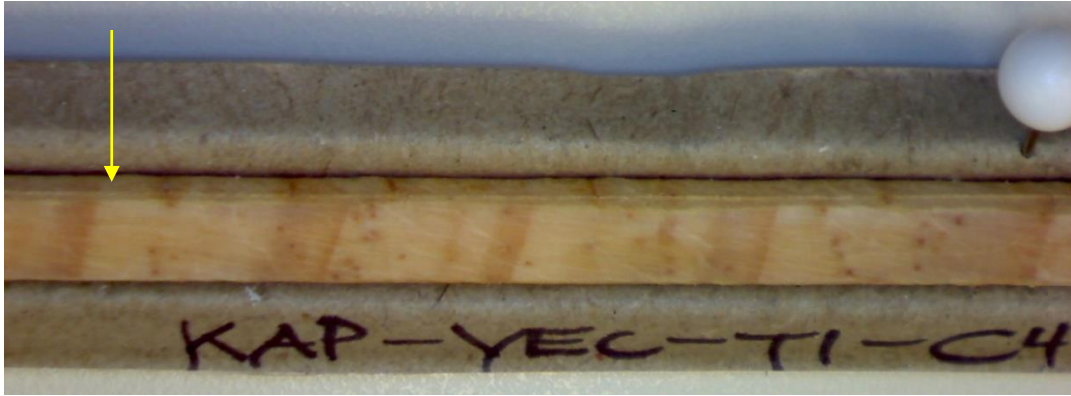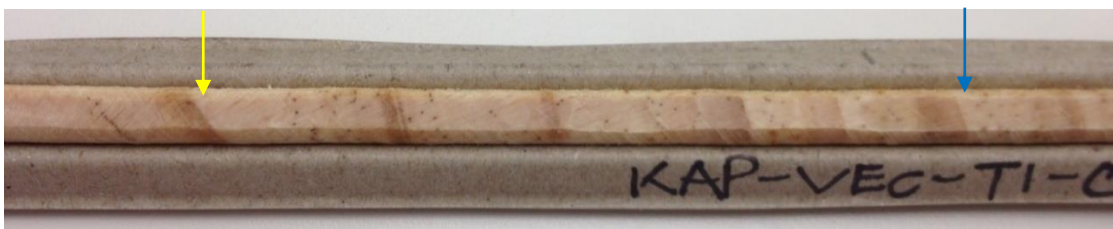Figure A6.15a

Figure A6.15b

Figure A6.15c

Figure A6.15d

Figure A6.15a-d   Photos Vector Pine cores R40447 & R40448 (1992–1996).

The photos in Figure A6.15a-d show cores C1-C4 in order a-d. The yellow arrows points to the boundary between 1991-1992. The blue arrow points to boundary between 1996-1997. Explanations of the interpreted patterns for the years 1992 through 1996 are found below:

- Core samples C1 and C3 show a similar tree ring pattern. Starting from 1992 there is a narrowing of ring width through 1993, followed a widening in 1994. In C1, the ring for 1994 is approx. the same width as for 1992, however, this is not true for C3. In 1995, there is again a narrowing of ring width, which is particularly noticeable in sample C1 where the ring is significantly narrower. Widening again occurs in 1996, with the ring for 1996 being wider than the previous year.

- Sample C2 shows a progressive widening of ring width from 1992 through 1994. This is followed by a narrowing in the year 1995, followed by widening again in 1996. Looking at the sample for the block of time from 1994 to 1996, it follows the same pattern mentioned above for samples C1 and C3. However, the ring for 1996 is only a little wider than for 1995.

- In sample C4, the rings for 1992 and 1993 are very close in width, with the ring for 1992 possibly only slightly wider. The rings for 1994 and 1995 are also about the same width, however, they are wider than the rings for 1992 and 1993. The ring for 1996 is the widest of the time frame from 1992 to 1996. The overall pattern seems to be that of ring widening.

6.1.4　Correlation of tree rings Baring Head tree R40454 and R40456

Core samples from tree BHD-T1, a Radiata Pine, have been a bit challenging to correlate due to the absence of significant patterns that span more than 3–4 growth years. Core C1 (R40454) and C3 (R40456) were used for the research project. A few noticeable patterns have emerged and are discussed below, but even they are bit subtle in many places making it difficult to sometimes say with certainty that they correlate well. Every effort has been made to show the most readily visible patterns. With all that said, the annual rings as allocated do match when extending all the way to the centre of the tree. That is, towards the centre of the tree, it's clear that overall accounting of the rings matches and that if no interpreted annual rings are false rings, then age of the tree is approx. 32 years.

2009–2013
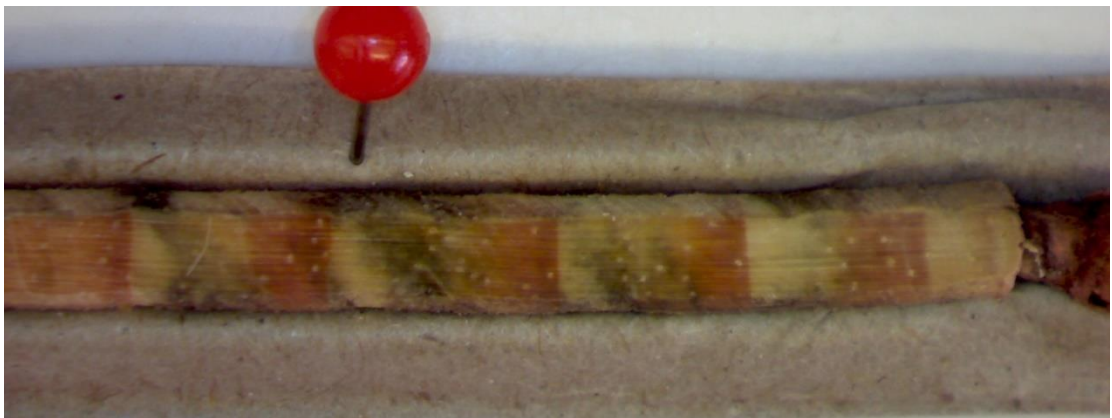
Figure A6.16a
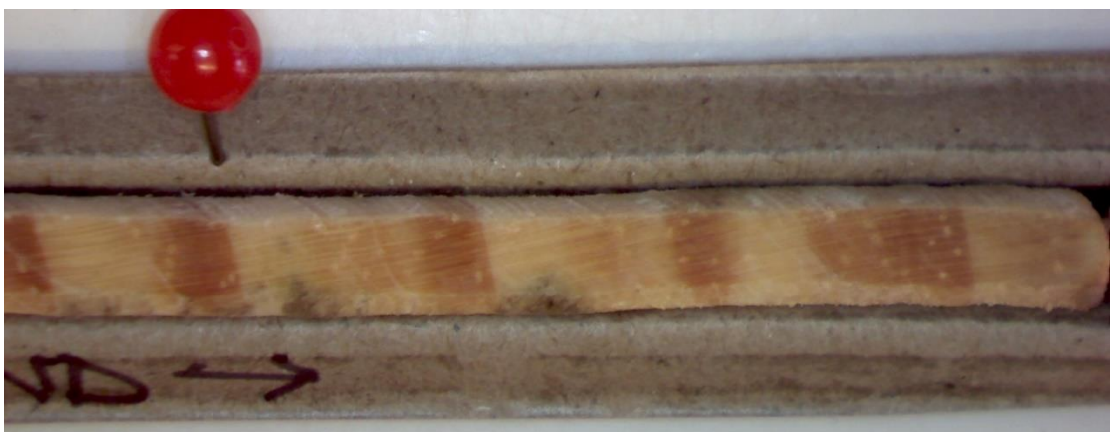
Figure A6.16b
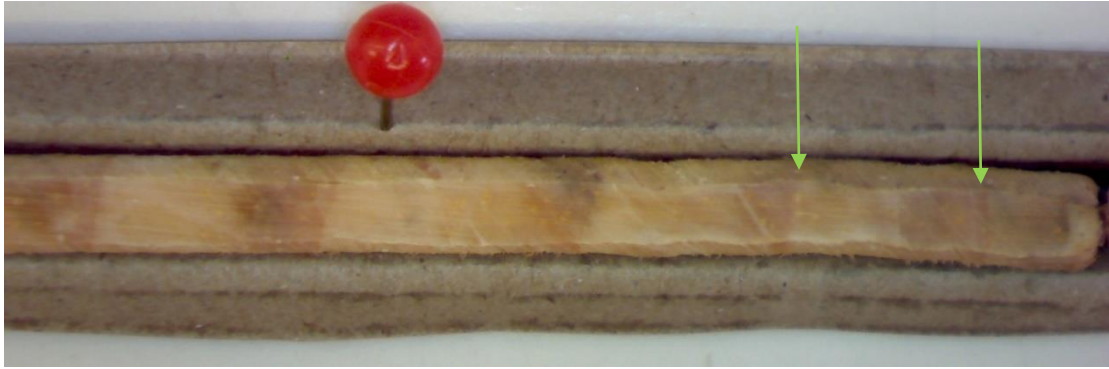
Figure A6.16c

Figure A6.16d

Figure A6.16a–d Photos Baring Head Pine cores R40454 & R40456 (2009–2013).

The photos in Figure A6.16a–d show cores C1-C4 in order a-d. The red pin indicates the boundary between 2009-2010 growth seasons. The green arrows indicate hard to see ring boundaries. The pattern is interpreted below:

- Across all 4 cores, the ring for 2009 is narrower than the ring for 2010.

- Examining the ring widths from 2010–2013, inclusive, it's clearly visible that there is a progressive narrowing of the rings. The pattern is more subtle in sample C1, but is still there. However, sample C2 shows a ring for 2012 that is wider than for 2011 and about the same size as the ring for 2010. It should be noted that for the ring representing the growth beginning in the year 2013 is not complete.

1998–2001
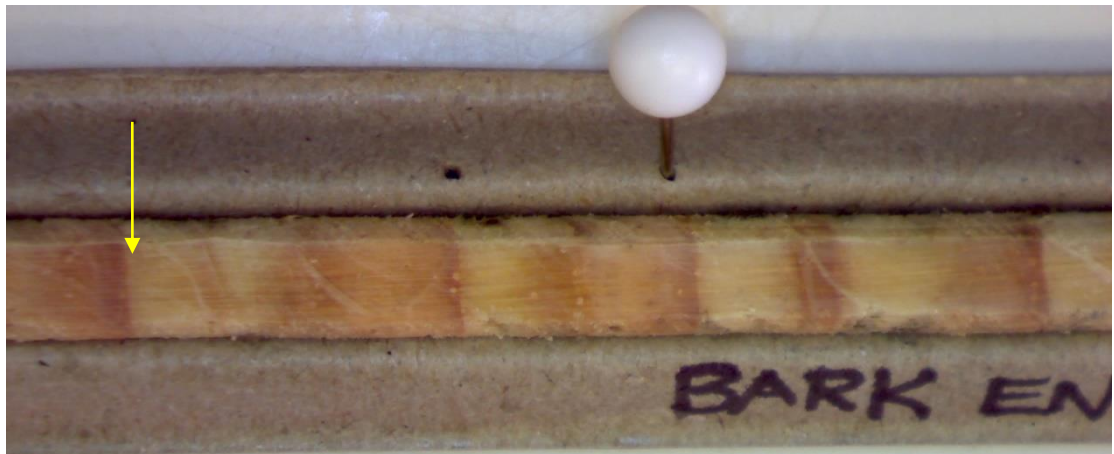
Figure A6.17a
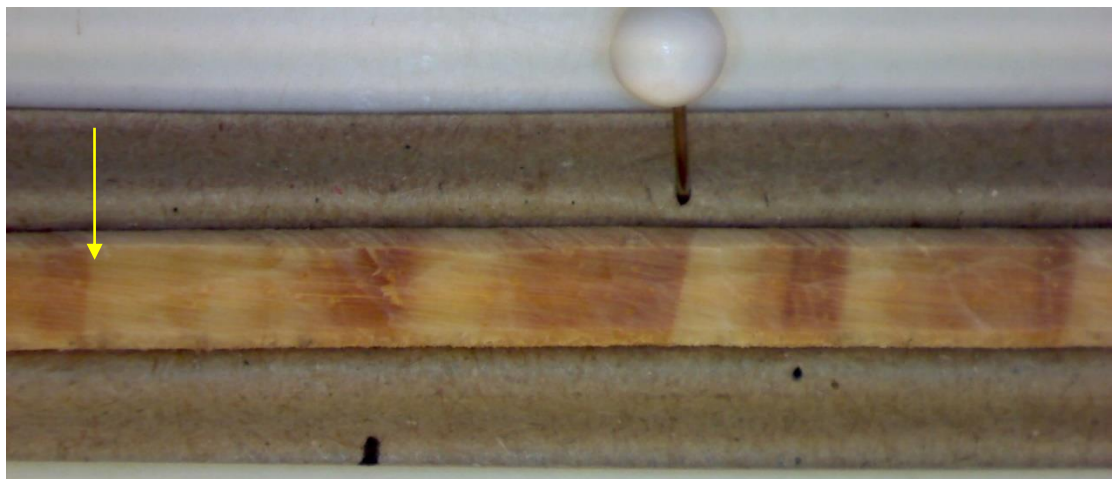
Figure A6.17b
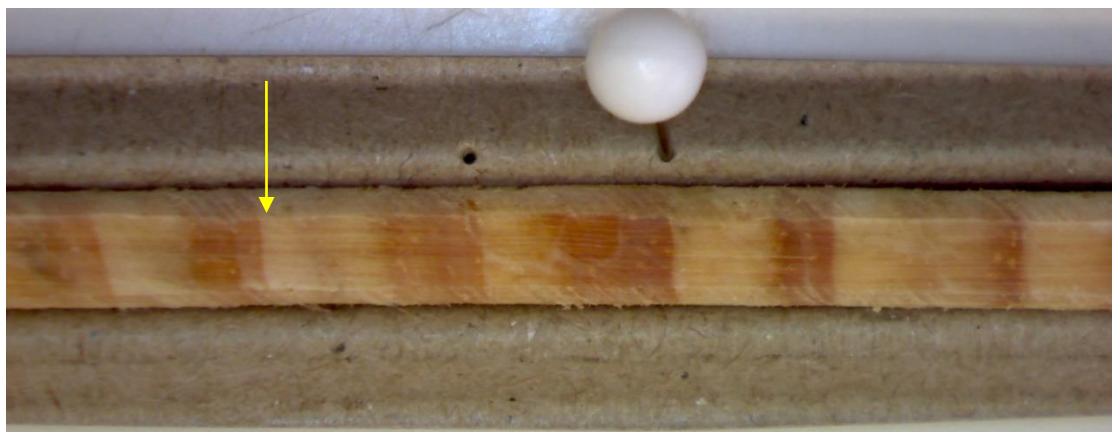
Figure A6.17c
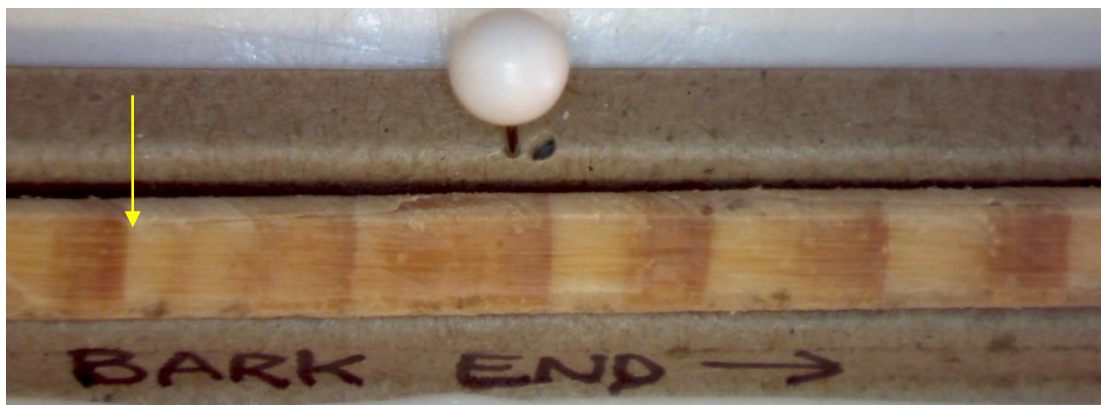
Figure A6.17d

Figure A6.17a–d Photos Baring Head Pine cores R40454 & R40456 (1998–2001).

The pattern for the years 1998–2001 can be seen in the photos above in Figure A6.17a–d. below is an explanation of the interpreted patterns:

- Looking at the rings for the years 1998 and 1999, across all cores samples the ring for 1999 is narrower than the ring for 1998.

- Moving on to the years 2000 through 2001, the narrowing mentioned above continues through the year 2000. This is followed by a considerable widening in 2001. However, this widening is less evident in sample C4.

- In correlating the samples over this time period, for samples C1 through C3, the main feature that stood out was the ring for 2000 and more specifically, its late-wood as it was fairly consistent across the 3 cores. This was initially due to the fact that in sample C1 it appeared to be a false ring, however, after examining C2 and C3, it was counted as an annual ring.

1984–1989
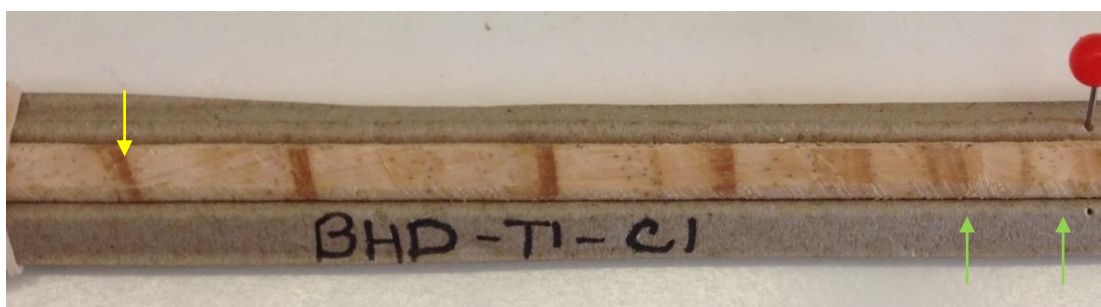
Figure A6.18a
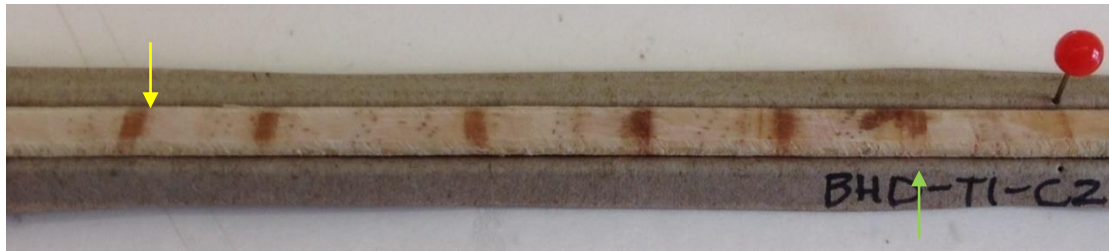
Figure A6.18b

Figure A6.18c

Figure A6.18d

Figure A6.18a–d Photos Baring Head Pine cores R40454 & R40456 (1984–1989).

The patterns from 1984 through to 1989 can be seen in the photos above. An explanation of the interpreted patterns can be found below:

- The ring width for 1985 shows an increase in width over the previous year across all 4 samples. Following on from 1985, the ring for 1986 shows a narrowing over the previous year, which in samples C2 and C4 is slight.

- For the growth year of 1987, the ring width is slightly narrow or about the same in width to 1986. The narrowing is most clearly evident in samples C1 and C2.

- From 1988 to 1989, there is widening of the rings across the 4 samples. The ring for 1988 is also narrow than the ring for 1987, with the exception of core sample C2 where ring for 1988 is as big as or slightly larger than the ring for 1987.

6.2 Calculated CO_{2ff} emissions

Table A6.1 CO_{2ff} Luscombe chestnut tree.

Year	CO₂ ppm	CO₂ std deviation	ΔObs	ΔObs error	ΔBHD	ΔBHD error	Δff	CO₂ff	CO₂ff uncertainty
1964	318.72	2.16*	444.21	1.74	435.17	42.98	-1000	-2.00	-9.49
1965	319.11	1.98*	604.03	2.49	620.55	37.48	-1000	3.29	7.47
1966	320.23	2.30*	636.79	2.58	635.64	7.91	-1000	-0.22	-1.63
1969	323.19	2.40*	538.05	1.83	539.67	4.27	-1000	0.34	0.98
1972	325.54	0.18	476.74	2.27	482.40	4.11	-1000	1.25	1.04
1975	329.48	0.24	381.49	1.99	398.45	1.68	-1000	4.04	0.62
1978	332.96	0.24	315.13	1.65	321.76	1.41	-1000	1.68	0.55
1982	338.90	0.28	251.81	1.95	255.73	2.15	-1000	1.06	0.79
1985	342.83	0.42	206.8	1.74	207.76	4.47	-1000	0.27	1.36
1987	345.92	0.33	182.77	1.52	189.23	4.16	-1000	1.89	1.30
1993	354.88	0.61	121.97	1.77	133.88	0.65	-1000	1.89	1.30
1994	355.66	0.14	115.48	1.8	127.13	3.39	-1000	3.77	0.60
1996	359.36	0.15	111.53	1.47	111.93	1.89	-1000	0.13	0.77
1999	364.81	0.21	90.1	1.44	102.53+	2.32	-1000	4.16	0.91
2001	367.52	0.18	84.72	1.74	90.81	0.66	-1000	2.06	0.63
2002	368.39	0.24	76.98	1.62	82.63	4.27	-1000	1.93	1.56
2004	373.64	0.30	62.67	1.69	73.47	3.33	-1000	3.80	1.31
2005	375.47	0.15	63.64	1.55	71.26	2.25	-1000	2.69	0.97
2006	377.77	0.29	59.23	1.74	61.28	1.80	-1000	0.73	0.89
2007	379.41	0.38	50.54	1.7	58.95	0.84	-1000	3.04	0.69
2008	381.54	0.13	50.93	1.4	55.56	1.82	-1000	1.68	0.83
2010	384.86	0.16	40.32	1.66	49.79	1.06	-1000	3.50	0.73
2012	388.67	0.25	35.28	1.51	38.55	1.21	-1000	1.23	0.73

*Denotes CO_2 concentration data accessed from Mauna Loa record as Baring Head CO_2 concentration record starts in 1970. The Mauna Loa data is not seasonally adjusted for Southern hemisphere conditions, but even if the CO_2 concentration is 2ppm lower CO_{2ff} does not change.

In the original $^{14}CO_2$ data set there were no $^{14}CO_2$ measurements in 1999 (Currie et al. 2009). In the new data set a smooth curve fit analysis has allowed the calculation of some 1999 $^{14}CO_2$ data. For the purposes of calculating CO_{2ff} here an average ^{14}C value for 1999 was calculated from data points from $^{14}CO_2$ smooth fit analysis. (Turnbull et al. 2015).

Table A6.2 CO_{2ff} Vector pine tree R40447 core.

Year	CO$_2$ ppm	CO$_2$ std deviation	ΔObs	ΔObs error	Δbg BHD	Δbg BHD error	Δff	CO$_{2ff}$	CO$_{2ff}$ uncertainty
1993	354.88	0.61	120.89	1.75	133.88	0.65	-1000	4.11	0.59
1994	355.66	0.14	110.47	1.63	127.13	3.39	-1000	5.33	1.20
1996	359.36	0.15	97.07	1.44	111.93	1.89	-1000	4.87	0.78
1999	364.81	0.21	86.6	2.11	102.53 [+]	2.32	-1000	5.35	1.05
2001	367.52	0.18	75.02	1.69	90.81	0.66	-1000	5.40	0.62
2002	368.39	0.24	69.31	1.56	82.63	4.27	-1000	4.59	1.57
2004	373.64	0.30	53.84	1.66	73.47	3.33	-1000	6.96	1.32
2005	375.47	0.15	54.97	1.56	71.26	2.25	-1000	5.80	0.98
2006	377.77	0.29	47.88	1.68	61.28	1.80	-1000	4.83	0.89
2007	379.41	0.38	45.47	1.69	58.95	0.84	-1000	4.89	0.69
2008	381.54	0.13	42.96	1.37	55.56	1.82	-1000	4.61	0.83
2010	384.86	0.16	31.88	1.65	49.79	1.06	-1000	6.68	0.73
2012	388.67	0.25	24.44	1.5	38.55	1.21	-1000	5.35	0.73

Table A6.3 CO_{2ff} Vector pine tree R40448 core.

Year	CO_2 ppm	CO_2 std deviation	ΔObs	ΔObs error	Δbg BHD	Δbg BHD error	Δff	CO_{2ff}	CO_{2ff} uncertainty
1999	364.81	0.21	87.42	1.44	102.53 [+]	2.32	-1000	5.07	0.92
2002	368.39	0.24	69.31	1.56	82.63	4.27	-1000	5.42	1.57
2004	373.64	0.30	53.84	1.66	73.47	3.33	-1000	4.80	1.32
2005	375.47	0.15	54.97	1.56	71.26	2.25	-1000	6.19	1.01
2006	377.77	0.29	47.88	1.68	61.28	1.80	-1000	4.75	0.90
2007	379.41	0.38	45.47	1.69	58.95	0.84	-1000	5.23	0.69
2008	381.54	0.13	42.96	1.37	55.56	1.82	-1000	4.70	0.84

Table A6.4 $Δ^{14}C$ data from Baring Head $^{14}CO_2$ supplied by Turnbull et al. (2015).

Year	$Δ^{14}C$	$Δ^{14}C$ standard deviation	Number of analysis
1955	-10.70	6.17	3
1956	-1.08	8.84	3
1957	20.75	8.49	4
1958	60.27	11.08	3
1959	116.56	13.96	6
1960	176.32	10.20	5
1961	198.17	3.66	6
1962	210.57	6.84	6
1963	261.68	16.90	6
1964	435.17	42.98	6
1965	620.55	37.48	6
1966	635.64	7.91	6
1967	613.47	5.96	7
1968	575.74	8.01	7
1969	539.67	4.27	8
1970	523.46	6.67	6
1971	499.98	2.53	8
1972	482.40	4.11	7

Year	$\Delta^{14}C$	$\Delta^{14}C$ standard deviation	Number of analysis
1973	450.27	2.40	7
1974	417.62	7.74	8
1975	398.45	1.68	8
1976	365.75	3.79	8
1977	338.36	1.45	6
1978	321.76	1.41	3
1979	308.59	4.44	6
1980	284.04	2.50	6
1981	270.14	5.86	8
1982	255.73	2.15	4
1983	236.58	5.22	6
1984	222.36	1.50	3
1985	207.76	4.47	6
1986	198.43	4.13	8
1987	189.23	4.16	7
1988	175.90	2.15	1
1989	170.72	3.44	7
1990	154.86	0.92	6
1991	147.62	0.96	6
1992	139.86	0.96	4
1993	133.88	0.65	2
1994	127.13	3.39	4
1995	123.27	4.41	6
1996	111.93	1.89	7
1997	111.49	6.31	4
1998	104.05	3.38	1
1999	102.53 [+]	2.32	8
2000	90.05	4.69	5
2001	90.81	0.66	5
2002	82.63	4.27	7
2003	83.00	1.04	8
2004	73.47	3.33	8

Year	$\Delta^{14}C$	$\Delta^{14}C$ standard deviation	Number of analysis
2005	71.26	2.25	6
2006	61.28	1.80	5
2007	58.95	0.84	2
2008	55.56	1.82	6
2009	48.10	4.55	4
2010	49.79	1.06	4
2011	44.74	3.38	6
2012	38.55	1.21	7
2013	34.32	1.11	6

Data averaged for the months September to April to create an annual value. The data was averaged as per section 4.6.2. [+]Originally no data existed for 1999 and it has since been gap filled by Turnbull et al. (2015).

Table A6.5 CO_2 concentration data Baring Head record (Brailsford et al. 2012).

Year	CO_2 concentration	CO_2 concentration std deviation	Number of analyses
1971	324.74	0.11	6
1972	325.54	0.18	7
1973	326.61	0.50	5
1974	328.45	0.38	8
1975	329.48	0.24	8
1976	330.51	0.27	7
1977	331.61	0.25	8
1978	332.96	0.24	6
1979	334.28	0.55	4
1980	335.88	0.23	3
1981	337.58	0.24	7
1982	338.90	0.28	5
1983	340.24	0.14	6
1984	341.87	0.08	7
1985	342.83	0.42	7
1986	344.32	0.22	5
1987	345.92	0.33	8
1988	348.36	0.20	7
1989	350.16	0.34	7
1990	351.30	0.42	8
1991	352.59	0.29	7
1992	353.55	0.77	7
1993	354.88	0.61	7
1994	355.66	0.14	7
1995	356.82	0.42	3
1996	359.36	0.15	8
1997	360.55	0.30	6
1998	362.30	0.52	6
1999	364.81	0.21	7
2000	365.98	0.17	7

Year	CO₂ concentration	CO₂ concentration std deviation	Number of analyses
2001	367.52	0.18	6
2002	368.39	0.24	8
2003	371.51	0.39	8
2004	373.64	0.30	8
2005	375.47	0.15	4
2006	377.77	0.29	3
2007	379.41	0.38	8
2008	381.54	0.13	8
2009	383.44	0.40	6
2010	384.86	0.16	7
2011	387.48	0.63	7
2012	388.67	0.25	4

The Baring Head CO_2 concentration record accessed from NIWA website was averaged as per results section 4.6.1

Table A6.6   Emissions of CO_{2ff} data reported by Vector Plant.

Year	Annual Vector emissions 2000–2004 tonnes CO₂ P Stephenson	Daily total Tonnes per day CO₂	Daily total as carbon gCS⁻¹	TgC yr⁻¹
1990/1991	252416	692	2184	0.08
1991/1992	286519	785	2479	0.09
1992/1993	268508	736	2323	0.08
1993/1994	258461	708	2237	0.08
1994/1995	269487	738	2332	0.09
1995/1996	251175	688	2174	0.08
1996/1997	233686	640	2022	0.07
1997/1998	238186	653	2061	0.08
1998/1999	220566	604	1909	0.07
1999/2000	246215	675	2131	0.08

Year	Annual Vector emissions 2000–2004 tonnes CO_2 P Stephenson	Daily total Tonnes per day CO_2	Daily total as carbon gCS^{-1}	$TgC\ yr^{-1}$
2000/2001	252241	691	2183	0.08
2001/2002	320874	879	2777	0.10
2002/2003	266148	729	2303	0.08
2003/2004	477492	1308	4132	0.15
Year	Calculated Monthly total for Sep–April provided by P Stephenson.	Daily total April–Sep average as CO_2	April–Sep average 2004–2013 converted to gCS^{-1}	$TgC\ yr^{-1}$
2003/2004	6379 *	1595	5037	0.18
2004/2005	13500	1687	5330	0.19
2005/2006	14460	1808	5709	0.21
2006/2007	14474	1809	5715	0.21
2007/2008	11678	1460	4611	0.17
2008/2009	12588	1573	4970	0.18
2009/2010	14319	1790	5653	0.21
2010/2011	13772	1721	5437	0.20
2011/2012	13423	1678	5299	0.19
2012/2013	11743	1468	4636	0.17

2003/2004 * based on 4 months of data only.

Table A6.7   Analysis of wind parameters Hawera meteorological data.

Year	Total No of obs	% Freq West>230 <330	Mean wind speed m^{-s} West	% Freq wind NE>330 <80	Mean wind speed m^{-s} NE	% Freq NE>330 <80	Mean wind speed m^{-s} NE
2005	2624	52	6.98	24	5.98	18	6.21
2006	2651	47	6.62	30	6.11	18	5.99
2007	2662	54	6.75	24	5.81	17	5.56
2008	2639	38	6.67	31	6.50	25	6.17
2009	2662	47	6.76	22	5.81	26	6.50
2010	2659	52	6.85	27	6.46	20	5.56
2011	2662	46	6.53	32	6.45	17	6.44
2012	2658	40	6.68	34	6.11	24	5.86